ISSN 1146-609X

1999

Vol. 20 • No. 3

May
June

ACTA OECOLOGICA

INTERNATIONAL JOURNAL OF ECOLOGY

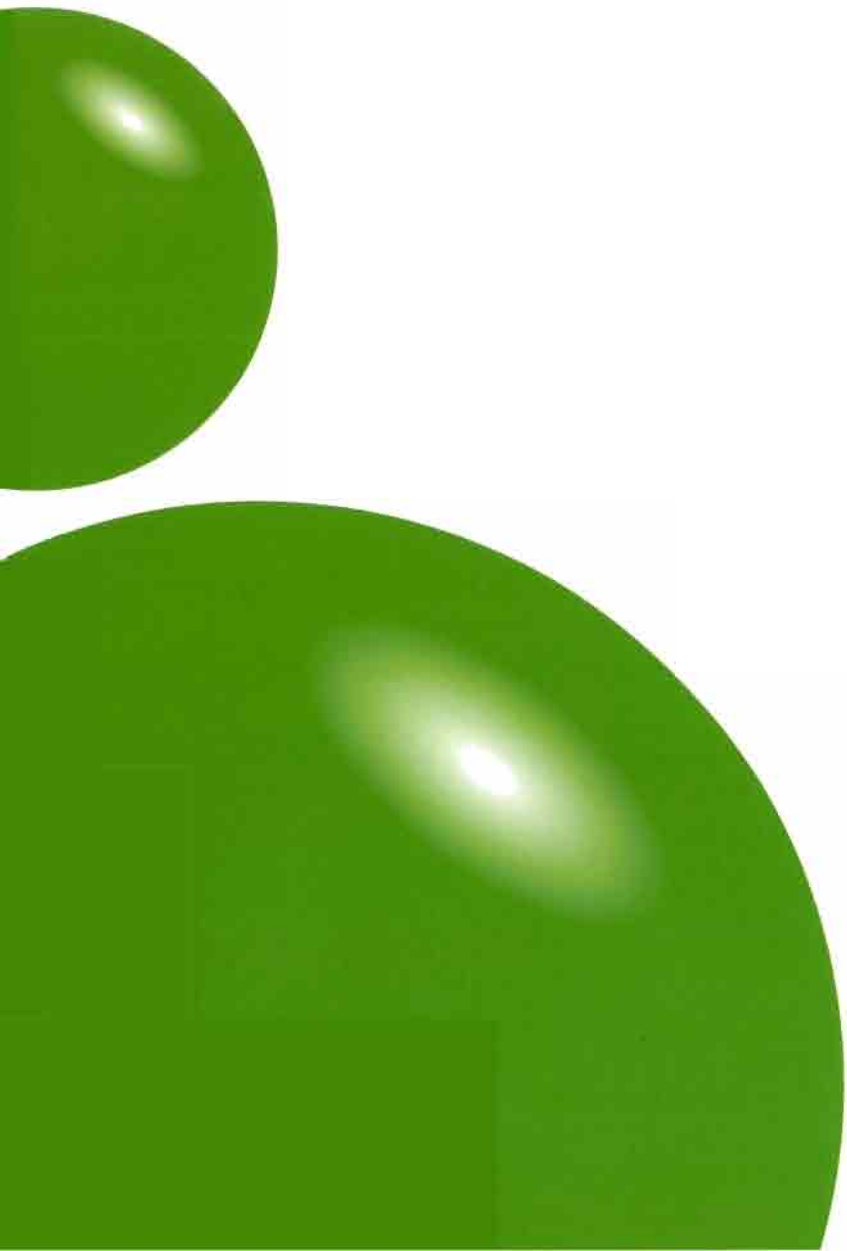

ELSEVIER

ACTA OECOLOGICA

INTERNATIONAL JOURNAL OF ECOLOGY

Aims and Scope

Acta Oecologica is a venue for the publication of original research articles and reviews in ecology. We encourage studies in behavioural ecology, community ecology, conservation biology, evolutionary ecology, physiological ecology and population ecology. There is no bias with respect to taxon, biome or geographic area. Both theoretical and empirical papers are welcome, but combinations are particularly sought. Priority is given to papers based on explicitly stated hypotheses. Papers explaining variation are preferred over those concentrating on average values. The forum section is reserved for short papers with critical discussion of current issues in ecology, as well as comments and viewpoints on previously published papers. *Acta Oecologica* does not publish book reviews, but comments on new books are welcome in the forum section.

Acta Oecologica is indexed in:

Current Contents (AB & ES, Ecological Abstracts, Current Advances in Ecological and Environmental Sciences, the INIST pascal Database, IBZ Database and Chemical Abstracts, Science Citation Index, Sci Search, Research Alert.

Editor-in-Chief

ARIE VAN NOORDWIJK
Behavioral and evolutionary ecology

Executive Editors:

STEPHAN HÄTTENSCHWILER
Plant population and physiological ecology, ecosystems ecology, global change

MARTINE HOSSAERT-MCKEY
Evolutionary biology, plant-insect interactions

JOAO CARLOS MARQUES
Marine ecology/modelling

HANS PETER KOELEWIJN
Plant population

MARCEL KLAASSEN
Animal Ecophysiology

Managing Editor

CHIARA MARCHETTI
NIOO-CTO
P.O. Box 40
NL 6666 ZG Heteren - The Netherlands
Fax: (31) 26 47 23 227.
e-mail: actaoec@cto.nioo.knaw.nl

ÉDITIONS ELSEVIER
23, rue Linois
75724 Paris cedex 15, France
http://www.elsevier.fr
A member of Elsevier Science
Éditions scientifiques et médicales Elsevier
SAS au capital de 80 250 000 F - 399 113 876 RCS Paris

LIFE SCIENCES DEPARTMENT
Tel.: (33) 1 45 58 90 67 - Fax: (33) 1 45 58 94 24.
Desk editor - Béatrice Fournier: (33) 1 45 58 90 33; b.fournier@elsevier.fr
Advertising - Marc Essodaigui : (33) 1 45 58 90 48; m.essodaigui@elsevier.fr

SUBSCRIPTIONS Tel.: (33) 1 45 58 90 67 - Fax: (33) 01 45 58 94 24; abt2@elsevier.fr
1999 (Vol 20) annual subscription; 6 issues.
- France: FF 1 480.
- EU (with 2.1% VAT*): FF 1 787.
- Rest of the world: FF 1 884.
- North, Central and South America: US$ 318.

Including air delivery.
* For tax exemption, VAT registration number must be indicated.

Address order and payment to: Éditions scientifiques et médicales Elsevier:
23, rue Linois, 75724 Paris cedex 15
- by check or credit card (CB, EuroCard, MasterCard or Visa) indicate No. and expiry date
- by transfer: CCP Paris n° 30041 00001 1904540 H 020/70.

Subscriptions begin 4 weeks upon receipt of payment and start with the first issue of the calendar year. Back issues and volumes are available from the publisher. Claims for missing issues should be made within 6 months of publication.

© 1999 Éditions scientifiques et médicales Elsevier, Paris

En application de la loi du 1er juillet 1992, il est interdit de reproduire, même partiellement, la présente publication sans l'autorisation de l'éditeur ou du Centre français d'exploitation du droit de copie (20, rue des Grands-Augustins, 75006 Paris).
All rights reserved. No part of this publication may be translated, reproduced, stored in a retrieval system or transmitted in any form or by any other means, electronic, mechanical, photocopying, recording or otherwise, without prior permission of the publisher.

Imprimé en France par STEDI
1, bd Ney, 75018 Paris
Dépôt légal : 5719 – À parution

Président-directeur général et directeur de la publication : Catherine Lucet
Commission paritaire : 0103 T 78049
Périodicité: 6 nos / an

Acta Oecologica **20** (3) 133 / © Elsevier, Paris

Foreword

In many arid and semi-arid environments in the world, the landscape is spectacularly patterned with alternating stripes of dense vegetation and almost bare soil. These banded landscapes are found in biomes as diverse as grasslands, shrublands, woodlands and forests. Land use and the socio-political systems that utilise banded landscapes are almost as diverse. Their typical spatial structure, mainly related to noteworthy hydrological processes, invites the development of elegant models to describe their function and to conjecture about their origins. Studies of banded landscapes have developed from purely descriptive to causal processes summarised in mathematical models.

This special issue of *Acta Oecologica* treats ecological and biological aspects (plants, mesofauna, organic matter) of banded landscapes. Except for one 'Forum' contribution, the papers result from an international Symposium held in Paris in April 1996 under the auspices of the Orstom institute (now IRD) and the SALT research project (SAvana on the Long Term, one of the core projects of the IGBP programme). Papers presented at the symposium on physical and geochemical aspects have been assembled in a special issue of *Catena*, to be published in 1999. Most of the work on banded landscapes was originally carried out as isolated individual studies. The convergence of results is pleasing and a good reason to publish these papers together. Already the concepts of function/dysfunction in landscapes and the associated field methodologies developed in studying banded landscapes have been applied to other less overtly patterned landscapes with success. This issue should help in stimulating this extension.

David Tongway
'Gungahlin Homestead'
CSIRO Wildlife and Ecology
GPO Box 284, Canberra 2601 ACT, Australia

Josiane Seghieri
IRD
B.P. 5045
34032 Montpellier, France

Acta Oecologica **20** (3) (1999) 135–146 / © Elsevier, Paris

Banded vegetation patterning in a subantarctic forest of Tierra del Fuego, as an outcome of the interaction between wind and tree growth

Juan Puigdefábregas [a*], Francesc Gallart [b], Oscar Biaciotto [c], Mario Allogia [d], Gabriel del Barrio [a]

[a] *Estación Experimemental de Zonas Aridas (CSIC), General Segura 1, 04001 Almería, Spain.*
[b] *Instituto de Ciencias de la Tierra 'Jaume Almera'(CSIC), Marti i Franqués s/n, 08028 Barcelona, Spain.*
[c] *Centro Austral de Investigacion Cientifica (CONICET) Ushuaia, Argentina.*
[d] *Instituto Forestal Nacional Ushuaia, Argentina.*
* *Corresponding author (fax: +34 50 27 71 00; e-mail: puigdefa@eeza.csic.es)*

Received March 17, 1997; revised October 23, 1998; accepted November 12, 1998

Abstract — Banded patterns have been investigated in a *Nothofagus betuloides* primeval forest from Bahía del Buen Suceso, on the eastern edge of Tierra del Fuego island (Argentina). These forests grow on spodosols developed upon silicic shales, in a cold oceanic climate, with 5 °C mean annual temperature and 600 mm mean annual rainfall. Bands are oriented perpendicular to the prevailing wind direction, with older and dying trees in the windward edge and a seedling regrowth in the lee side of each band. Forest structure, species composition and relevant soil properties were sampled in a wind-affected forest and in an undisturbed stand. In the former, samples were obtained in transects across the banding and along a hill-slope gradient. Results show that wind causes about 50 % reduction of stand basal area and of size of overstorey trees. Stand growth processes, such as self-thinning, basal area and height growth, and specific composition of the understorey, occur in a windward direction, as well as changes in soil properties such as C/N ratio and redox potential increase. Based on field observations, we have developed an hypothesis of how wind is able to generate this pattern. Its core is that bands develop when vulnerability of trees to wind damage increases with age and with lack of protection from older windward trees. In such conditions, bands are the outcome of a tuning between tree growth rates and wind killing capacity. On the basis of this hypothesis, a simulation model, based on the cellular automata approach, was constructed. Simulated patterns that arise from heterogeneous forests with random age distributions match successfully with those observed in nature. Increasing tree growth rates lead to longer wavelengths and higher wave propagation rates, while increasing wind killing potential leads to shorter wavelengths and lower propagation rates. This interpretation of banded patterning involves a resonance between a directional disturbance and an oscillatory process, such as stand regeneration, growth and decay. © Elsevier, Paris

Banded spatial pattern / wind waves / subantarctic forest / *Nothofagus* / Patagonia / cell automata modelling / directional disturbances in ecosystems

1. INTRODUCTION

Wave regenerating forests, with stripes perpendicular to the direction of the prevailing wind, have been described in north-eastern United States [14, 16, 18] and in central Japan [11, 15]. Parallel dieback stripes travel slowly downwind giving place to a succession of regeneration phases that occur between them. Several factors have been cited as possible causes of such striped dieback, all related to wind effects such as winter desiccation, summer cooling, rime deposition and branch breakage [15].

The reported cases of wind wave regenerating forests are restricted to subalpine conifers [17], i.e. *Abies balsamea* in the United States and *A. veitchii* in Japan. Here, a case of striped forest is described for a new geographic region, the eastern part of Tierra del Fuego in South America, involving a broad-leaved tree species, *Nothofagus betuloides* (Fagaceae).

The maintenance of this striped pattern, once formed, has been explained in terms of a sharp increase of mortality once trees exceed a critical age [16, 18]. Nevertheless, the question of how such patterns are generated is still a topic of active research.

Are stripes initiated by linear discontinuities caused by disturbances or topographic features in the forest? Can they be generated by the effect of wind on an initial random patterned forest? One of us [7] showed that striped patterns could dynamically evolve from random patterns, using a very simple model in which wind-exposed trees had an increased probability of death as age increased. That model was a crude over-simplification of reality, because cells were supposed to be occupied by a single tree representing a cohort. Subsequently Sato and Iwasa [15] published another model to explain the central Japan case. It was based on a cellular-automata approach, which assumed that tree height grows at a constant rate, and that trees die if they are taller than their windward neighbours by a difference larger than a certain threshold. A series of additional rules were incorporated to make the model more robust and stable in producing two-dimensional patterns. This second model was also able to successfully generate stripes from initial random patterns, but it was still far from reality because its rigid deterministic structure and its assumption that trees, each representing a cohort, grow on sites arranged in a two-dimensional lattice.

In this work, a further step towards a more realistic model of wave regeneration systems is proposed by using ad hoc field information, and by managing the demographic evolution of cohorts across space. Forest responses to a range of parameter values are explored and simulation outputs are qualitatively compared to observed patterns in the field.

2. FIELD SITES AND METHODS

The study site is located in Bahia del Buen Suceso, in the eastern edge of the Isla Grande de Tierra del Fuego, Argentina (54°51'50'' S, 65°13'36'' W) (*figure 1*). The littoral eastern sector of the island is characterised by a cold, oceanic and windy climate [2, 5, 10, 13] with mean temperatures of 10 °C in February, 2 °C in August, and 5 °C round the year. Mean annual rainfall is around 600 mm, precipitation exceeds the atmospheric evaporative demand throughout the year and prevailing winds flow from the northwestern sector.

Bedrock is made mostly by silicic shales which, in conjunction with the cold and wet climate, facilitate the formation of stagnopodzols and peat soils in the valley bottoms and flat summit areas [3]. On hillslopes and well drained areas, podzolic soils are formed which support extensive evergreen forests, with a nearly mono-specific overstorey of *Nothofagus*

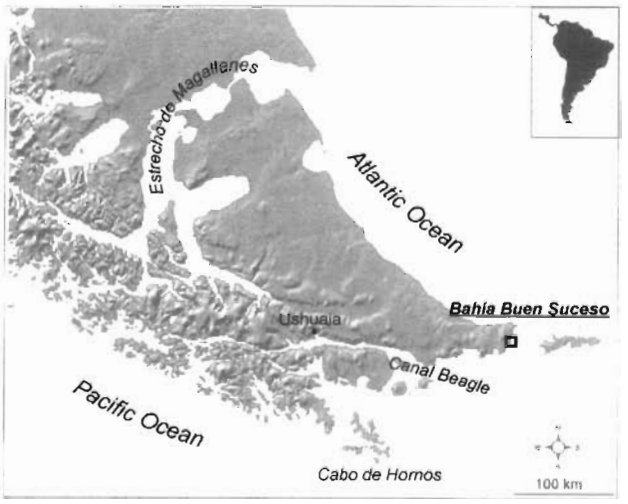

Figure 1. Location of the study area.

betuloides. Some small tree species, e.g. *Drymis winteri*, and in much smaller proportion, *Maytenus magellanica* and *Berberis ilicifolia*, are the main understorey components. Small deciduous patches of *Nothofagus antarctica* colonise the more extreme environments such as the fringes of peatbogs or areas exposed to strong winds.

Owing to inaccessibility by road, the landscape of the area is largely primeval and forest dynamics are mostly controlled by peat soil flows and wind. The former cause large strips where forest is peeled away downslope and new regeneration phases start again [8]. The latter causes a pattern of parallel stripes of regeneration waves perpendicular to the dominant wind direction. Regeneration waves often occur on northern exposed hill-slopes where prevailing northwestern winds can flow freely along.

Available aerial photographs from the Cartographic Service of Argentina, and an ad hoc helicopter survey allowed us to find suitable sites for field observation and provided images for contrasting simulation outputs (*figure 2*). A study site was selected on a hill-slope with altitude ranging between 20 and 340 m, a mean gradient of 40 % and a mostly north aspect. The sampling design consisted of three circular plots along a mature forest band adjacent to and downwind from a dieback stripe, and a transect across a whole regeneration wave. An additional circular plot was located on an east-facing hill-slope, protected from western wind, as a reference for undisturbed forest.

The three circular plots in the wind exposed hillslope were established at the low slope (LS), midslope

Figure 2. Low altitude photograph of wind regeneration waves in a *Nothofagus betuloides* forest of Bahia del Buen Suceso (Tierra del Fuego, Argentina). Prevailing wind blows from the right side of the image.

(MS) and upslope (US) sectors. Altitudes and gradients were 50, 120 and 235 m, and 21, 30 and 25 %, respectively. The undisturbed forest plot (UDF) was at an altitude of 75 m, with a slope gradient of 52 %.

All plots had a diameter of 20 m, except US, which was composed of four circular subplots with a 10-m diameter. In each plot, all stems larger than 5 cm in diameter at breast height (DBH) were tallied, their DBH measured and condition (dominant, codominant or suppressed; alive, senescent or dead) recorded. A small sample of three to five overstorey trees was selected for measuring total height and for extracting a core of wood for age estimation. Total lengths of the three regeneration waves downwind from each circular plot were measured at the three hill-slope sectors.

A transect was set up downwind from the midslope circular plot, stretching 125 m across the whole regeneration wave, from one dead front to the next. Along this transect, 25 contiguous rectangular plots of 5×10 m were established. The data recorded in each plot were equivalent to those obtained in the circular plots, with some additional information concerning litter, organic and top mineral layers of soil. Depth, pH, redox potential (rH) and temperature were measured in each layer, in a 0.5×2 m subquadrat at the centre of each plot, using portable electrodes and a temperature sensor. Samples were taken from the organic layer for laboratory C and N determination, using the Walkley and Black and Kjelldall methods, respectively.

3. THE SPATIAL PATTERN OF FOREST STRUCTURE

3.1. Field description of the regeneration wave system

The regeneration wave system displays a conspicuous pattern of parallel bands perpendicular to the direction of the prevailing wind. Immediately windward from a front of dead and senescent trees, there is an open field with young saplings that progressively changes windward to mature forest up to the next dieback front. The midslope transect that was sampled across this pattern provides quantitative information about forest structure and soil changes.

3.1.1. Spatial variation in the forest structure

Stand age shows a linear windward increase at a rate of 1.17 year·m^{-1} ($r = 0.806$, $P < 0.001$). The mature forest standing immediately leeward from the dead front has an age of 209 years at the stem base. The ordinate intercept (62 years), indicates that forest recruitment occurs in the floor of the previous mature phase and grows upward when the canopy becomes open following the death of large trees. This lag of circa 62 years between stand age and plot age counted from the dieback front, means that the period, or the time elapsed between two consecutive dead stripes in the sampled transect is of 147 years. As wavelength is 125 m, the dieback front is travelling downwind at a rate of 0.85 m·year^{-1}.

Canopy height shows a sigmoidal trend with time (*figure 3*). Once trees have reached the measurement

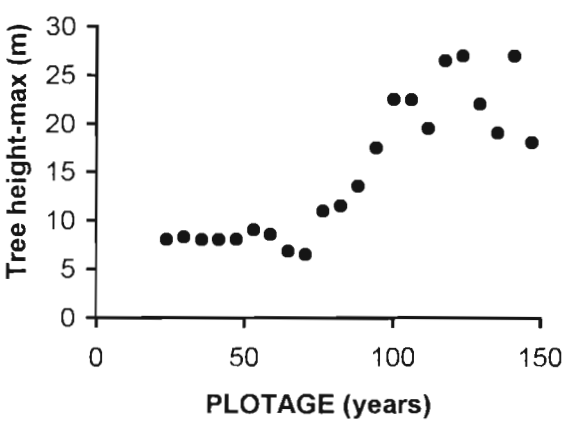

Figure 3. Plot of maximum tree heights, observed in 50-m^2 quadrats, versus elapsed time from the dieback front (PLOTAGE) along a regeneration wave in midslope position.

threshold of 5 cm DBH, at some 20 years elapsed from the dead front, maximum heights grow slowly from 8 to 10 m during the next 60 years. During the following 40 years, trees grow faster to reach heights between 20 and 25 m at 120 years after the dieback front. Thereafter, maximum heights become more variable, but on average, they maintain height or even decline.

Stem basal area of *N. betuloides* (*figure 4*) grows windward from the dieback zone up to maximum values of around 90 $m^2 \cdot ha^{-1}$ at a plot age of 100–120 years and thereafter, it declines steadily to the next dead front while the proportion of senescent and dead trees increases. During the initial phases of stand growth, up to 60–70 years after the dead front, large scattered dead trees of the previous wave share a large proportion of the total stem basal area.

D. winteri shows a pattern of stem basal area out of phase with that of *N. betuloides* and somewhat advanced to it (*figure 4*). Maximum values of around 40 $m^2 \cdot ha^{-1}$ occur at 70–80 years after the dieback zone. Thereafter, stem basal area of *D. winteri* declines and virtually disappears at the peak phase of *N. betuloides*. In mature stands, when the overstorey begins to open, recruitment of *D. winteri* starts again.

In the case of *N. betuloides*, the density of stems larger than 5 cm DBH reaches a maximum at 60 years windward from the dead front (*figure 5*). Before this time, the regrowth has not yet reached the measurement threshold of 5 cm DBH. This maximum density at 60 year plot age and around 120 year stand age is very high (around 9 000 stems·ha^{-1}), and it declines exponentially with a coefficient of –0.036 89 to 387 stems·ha^{-1} in mature stands leeward of the dieback zone.

The increase in stem basal area together with the parallel decline in stand density are the outcomes of a biomass redistribution process. A larger proportion of the latter is progressively shared by fewer and bigger individuals. This trend is described by the ratio of stem basal area to stand density, the basal area of the average tree, that may also be expressed as a DBH (DBHm). DBHm grows exponentially with time, reaching values of 30 cm in mature stands leeward of the dieback zone, at 147 years plot age and 209 years stand age. The equation which describes this trend is:

$$DBHm = 5.1418 \times \exp(0.0128 \times PLOTAGE)$$

$$r = 0.878,\ P < 0.001$$

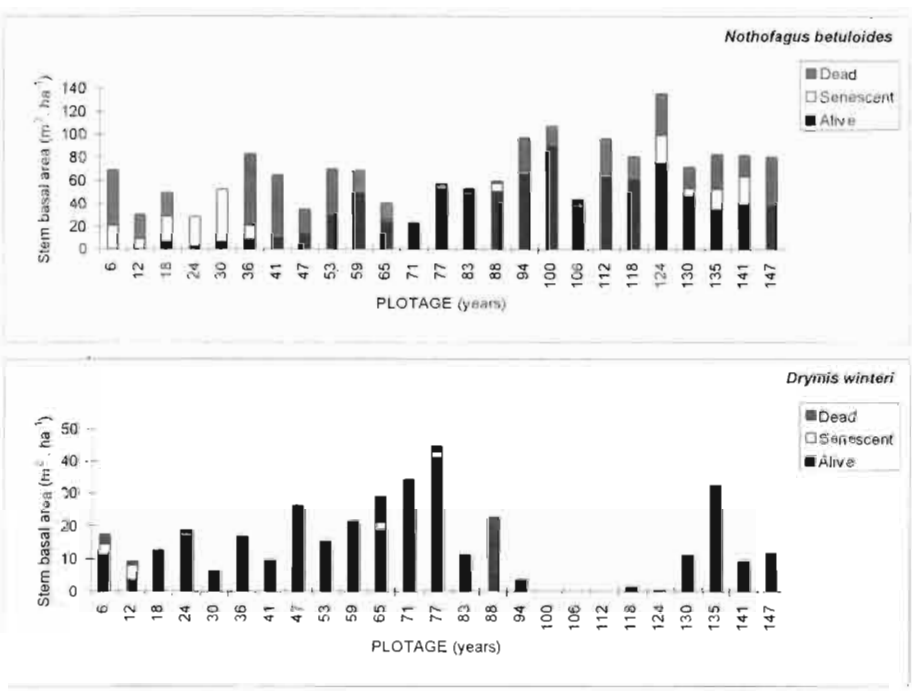

Figure 4. Trends of stem basal area with time elapsed from the dieback front (PLOTAGE) along the sampled regeneration wave. Waves are travelling from the right to the left. dead, Dead stems; sen, senescent stems; alive, live stems.

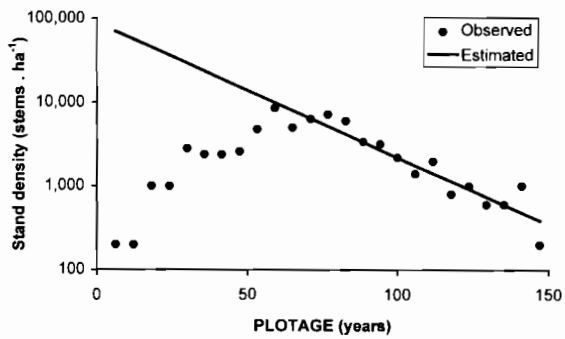

Figure 5. Trend of *N. betuloides* stand density with time elapsed from the dieback front (PLOTAGE) across the sampled regeneration wave. Fitted curve: stand density = 87 680 × exp (–0.036 89 × PLOTAGE); $r = 0.947$; $P < 0.001$.

3.1.2. Changes in soil properties

Only three out of all the soil attributes recorded at the organic and upper mineral horizon showed a significant trend with the time elapsed from the last dieback zone (*table I*). The three were concerned with the mineral horizon (A_h layer). N content, relative to soil dry weight, declined at a rate of –0.0016 %·year^{-1}. As soil organic matter became impoverished in N, C/N ratio increased from 22 to 30, at a rate of 0.0536 year^{-1}. Coincidentally, oxidation conditions at the top soil became enhanced and the redox potential (rH) increased from 271 to 355 mV, at a rate of 0.65 mV·year^{-1}.

3.2. Changes of the forest structure along hill-slopes and in undisturbed conditions

The largest structural differences in mature stands leeward of the dieback zone are found between the upper hill-slope stands and those from middle or lower sectors (*table II*). Differences between the latter two are slight and cannot be considered significant. Mature upslope stands lack *D. winteri* in the understorey, they are 3-fold denser and trees are also around three times smaller than those located downslope. On the contrary, stem basal areas and stand ages are of the same order as those in downslope stands.

Wavelengths are rather variable because they are influenced by hill-slope local topography. Measured wavelengths at the sampled stands, which are located in the most regular hill-slope sector, showed an upwards decrease ranging from 150 m at the foot-slope to 60 m in the upper-slope.

Compared to mature stands in the wind-affected hill-slope, the undisturbed mature stand, sampled in a wind-protected slope, showed a much greater stem basal area (× 2) and a larger mean tree diameter (× 1.3). Its *D. winteri* population consisted of larger individuals than in mature stands of the wave regeneration system. *D. winteri* stem basal area was within the same range of values in both cases, but density was four to five times lower in the undisturbed mature stand. Surprisingly, the latter did not show a higher canopy nor a lower stem density of *N. betuloides*.

4. DISCUSSION OF FIELD RESULTS

4.1. Causes of regeneration waves

The interpretation that the studied regeneration wave system is caused by wind relies not only on morphological comparisons with published references [15, 16, 18] but also on other field evidence. First, these forest patterns are observed in north-easterly exposed hill-slopes that lay parallel to the prevailing north-western wind. Secondly, undisturbed

Table I. Pearson correlation matrix of top soil properties and PLOTAGE (time elapsed from the last dieback front). org, Organic layer; min, upper mineral layer; LITD, litter depth; ORGD, depth of the organic layer ($n = 22$; $P < 0.05 = 0.404$; $P < 0.005 = 0.537$; $P < 0.001 = 0.652$).

	PLOTAGE	C	N	C/N	pH (org)	pH (min)	rH (org)	rH (min)	LITD
PLOTAGE	1								
C	0.11	1							
N	**–0.48**	0.35	1						
C/N	**0.47**	**0.44**	**–0.42**	1					
pH (org)	–0.39	–0.33	–0.06	–0.38	1				
pH (min)	0.21	**–0.54**	**–0.40**	–0.07	0.40	1			
rH (org)	**0.70**	0.08	–0.32	0.36	–0.25	–0.15	1		
rH (min)	0.31	0.16	–0.20	0.08	0.16	–0.10	**0.57**	1	
LITD	–0.35	–0.10	–0.08	–0.02	–0.01	–0.10	–0.34	**–0.48**	1
ORGD	–0.28	–0.01	0.11	–0.20	–0.25	–0.08	–0.32	–0.18	**0.60**

Table II. Forest structure of mature stands of *Nothofagus betuloides* at Bahia del Buen Suceso (Tierra del Fuego, Argentina). UDF, Undisturbed forest; US, upper slope sector; MS, midslope sector; LS, lower slope sector; SBA, stem basal area; DENS, density of stems; DBHm, diameter at breast height of the average tree; HEIGHT DOM/COD, canopy height of dominant and co-dominant trees; SBADEAD, stem basal area of dead stems; DENSDEAD, density of dead stems; AGEm, mean age of sampled dominant and co-dominant trees; PLOTAGE, time elapsed from the last dieback front; WAVE PROP RATE, wave propagation rate; nd, no data; brackets, 1 SE.

	UDF	US	MS	LS
Nothofagus betuloides				
SBA (m^2·ha)	97	45	52	44
DENS (n·ha)	700	1 623	600	541
DBHm (cm)	42	19	33	32
HEIGHT DOM/COD (m)	19/0.28	7.4/0.27	21/2.3	18/1.47
SBADEAD (m^2·ha)	8	24	27	32
DENSDEAD (n·ha)	255	1 560	650	987
AGEm (1.3 m) (year)	nd	168 (17)	192 (33)	184 (24)
PLOTAGE (year)	165	137	147	153
WAVELENGTH (m)	–	60	125	150
WAVE PROP RATE ($m \cdot year^{-1}$)	–	0.4	0.8	1
Drymis winteri				
SBA (m^2·ha)	11	0	15	12
DENS (n·ha)	637	0	2 400	2 897
SBADEAD (m^2·ha)	1.33	0	0.72	0.17
DENSDEAD (n·ha)	95	0	150	64

forest patches are restricted to south-easterly exposed hill-slopes, leeward of the wind and outside the tracks of peat soil flows. Thirdly, dieback zones are always on the windward side of the regeneration waves.

One of the main hypotheses describing key factors involved in wind-induced tree dieback is winter desiccation of canopies. This factor has already been claimed by Sato and Iwasa [15] and it is supported by the subalpine location of the two previously reported cases in Japan [11] and United States [16]. In the subantarctic climate of south-eastern Tierra del Fuego, soil freezing is rare, but soil temperatures remain between 0 and 1 °C during long periods [6]. Conductances to water flow through the plant are known to be dramatically lowered when roots reach such temperatures [9]. Loss of foliage by wind abrasion and root breakage by stem swaying and subsequent infection by parasitic root fungi have also been suggested as a possible cause of tree dieback associated to wind [12].

Mechanical wind damage to branches is not likely to cause regeneration waves because no evidence thereof was observed in tree crowns. Moreover, intense wind storms would cause a more irregular pattern with patches of fallen trees and broken stems. A continuous and additive effect of long-lasting or continuous wind flow is also to be discarded because this would produce adaptations in the canopy architecture that probably start at young tree ages. This is the case of flagged crowns and prostrate trees in the littoral or high altitude timberlines.

Initially, field observations in the study area suggested some connection between regeneration waves and peat flows. Linear discontinuities created by peat flow tracks in forest canopies would act as a permanent trigger of dieback front waves. However, further evidence did not support this view and we turned to the alternative hypothesis, also raised by Gallart [7] and Sato and Iwasa [15], that regeneration waves could result solely from the effect of wind acting on a spatially heterogeneous forest. This hypothesis assumes that trees, after reaching a height threshold, are subject to increased probability of death if they lack protection from larger neighbours windward of them. It is thought that this process, if maintained long enough, is able to yield regeneration waves. A cluster of trees produces a cone-shaped wind shadow that protects a larger cluster leeward, this process being repeated and enlarged through a positive feedback mechanism.

4.2. Changes of forest structure and soil along the regeneration wave

DBHm-PLOTAGE curves obtained from the wind-disturbed forest sample, where PLOTAGE is the time elapsed since the dieback, enabled the estimation of a comparable age for the undisturbed stand as 165 years

(*table II*). The corresponding estimate of the forest band just leeward of the dieback front in the sampled wave transect was 147 years, which is 89 % of the undisturbed stand estimate. Wind does not appear to affect mature stand ages significantly. However, mean stem density just leeward of the dead front in the sampled wave (387 stems·ha^{-1}) was only 55 % of the density found in undisturbed forest (*table II*).

Such differences in age-density proportions allow an estimate to be made of the change in the mortality or exponential decay coefficient, by assuming the same equation and ordinate intercept value for both disturbed and undisturbed conditions. This is not unrealistic because the initial density of saplings is not likely to be affected by wind. In this way, it is estimated that mortality coefficients in undisturbed and wind-disturbed conditions are 0.029 35 and 0.036 89, respectively. This means a 25 % increase in mortality in wind-affected forest.

Observed values of stem density and basal area in juvenile stands (around 100 years plot age) are extremely high (9 000 and 90 m^2·ha^{-1}, respectively). Similar values were found elsewhere in *N. pumilio* [1] and they are interpreted as a forest adaptation to the risk of paludification or soil swamping and blanket bog development. By building up as quickly as possible an efficient transpiring system that ensures soil drainage, paludification is avoided. Maturation of forest stands leads to a redistribution of basal area in a smaller number of big trees.

Understorey changes along the regeneration wave are controlled by the strong competition that occurs during the intermediate stage of the overstorey regeneration. High tree densities and stem basal areas exclude understorey shrubs and force *D. winteri* to advance its seedling phase as soon as the *N. betuloides* canopy starts to break down. In this way, maxima of the stem basal area in the understorey occur before those of the overstorey.

Topsoil changes along the regeneration wave concern redox potential values and C/N ratios. The former may be interpreted as an effect of the progressive drainage of the upper soil layers by the growing stand. The second is the result of leaf litter input from the growing *N. betuloides* canopy, whose leaves are sclerophyllous, slowly decomposing and have large C/N ratio [6]. Herbs and grasses (*Gunnera* sp., *Luzuriaga* sp., *Senecio* sp. and *Carex* sp.), which could supply litter with lower C/N ratio, are progressively excluded and, once the high density stage has been established, only lichens and bryophytes remain in the ground layer.

4.3. Changes of the wave regeneration system along hill-slopes

The lower travelling velocity of regeneration waves in the upper slope sectors may be explained by denser mature stands with smaller trees than in downhill stands and therefore also requiring more time to die.

The decrease in tree height along the altitudinal gradient in hill-slopes has also been reported in other Fueguian forests [1]. One of the main factors that may cause stunted trees in the upper slope sectors is the temperature decrease with altitude. As mean summer temperatures are already low (8 °C at sea level), a gradient of –0.005 °C·m^{-1} means a temperature of 6.5 °C at 300 m altitude in the upper hill-slope sector. This is already a critical summer temperature for tree growth, not far from the 5–6 °C which have been estimated for the timberline in the area [4].

5. MODELLING THE WAVE REGENERATION SYSTEM

Based on these field observations, we propose a set of simple hypotheses to explain the generation and dynamic persistence of striped patterns in forests. The main assumption is that trees that have grown protected from wind by taller windward neighbours, after being suddenly exposed by dieback of the latter, suffer increased probability of death, and are finally killed by wind. Field observations also suggest that banded patterns are not triggered by linear discontinuities in the forest, but rather result from an initially random distribution of ages, and a subsequent spatial synchronisation of the regeneration, maturation and senescence phases of the forest.

This hypothesis is formalised in a system structure and a model which describes its behaviour. Simulation outputs using this model allow the above-mentioned hypothesis to be tested. A qualitative contrast with field observed patterns will help to strengthen the consistency of the proposed structure.

The model assumes that a forest grows in a two-dimensional space, divided in square cells or plots. Each cell supports a cohort of trees which declines by self-thinning according to the exponential decay curve: $DENS_t = DENS_0 \exp(-k \times t)$, where $DENS_0$ and $DENS_t$ are densities at time 0 and t, while k is a mortality coefficient which is converted to a yearly intrinsic death probability IDP, as $IDP = 1 - \exp(-k)$, and added with a random factor. Once self-thinning has been applied, a wind dieback factor (WDF) comes into operation. This factor depends on a protection factor (PF) from windward neighbours, on the age of

the cohort and on the number of trees that can be killed in one iteration.

The protection factor is calculated as a sum of four scores produced by the three adjacent windward cells, one straight forward, the two side diagonals, and a fourth one straight forward in the second row windward. If one of these cells is occupied by at least one tree, and its cohort is older that the target cell cohort, its score is 1, except the two rows windward cell, which scores 0.5. If cohorts in windward cells are younger than those in the target one, their score is 0. In each case, the total score is brought to the range 0–1, by expressing it as a ratio to the maximum possible value which is 3.5. The age factor (AF) is introduced as a linear function that varies between 0 and 1, when the cohort is 1-year-old or has reached the age (AMAX) at which wind will kill the trees if they are exposed. AMAX is therefore a parameter that expresses the inverse of wind killing capacity.

NTREE is the maximum number of trees that can be killed by wind in a single iteration. It is a scaling and tuning factor to adjust wind killing capacity to the cell dimension and self-thinning coefficient chosen in each run.

The global wind dieback factor (WDF) is then calculated as a product:

$$WDF = PF \times AF \times NTREE$$

WDF score, rounded to the nearest integer value, yields the number of trees killed in each cell, at each iteration, in addition to the self-thinning ageing mortality. WDF may therefore take integer values ranging between 0 and NTREE.

Each run is initialised by distributing cohorts in the simulation field in which age varies at random between 0 and 50 years. This upper limit for age is adopted in order to provide cohorts with some initial resistance to wind. Otherwise, the presence of old stands from the start easily produces artefacts. This assumption is realistic because wind action is not expected to start suddenly on an already developed forest, but rather to precede the forest occupation of a given area.

In order to simulate variations of wind effect along hill-slopes, an option is provided in which parameters can change in a linear way between extreme values that are set at the left and right sides of the simulation field.

6. RESPONSES OF THE REGENERATION WAVE SYSTEM TO PARAMETER CHANGES

The above-described model has four parameters: $DENS_0$, tree density in terms of number of trees per cell at starting regeneration; IDP, yearly intrinsic death probability in undisturbed conditions; AMAX, age at which a tree may be killed if exposed to wind; and NTREE, maximum number of trees that can be killed by wind in each cell at each iteration.

Field information provides a basis for setting realistic values to these parameters. Starting density is set at 87 680 individuals·ha^{-1}, as obtained from the empirical density-age curve (*figure 5*). It has to be noted that this initial density is considered at the so-called PLOTAGE = 0. That means that time starts to be counted for ageing and height increments when overstorey trees have died out. $DENS_0$ acts as a scale factor because it sets the cell dimension. For this simulation survey, a cell size of 30 m^2 has been adopted, resulting in 263 saplings per cell in starting regeneration cells.

IDP was set at 0.03, a value close to the field estimate for undisturbed stand which was 0.029. AMAX was set at 150, also close to the field record of wave period or time elapsed between two consecutive dead fronts. NTREE was set at a value of 2 per iteration, which is the approximate number of trees per cell in mature stands leeward of dead stripes in midslope and foot-slope positions.

6.1. Exploring responses to parameter changes

A survey was made on the system responses to changing values of the two parameters IDP and AMAX. In both cases, parameter values were allowed to vary in a range of ± 50 % around the baseline values indicated above. In each run, a total of 3 000 iterations were performed. Images of the resulting outputs are shown in *figures 6* and *7*.

Results show that bands perpendicular to wind direction are formed, in patterns similar to regeneration waves observed in the field. Output images show also that there is a fetch or critical length that is needed to start the formation of bands.

Simulation outputs show that decreasing IDP values lead to shorter wavelengths and older trees in the wind exposed mature stripes (*figure 6*). IDP changes are linked to site productivity changes, because in fertile sites, trees develop faster, intra-cohort competition for light is stronger and therefore, self-thinning and IDP are also larger. This means that stands in less productive sites attain maturity with higher densities than

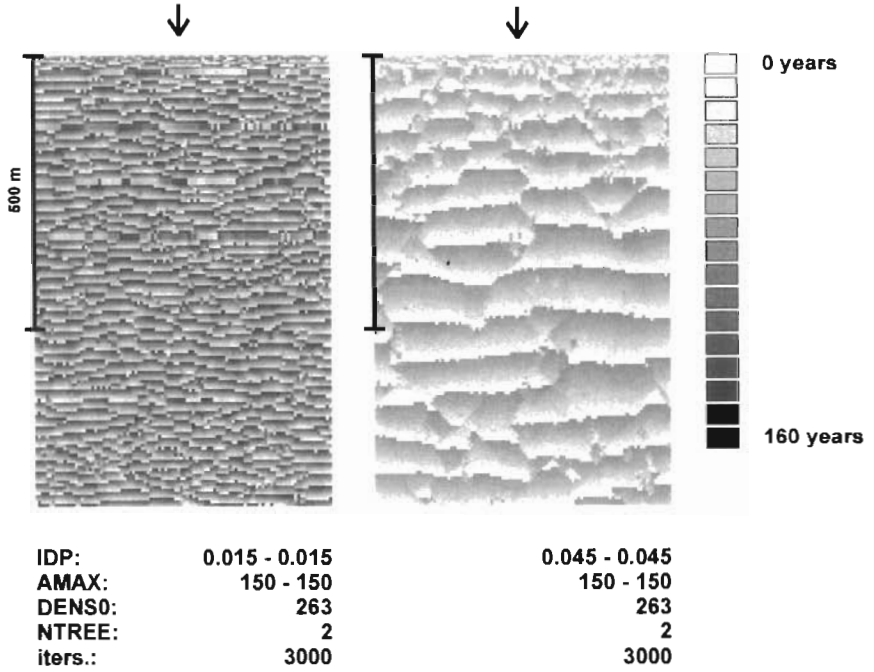

Figure 6. Simulation output showing the effect of changing intrinsic death probability (IDP) on wavelengths and age distribution of wave regeneration systems. The grey tone scale represents the ages of the cohorts in each pixel. Waves propagate downwind, from the top to the bottom of the figures. IDP may be considered as a surrogate of the site productivity. Values of the parameters are shown at the bottom of each image. AMAX, Age at which trees may be killed by wind; $DENS_0$, number of trees per pixel at starting regeneration; NTREE, maximum number of trees that can be killed by wind in each pixel at each iteration; iters., number of iterations. For IDP and AMAX, the values set at the right and left hand of the images are supplied.

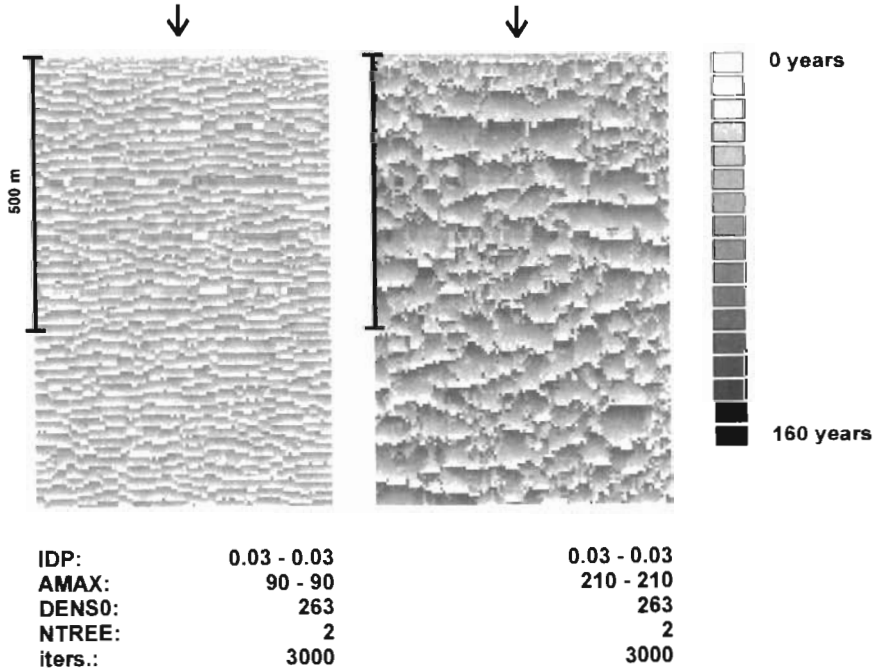

Figure 7. Simulation output showing the effect of changing wind killing capacity on wavelengths and age distribution of the wave regeneration system. The grey tone scale represents the ages of the cohorts in each pixel. Wind killing capacity is expressed by the inverse of AMAX, the age at which trees may be affected by wind, and it is higher at lower AMAX values. Waves propagate downwind, from the top to the bottom of figures. Abbreviations as in *figure 6*.

those of more productive ones. Consequently, even with the same wind dieback factor (WDF), killing the trees of an exposed cell takes more time in less productive sites, where wave systems are expected to travel more slowly, as shown by their shorter wavelengths and older ages of mature stands.

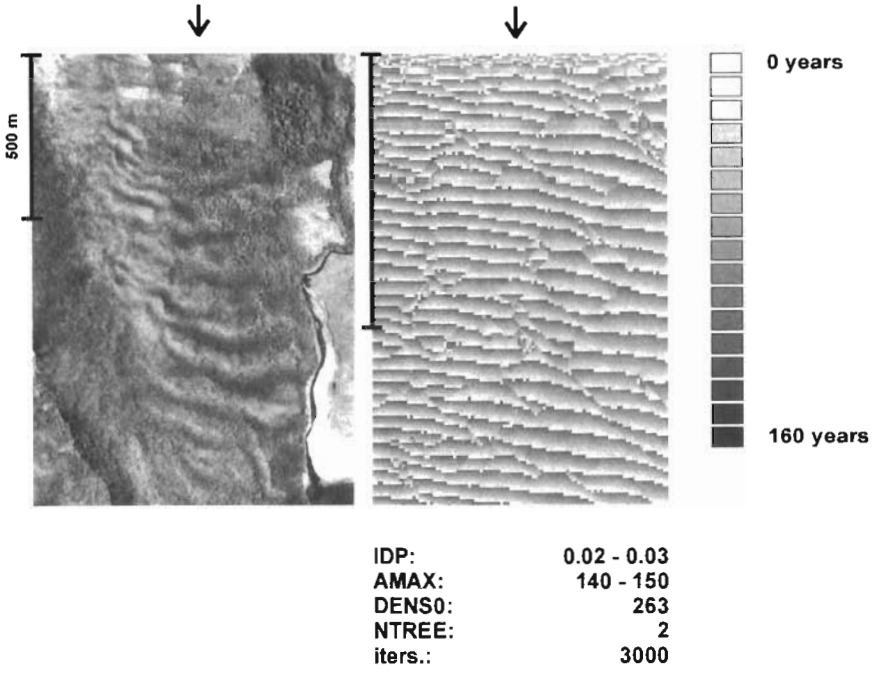

Figure 8. Field (left) and simulation (right) comparison of the hill-slope effect on wave regeneration patterns. The system propagates downwind from the top to the bottom. In both cases, upper hill-slope is on the left and lower hill-slope on the right. Values of the parameters are shown at the bottom of the simulation image. IDP (intrinsic death probability) and AMAX (age at which trees may be killed by wind) change from left to right, and they can be taken as surrogates of site productivity and wind killing capacity, respectively. The grey tone scale represents the ages of the cohorts in each pixel. The image on the left is an aerial photograph of the studied north-exposed hill-slope at Bahía del Buen Suceso (Tierra del Fuego, Argentina). Abbreviations as in *figure 6*.

Decreasing AMAX is a way to increase wind killing potential by increasing WDF. The resulting pattern (*figure 7*) shows younger forest stripes exposed to wind, shorter wavelengths and, therefore, slower motion of the wave system. A larger WDF means that forest stands are exposed to wind at younger stages but still keeping high densities, because self-thinning did not operate during long periods. Therefore, killing the trees of an exposed cell takes more time than with large AMAX values, and resulting wavelengths are shorter.

6.2. Qualitative contrast with field observations

The wind dieback factor (WDF) has not been fully parametrised with field data and therefore, at this stage, the model does not provide simulation outputs that can be quantitatively compared with reality, particularly for band dimensions. However, relative changes of WDF across the land can be reproduced reasonably well, allowing qualitative comparisons between field and simulated patterns, as shown in *figure 8*.

The field pattern image was obtained from an aerial photograph of the studied hill-slope, where altitudes range from 20 to 340 m. In the western sector of the hill-slope (upper part of the image), the forest has been completely stripped off by peat soil flows. The simulated pattern was obtained by using parameter values similar to those observed in the real hill-slope. For this purpose, IDP and AMAX values were changed laterally across the simulation field. In both images, wind flow comes from the west (top).

Upper hill-slope IDP value was estimated at 0.02, assuming that it changes with altitude at the same rate as observed total mortalities in the sampled stands. Field information shows that ages of stands next to dieback front are slightly lower in the upper than in lower hill-slope sectors, although differences are hardly significant. Therefore, upper hill-slope AMAX was rated only 10 years younger than the lower hill-slope one.

Simulated and real images show that regeneration waves are wider and travel faster in the downslope sector. For this reason, the overall pattern appears down-curved in the right side of both images. The existence of a fetch can also be appreciated in the top of the images, where the most windward sector of the forest is located. The fetch feature demonstrates that dieback fronts caused by wind acting from linear disturbances or accidents cannot start a wave system. Dead fronts so initiated are quickly absorbed by the existing heterogeneity of the downwind forest structure, and they can only progress if an existing wave pattern catches and transmits them forward.

In the image of the real situation, bands do not reach the uppermost hill-slope. Instead, small tree islands and irregular features are observed. Near to the water divide, wind velocity increases and becomes more

persistent. In such conditions, trees are exposed to wind since their youth, and their crowns adopt a variety of adaptive architectures that increase their survival probability. Wind protection is dependent on the local existence of wind-adapted individuals and, therefore, spatial patterns are less regular and bands are no longer formed. The proposed model is not able to reproduce such local features because individual adaptive processes are not included in it.

7. CONCLUSIONS

Field observations on wave regeneration patterns from a subantarctic forest of *Nothofagus betuloides* in eastern Tierra del Fuego show that wind action is the main controlling factor. Compared to undisturbed forest stands, the most mature stages of wind-affected forests show a significant reduction of stem basal area. Across the regeneration waves, growth and decay phases occur, together with self-thinning, biomass redistribution, and temporary exclusion of the understorey, which is mainly composed of *Drymis winteri*. Some topsoil properties, such as C/N ratio and redox potential, increase across the regeneration wave, during the growth of the stand. Field evidence suggests that banded patterns arise dynamically as a consequence of the formation of a circular sector, leeward of each tree, where younger trees can grow protected from wind.

A model has been proposed to explore the consistency of this hypothesis by comparing the variation of simulated patterns, as a response to changes of key factors and parameters, with those observed in nature. The model incorporates some demographic processes and is therefore able to simulate real situations observed on hill-slopes.

Some assumptions of the model are as follows. The relationship between tree height and age is supposed to be linear, while field results show a logistic trend. Any younger stand windward means unprotection, and no threshold is considered for such age differential. Tree resistance of a tree suddenly exposed to wind damage decreases linearly with age. Wind protection is independent of tree density of windward stands. Despite these over-simplifications, simulation outputs qualitatively match field observations.

The model predicts that larger tree growth rates lead to longer wavelengths and higher propagation rates, while an increase of wind killing capacity leads to shorter wavelengths and lower propagation rates. This is supported by field observations according to which in upper slope sectors with lower growth rates and higher wind intensity, wavelengths are shorter than in foot-slope situations.

Therefore, wave regeneration patterns would be the outcome of a resonance between tree growth-decay cycles and wind killing capacity, and might arise by wind action on an initial forest with random age distribution. This case suggests a more formal research on how anisotropy may result from the interaction between a vectorial process and an initially isotropic system.

Acknowledgments

This work was funded by the CONICET (Argentina) / CSIC (Spain) Convention and the SUBANTARCTIS Project (CONICET). The support from both programmes is gratefully acknowledged.

REFERENCES

[1] Allogia M., del Barrio G., Bianciotto O., Ferrés L., Gallart F., Puigdefábregas J., Efectos de los aludes sobre la dinámica del bosque de *Nothofagus betuloides*, in: Puigdefábregas J., García-Novo F., Frangi J., Vila A. (Eds.), Los Sistemas Naturales Subantárticos y su Ocupación Humana, CSIC, Madrid, 1999, in press.

[2] Burgos J.J., Clima del extremo sur de Suramérica, in: Boelcke O., Moore D.M., Roig F.A. (Eds.), Transecta Botánica de la Patagonia Austral 2, CONICET-Royal Society-Instituto de la Patagonia, Chile, 1985, pp. 10–40.

[3] Cabaneiro A., Solé A., Bianciotto O., Puigdefábregas J., Formación y evolución de suelos en los principales sistemas forestales del sector oriental de Tierra del Fuego, in: Puigdefábregas J., García-Novo F., Frangi J., Vila A. (Eds.), La Tierra del Fuego: Los Sistemas Naturales y su Ocupación Humana, CSIC, Madrid, 1999, in press.

[4] del Barrio G., Puigdefábregas J., Iturraspe R., Régimen térmico estacional en un ambiente montañoso de Tierra del Fuego, con especial atención al límite superior del bosque, Pirineos 132 (1988) 137–148.

[5] Etchevere P.H., Maczynski C.R.O., Los Suelos de Tierra del Fuego, INTA, Buenos Aires, 1963, 25 p.

[6] Frangi J.L., Richter L.L., Estructura y función de ecosistemas forestales fueguinos, in: Puigdefábregas J., García-Novo F., Frangi J., Vila A. (Eds.), La Tierra del Fuego: Los Sistemas Naturales y su Ocupación Humana, CSIC, Madrid, 1999, in press.

[7] Gallart F., Algunos ejemplos de utilización de técnicas de simulación en geomorfología, in: Gutierrez M., Peña J.L., Lozano M.V. (Eds.), Actas de la I Reunión Nacional de Geomorfología, vol. 2, Instituto de Estudios Turolenses, Teruel, Spain, 1990, pp. 773–787.

[8] Gallart F., Clotet-Perarnau N., Bianciotto O., Puigdefábregas J., Peat soil flows in Bahia del Buen Suceso, Tierra del Fuego (Argentina), Geomorphology 9 (1994) 235–241.

[9] Hinckley T.M., Goldstein G.H., Meinzer F., Teskey R.O., Environmental constraints at arctic, temperate-maritime and tropical treelines, in: Turner H., Tranquillini W. (Eds.), Establishment and Tending of Subalpine Forest: Research and Management, Rapports Institut Fédéral de Recherches Forestières n° 270, Birmensdorf, Switzerland, 1985, pp. 21–30.

[10] Iturraspe R., Sottini R., Schroeder C., Escobar J., Generación de información hidroclimática en Tierra del Fuego. Hidrología y Variables Climáticas del Territorio de Tierra del Fuego, Información básica, CONICET-CADIC, Contribución Científica n° 7, Ushuaia, Argentina, 1989, pp. 4–170.

[11] Kohyama T., Etiology of 'Shigamare' dieback and regeneration in subalpine *Abies* forests of Japan, GeoJournal 17 (1988) 201–209.

[12] Marchand P.J., Goulet F.L., Wave mortality in subalpine forest ecosystems with particular reference to foliage and root attrition in *Abies balsamea*, White Mountains, New Hampshire (USA), in: Turner H., Tranquillini W. (Eds.), Establishment and Tending of Subalpine Forest: Research and Management, Rapports Institut Fédéral de Recherches Forestières n° 270, Birmensdorf, Switzerland, 1985, pp. 173–177.

[13] Prohaska F., The climate of Argentina, Paraguay and Uruguay, in: Schwerdtfeger W. (Ed.), Climates of Central and South America. World Survey of Climatology, vol. 2, Elsevier Scientific Publishers, 1976, pp. 13–112.

[14] Reiners W.H., Lang G.E., Vegetational patterns and processes in the balsam fir zone, White Mountains, New Hampshire, Ecology 60 (1979) 403–417.

[15] Sato K., Iwasa Y., Modeling of wave regeneration in subalpine *Abies* forests: Population dynamics with spatial structure, Ecology 74 (1993) 1538–1550.

[16] Sprugel D.G., Dynamic structure of wave regenerated *Abies balsamea* forests in the north-eastern United States, J. Ecol. 64 (1976) 889–911.

[17] Sprugel D.C., Characteristics, causes and consequences of wave regeneration in high-altitude forests, in: Turner H., Tranquillini W. (Eds.), Establishment and Tending of Subalpine Forest: Research and Management, Rapports Institut Fédéral de Recherches Forestières n° 270, Birmensdorf, Switzerland, 1985, pp. 179–188.

[18] Sprugel D.G., Bormann F.H., Natural disturbance and the steady state in high altitude balsam fir forests, Science 211 (1981) 390–393.

Acta Oecologica **20** (3) (1999) 147–158 / © Elsevier, Paris

The influence of vegetation pattern on the productivity, diversity and stability of vegetation: The case of 'brousse tigrée' in the Sahel

Pierre Hiernaux [a*], Bruno Gérard [b]

[a] *International Livestock Research Institute (ILRI), ICRISAT, B.P. 12404 Niamey, Niger.*
[b] *International Crop Research Institute for the Semi-Arid Tropics (ICRISAT), ICRISAT, B.P. 12404 Niamey, Niger.*
* *Corresponding author (fax: +227 75 22 08; e-mail: p.hiernaux@cgiar.org)*

Received March 17, 1997; revised November 10, 1998; accepted November 12, 1998

Abstract — Sample sites of 'brousse tigrée' and related vegetation types are described for Mali and Niger. Species composition and physical structure of the herbaceous layer as well as woody plant population were recorded at all sites together with data on soils and natural resource management. Herbage yield was measured whereas foliage yield and wood mass were calculated using allometry equation calibrated for each species. 'Brousse tigrée' is characterized by the regularly alternating bare-soil stripes with dense linear thickets arranged perpendicularly to the slope. There was no clear superiority in total plant production of 'brousse tigrée' when compared to neighbouring site with diffuse vegetation. However, the pattern of 'brousse tigrée' tended to favour woody plant yield to the detriment of herbage yield. The number of herbaceous species recorded per site (22–26) was slightly above Sahelian vegetation average despite low number of species per 1-m^2 quadrat (6–9), bare soil excluded. This species richness reflects the diversity in edaphic niches resulting from the redistribution and local concentration of water resources and shade. The high spatial heterogeneity and species richness of the herbaceous layer in 'brousse tigrée' did not attenuate the interannual variation in herbage yield despite low yields. Except for the herb layer, little evidence was found of grazing influence on the vegetation structure and yield a few hundred metres away from livestock concentration points. On the other hand, the clearing of thickets for cropping led to severe soil erosion which threaten the resilience of 'brousse tigrée'. These observations and the well-defined climatic, soil and topographic situations under which the 'brousse tigrée' occurs invalidate the hypothesis of an anthropic origin of that vegetation pattern. © Elsevier, Paris

Vegetation pattern / patchiness / diversity / herbage yield / wood mass / vegetation dynamics / Sahel

1. INTRODUCTION

'Brousse tigrée' differs from other Sahelian vegetation types by the dominance of woody plants and a pattern characterized by the regularly alternating bare soil stripes with linear and dense thickets (*figure 1*). The bare stripes act as impluvium for the thickets which are linear shaped following the contours. 'Brousse tigrée' develops naturally in the Sahel between the isohyets 400 and 600 mm on poorly permeable soils, often composed of a very thin silty horizon that caps the bedrock or an indurated pan, located on uniform and very gentle slopes [10]. Variants of 'brousse tigrée' have been distinguished based on pattern characteristics such as width and shape of the thickets and bare stripes [2] and on the dominant woody species [17]. Locally, the vegetation pattern can range from uniform 'diffuse scrub' to well patterned 'brousse tigrée' of variable impluvium and thickets width, all with similar woody species composition. Neighbouring sites with diffuse scrub and 'brousse tigrée' sampled in Mali and Niger were analysed to test the following hypotheses: higher spatial heterogeneity of the vegetation pattern increases: 1) vegetation diversity; 2) vegetation productivity [21]; 3) higher spatial heterogeneity and species diversity of the herbaceous layer attenuate interannual fluctuations in herbage yields [1, 26]; 4) 'brousse tigrée' has an anthropic origin; 5) clearing, wood cutting and grazing by livestock cause the 'brousse tigrée' pattern to degrade [4].

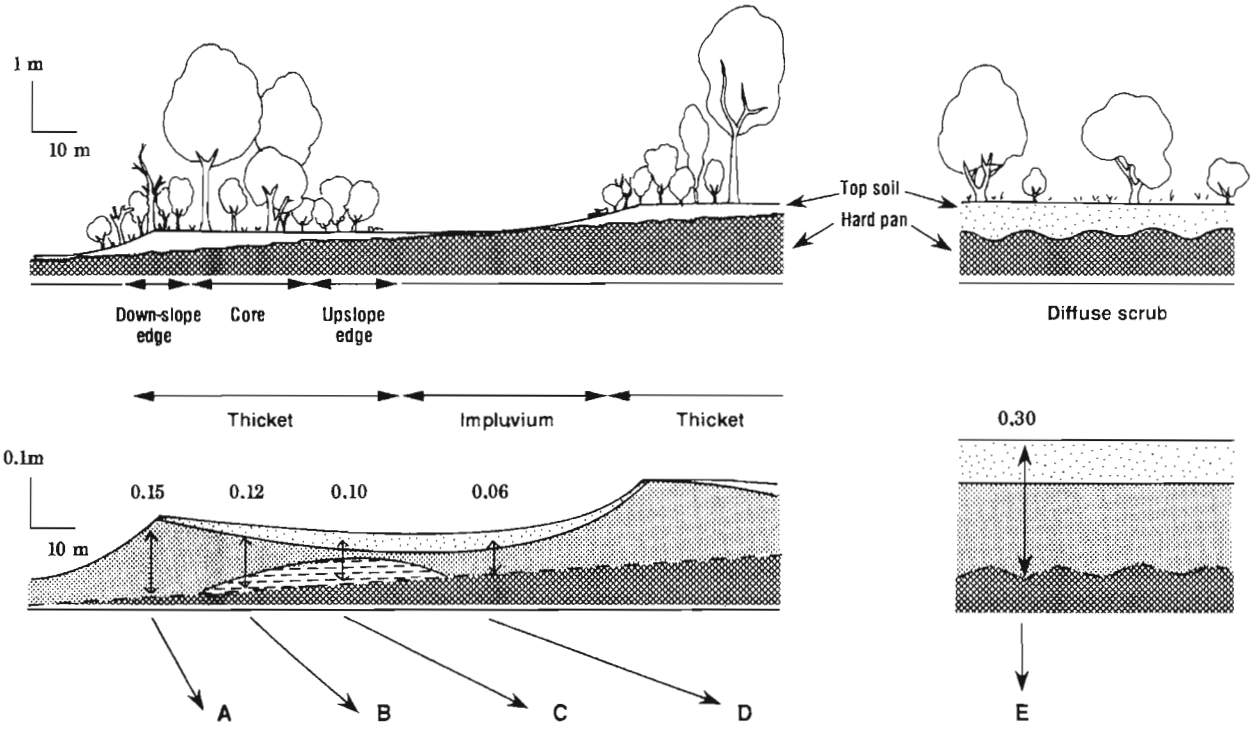

Soil horizons	S	L	C	S	L	C	S	L	C	S	L	C	S	L	C
0 - 6 cm	63	35	02	73	23	04	69	29	02	76	23	01	74	25	01
6 -12 cm	62	33	06	60	30	10	67	31	02	60	31	09	71	26	03
12 -25 cm	63	41	06	37	36	27	28	54	18	50	32	18	63	29	08
25 -50 cm	56	34	10	37	36	27	33	37	30	42	32	26	55	33	12

Figure 1. Scheme of the vegetation pattern, terrain topography and soil texture profiles (loose soil only) for neighbouring 'brousse tigrée' and diffuse scrub sites in Nampala (Mali).

2. METHODS

Data from three different studies by the International Livestock Centre for Africa (ILCA, now ILRI) in collaboration with the Malian Institute of Rural Economy (IER) and the National Institute of Agriculture Research in Niger (INRAN) have been used in this paper. 'Brousse tigrée' and related vegetation sites were characterized in the regional assessment and mapping of pastoral resources conducted in a region of Mali centred on the flood plain of the Niger River, known as Macina, and extending to adjacent uplands to the west and north (*figure 2*). Other sites were characterized in the Gourma study which extended to the south of the Niger river between Timbuktu and Gao down to the border with Burkina Faso. The objective of that study was to monitor changes in vegetation (1984–1993) following the major drought in 1983–84 [11]. The third group of 'brousse tigrée' sites were described and monitored (1994–1998) in western Niger (Fakara) in a study on the role of livestock in nutrient cycling within Sahelian agro-ecosystems.

2.1. Field measures

Herbage yields, pattern and species composition, as well as woody plant population density and species composition were recorded at all sites together with data on soils and resource management. However, because of differences in scale and aims, the sampling designs differed between studies. In the Macina study, the classification of the vegetation types was based on a correspondence analysis of descriptors including the list of herbaceous species, recorded in 400 plots, 10×10 m in size, distributed over the area stratified by climatic zones subdivided by edaphic units based

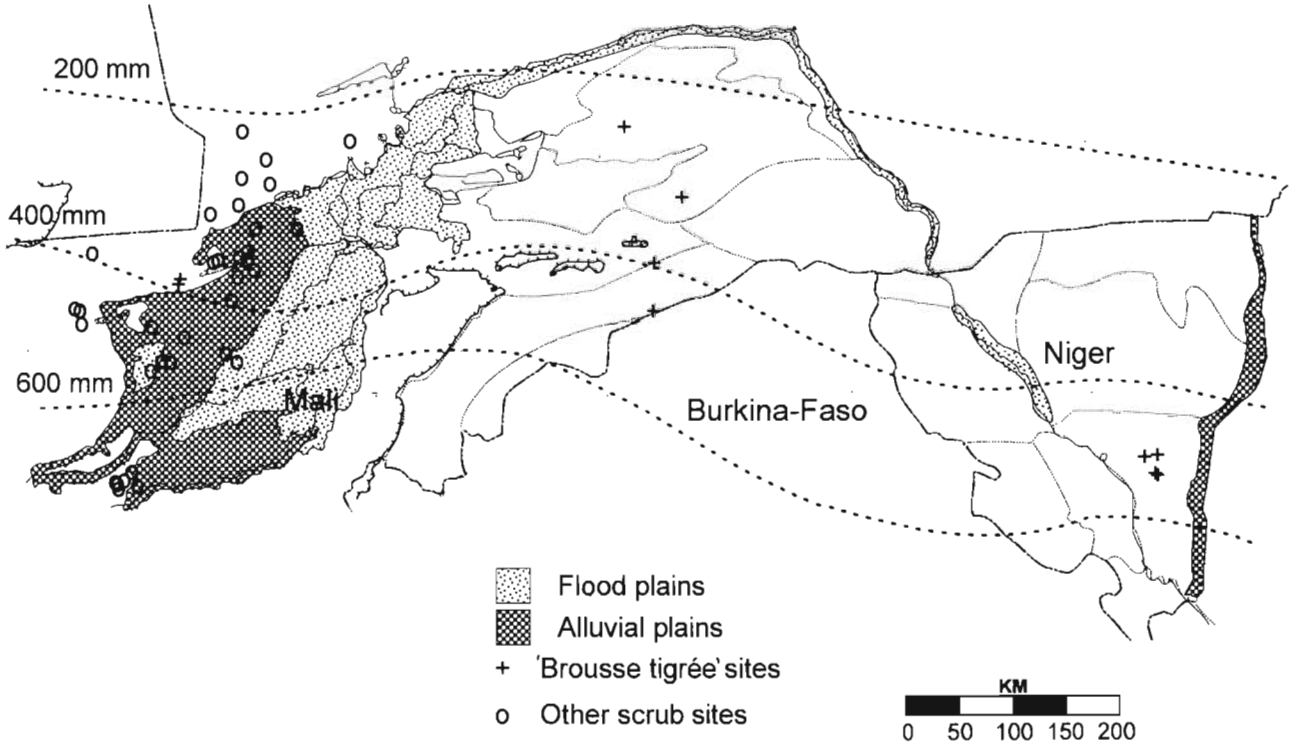

Figure 2. Situation map of the 'brousse tigrée' and related vegetation sites studied within the Sahel of Mali and Niger.

on soil texture and flood regime, in turn subdivided by the type of land use [31]. Herbaceous standing mass at the end of the growing season was destructively measured in 1×1 m plots placed in each facies whose area within the 10×10 m plot was visually assessed. To better characterize the woody plant population complementary observations were made in 100 of these sites. They consisted of exhaustive counting of the woody plants encountered in each of sixteen adjacent 10×10 m plots arranged in a 160-m long transect band [15]. Less frequent species were also recorded in bands adjacent to one side of the transect band and of increasing width (10, 20, 40, 80 m) so that the total area investigated was 160×160 m. Each plant recorded was characterized by its species name, canopy dimensions, number and trunk circumference.

The same woody plant descriptors were observed in the Gourma and Fakara studies but in a different sampling design. The plots were circular and centred on four points located randomly along a linear transect of 1 000 m (Gourma) or 200 m (Fakara) long, set perpendicular to the major ecological gradient in the site. The radius of the circular plot was chosen depending on the density of the species in the stand. As a result the size of the individual plots ranged between 1/64 and 1 ha. In patterned vegetation, thickets and impluvium were sampled separately. At all sites, foliage yield and wood mass were estimated using allometric relations established, for each species, between yield or mass and the basal circumference of the stems [6, 18, 28].

In the Gourma and Fakara studies, herbage cover, standing mass and species composition were recorded using a two-level stratified random sampling design: major differences in vegetation induced by terrain features (such as impluvium and thicket often subdivided into upstream, core and downstream bands) were identified as facies sampled individually. Four strata were systematically distinguished within each facies on the base of the apparent density of the vegetation: bare soil, low, medium and high density. The areas covered by each strata within facies were

measured along linear transects of 1 000 m (Gourma) or 200 m (Fakara), which were used to weigh the vegetation parameters. Weighed averages and variances were calculated for each site following Cook and Stubbendieck [7]. In the Gourma study, a virtual sample of fifty plots was created using a random generator for normal distribution applied to each strata in proportion of the area it covered, each strata being characterized by the mean and variance of the herbage mass measured in quadrats. The mean and variance of the virtual random sample were calculated and the coefficient of variation of that mean used to estimate spatial heterogeneity. Interannual variability was estimated by the coefficient of variation of the interannual means calculated over 10 years [16].

2.2. Remote sensing

To better characterize the vegetation pattern of 'brousse tigrée', aerial photographs were scanned at a resolution of 300 dpi for panchromatic prints whereas colour slides were processed and transferred to CD-ROM at a Kodak laboratory. After correction for contrasts, pixel brightness was used to classify vegetation and soils using Adobe Photoshop software. In the case of colour slides, the analysis was done on the red band reflectance data in order to enhance the contrast between vegetation and soils [14]. Neighbouring 'brousse tigrée' and 'diffuse scrub' sites located less than 5 km from large water points and across a major and historical transhumance track were studied to assess the effect of high intensity of trampling and grazing by livestock on the vegetation pattern. An aerial photograph (IGN mission 75 MAL 32/500, photo 875) was scanned over an area of 3×3 km centred on the transhumance track. Isolated trees and thicket were identified by a classification of pixel brightness. The image was then vectorized and imported in Atlas GIS. The mean and total areas occupied by tree crowns or thickets were derived for 100-m wide corridors drawn parallel to the central axis of the transhumance path and at distances ranging from 0 to 600 m on either side of the track.

3. RESULTS

3.1. Woody species composition

From the results of the correspondence analysis of the Macina data [17] and observations in Gourma and Niger, species composition of 'brousse tigrée' was related to average rainfall and to the texture of the top soil (*figure 3*). A few species including *Combretum micranthum*[1], *Pterocarpus lucens* (although absent in eastern Burkina Faso, Niger and northern Nigeria), *Boscia senegalensis*, *B. angustifolia*, *Grewia flavescens*, *G. bicolor*, *Acacia ataxacantha* and *Guiera senegalensis* constituted the core of what could be considered as the archetype 'brousse tigrée' (*figure 3A*). This archetype was found between the isohyets 400 and 600 mm·yr^{-1}, on poorly permeable soils with a thin silty horizon overlaid on ferralitic hardpans (*figure 1*). Variants were found when top soil was more loamy (*figure 3B*) or more sandy (*figure 3C*). Below 400 mm mean annual rainfall, 'brousse tigrée' was gradually replaced by open scrubs whose species composition depended on top soil texture (*figure 3D, E, F*), while above 600 mm there was gradual transition towards the 'low trees and shrub savannah' found on the shallow soils of the northern sub-humid zone (*figure 3H*). Whatever the variant considered, the woody species composition of 'brousse tigrée' was not distinctive of that particular vegetation pattern. Diffuse scrubs with similar woody species composition were found in environment very similar to those of 'brousse tigrée' except for the terrain slope (*figure 1*). Moreover, vegetation with similar species composition also occurred on deep alluvial soils of the fossil flood plain of the Niger river in Mali (*figure 2*). The flatness of the terrain and the low permeability of the alluvial soils resulted in ecological niches equivalent to the niches found on the shallow soils of 'brousse tigrée' [17].

3.2. Vegetation pattern

Patchy patterns are common in arid and semi-arid vegetation [8, 12, 30] among them the 'brousse tigrée' pattern is characterized by regularly alternating bare soil stripes with linear and dense thickets set perpendicular to the direction of the gentle slope. In the studied sites, the impluvium to thicket area ratio increased when annual rainfall decreased (*table I*). The average width of the pattern period (impluvium + thicket) varied with slope and top soil texture. In the dryer situations, sand may deposit across the bare strips and, depending on the orientation of the thicket relative to the dominant winds, sand may accumulate on the windward side of the thicket [20].

Two of the range sites monitored in northern Gourma between the isohyet 300 and 200 mm (indicated as 'very open scrub' in *figure 5*) were patterned and functioned as 'brousse tigrée' although their thickets were few and far apart at the onset of

[1] Taxa are named after the second edition of the *Flora of West Tropical Africa, 1954-1972*, by J. Hutchinson and J.M. Dalziel, re-edited by R.W.J. Keay and F.N. Hepper, Crowns Agents for Overseas Governments and Administrations, London, vol. 1–3.

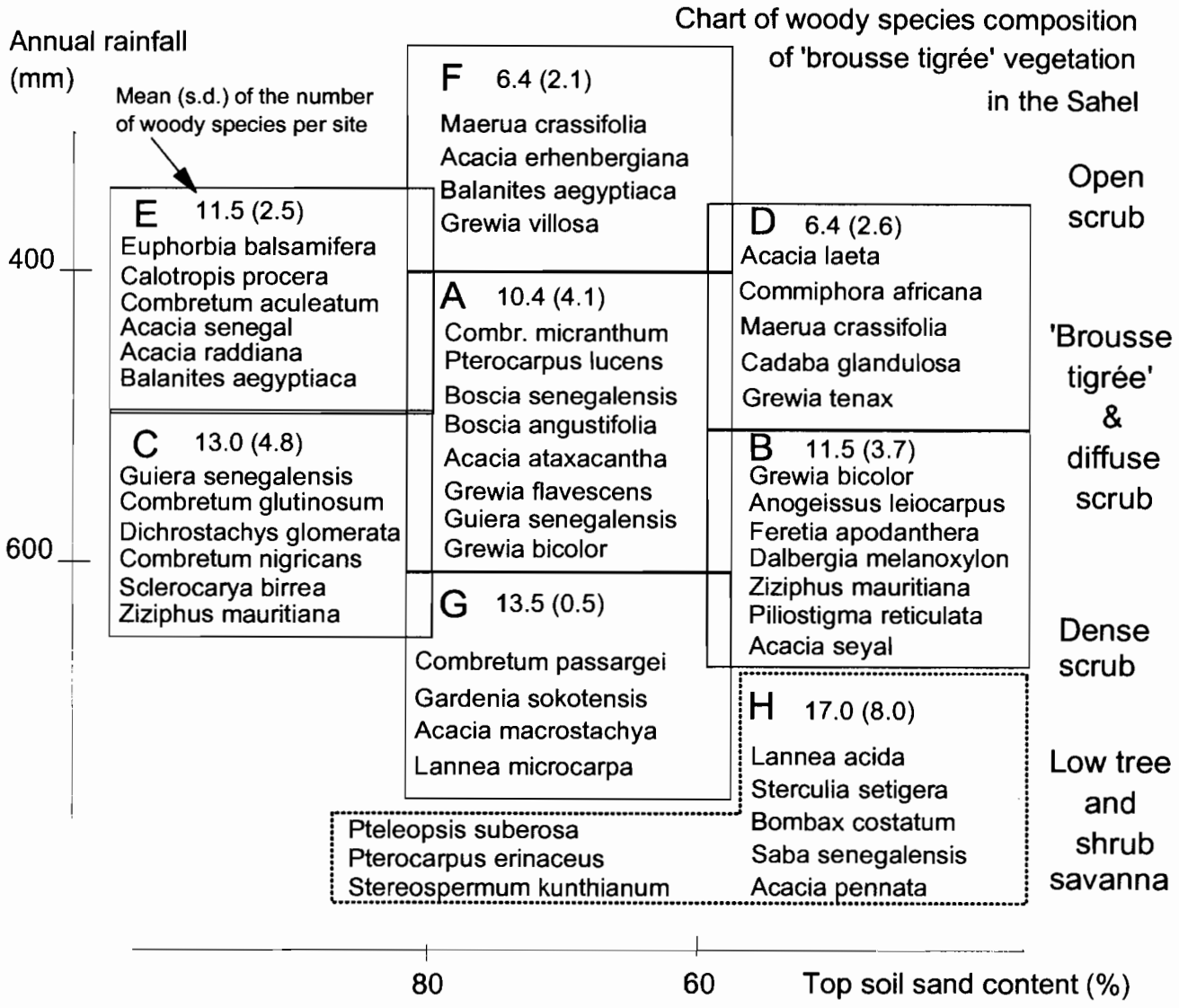

Figure 3. Species composition of 'brousse tigrée' and related vegetation in relation to climatic and soil texture conditions.

observations in 1984. Ten years later, the spatial pattern and composition of the vegetation were totally modified and the vegetation could not be considered part of 'brousse tigrée' any longer. The herbaceous layer has been the first to suffer from a succession of dry years. Herbaceous cover and yield declined and the herbaceous layer fragmented into scattered patches. However, herbaceous species diversity was maintained in a few refuge niches. Then, as the dry condition persisted, most of the woody plants died with the exception of *Boscia senegalensis* and *Maerua crassifolia* shrubs. A few species such as *Acacia erhenbergiana* and *Commiphora africana* for the woody plants, *Microchloa indica*, *Tragus berteronianus* and *Schoenefeldia gracilis* for the grasses started to establish with better rains in 1988 and 1990. However, these new comers spread in linear patterns along the new network of gullies that resulted from the change from sheet run-off to concentrated run-off.

'Brousse tigrée' and related diffuse scrub are distributed on shallow soils irrespective to rural popula-

Table I. Parameters of the vegetation pattern of 'brousse tigrée' (BT) and diffuse scrub (DS) sites observed along transects in the field and on aerial photographs.

Region Pattern	Rainfall (mm)	Slope (%)	Top soil texture	Period width[1] (m)		Thicket (%)			Impluvium (%)		
				mean	s.d.	Dense stand	Open stand	Total	Gravels or herbs	Silty flats	Total
Macina											
BT	320	0.6	silty sand	102	20	7.9	9.6	17.5	65	17.5	82.5
BT	510	0.3	silty sand	160	31	36.3	8.2	44.5	36.4	19.1	55.5
BT	510	0.4	silty sand	109	22	41	17	58	39.1	2.9	42
BT	510	0.5	silty sand	80	20	11.9	40.9	52.8	18.7	30.5	49.2
DS	510	0.1	Silty sand	–	–	5.7	29.9	35.6	53.7	10.7	64.4
BT	580	0.2	sandy silt	72	10	25.3	30.9	56.2	9.6	34.2	43.8
Gourma											
BT	390	0.5	sandy loam	126	29	10.6	2.8	13.4	69.8	16.8	86.6
DS	390	< 0.1	sandy loam	–	–	11.6	3.4	15	56.9	28.1	85
Fakara											
BT	440	0.4	silty sand	73	17	23.8	6.5	30.3	57.2	12.5	69.7
BT	440	0.5	silty sand	55	10	10.9	10	20.9	21.6	57.5	79.1
DS	440	< 0.1	sandy silt	–	–	54.6	9.3	63.9	19.2	16.9	33.8

[1] Period width = width of impluvium + downstream thicket.

tion density and livestock stocking rates. The vegetation pattern of neighbouring sites of 'brousse tigrée' and diffuse scrub located along a major transhumance track was very much affected in the first 50-m from the central axis of a major transhumance track: the relative area covered by scattered shrubs and thickets, as well as density of thickets largely decreased (*figure 4*). Further away from the axis but within 200 m, the density of thickets was still affected but the area covered by thickets (or individual shrubs) decreased or increased depending on the local orientation of slope relative to the transhumance track. Further away, no evidence was found of grazing influence on the vegetation pattern whether the track traversed the 'brousse tigrée' or the diffuse scrubs. On the contrary, a widespread and large reduction of the area covered by thickets and thicket fragmentation was observed when comparing 1995 to 1950 aerial photographs of 'brousse tigrée' and diffuse scrub sites located in a densely populated area of the Fakara region (*table II*). The decrease in woody plant cover was accompanied by a severe reduction of the herbaceous cover with the exception of newly formed thin sand deposits on the impluvium which were colonized by *Zornia glochidiata* and *Sida cordifolia*.

3.3. Flora diversity

In 'brousse tigrée', the average number of woody species recorded per site ranged between eight and nine (*table III*) which is below most of the other Sahelian natural vegetation types except for tempo-

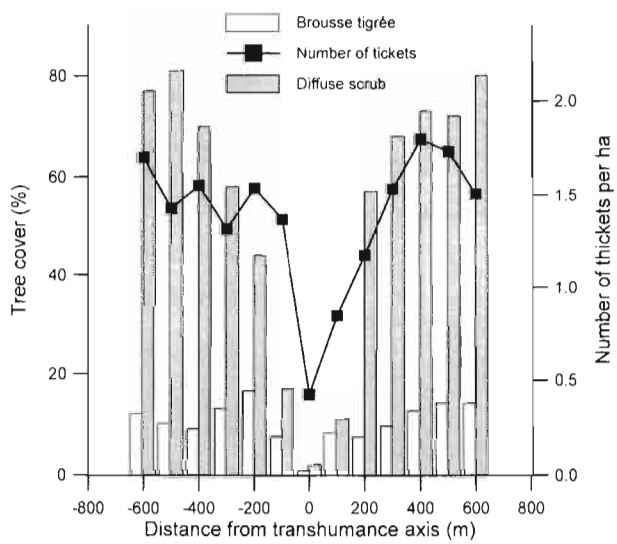

Figure 4. Effects of grazing on the number and area of thickets in a 'brousse tigrée' site and on the woody plant cover in a neighbouring diffuse scrub site, both located across a major transhumance track (Nampala, Mali).

Table II. Changes from 1950 to 1995 of the area covered by thickets and bare soil impluviums in two 'brousse tigrée' sites from the Fakara region (Kodey, Niger) subjected to intense forestry and pastoral use and partially cleared for shifting millet and sorghum crops.

Site	Year	Period width (m)		Thicket relative area (%)			Impluvium relative area (%)		
		mean	s.d.	Dense stand	Open stand	Total thicket	Gravels or herbs	Bare silty or sandy soils	Total impluvium
Peyrel	1950	55	10	10.7	45.9	56.6	27.1	16.3	43.4
	1995			10.9	10.0	20.9	21.6	57.5	79.1
Raneo	1950	95	21	19.0	30.7	49.7	15.0	35.3	50.3
	1995			3.6	6.3	9.9	4.8	85.3	90.1

rarily flooded sites. The direction of differences between neighbouring diffuse and patterned vegetation was not constant. The average numbers of herbaceous species recorded per site (flora richness) in 'brousse tigrée' and diffuse scrub were comparable and ranged between 22 and 26 (*table III*), while average numbers of species recorded per quadrat, excluding bare patches, ranged between 6.7 to 9.0. In contrast to woody plants, the flora richness of the herbaceous layer of 'brousse tigrée' and related diffuse scrub was slightly superior to Sahelian vegetation average, while the average number of species per quadrat was inferior.

3.4. Herbaceous plant production

In the Macina study, the herbaceous yield of 'brousse tigrée' was 489 kg DM·ha^{-1} compared to 1 194 kg DM·ha^{-1} for neighbouring diffuse scrub (*table IV*). In the Gourma, from 1984 to 1993, the annual herbage yields of the 'brousse tigrée' site averaged 177 (SE 42) kg·ha^{-1} compared to 927 (SE 203) kg·ha^{-1} for the neighbouring diffuse scrub and the average of the coefficient of variation of the mean herbage mass (virtual random sampling of fifty quadrats) were 441 % (SE 63) and 131 % (SE 11) respectively. The interannual variability of the herbage production was assessed by the coefficient of variation of the interannual production mean which was 76 % in 'brousse tigrée' and 69 % in the diffuse scrub. In the Fakara, from 1994 to 1996, the average herbage yield of the heavily grazed 'brousse tigrée' site was 363 (SE 137) kg DM·ha^{-1} compared to 507.3 (SE 134.7) kg·ha^{-1} in the heavily grazed diffuse scrub site, and the averages of the coefficient of variation of the mean herbage mass were 124 and 90 %, respectively. There was thus a large superiority of the herbage yield in diffuse scrub compared to 'brousse tigrée' in all sites and years. There also was a difference of magnitude in the spatial heterogeneity of the herbaceous layer as indicated by the coefficient of variation of the herbage mass which was much larger in 'brousse tigrée' than in diffuse scrub, at least when the site was not too heavily grazed.

Table III. Woody and herbaceous species richness per site, and average number of herbaceous species recorded per 1-m^2 quadrat in 'brousse tigrée' (BT) and diffuse scrubs (DS) sites from three study zones in the Sahel.

Study zone	Vegetation pattern	Woody plants				Herbaceous plants					
		Area sampled × replicates	Sites × years	Species recorded per site		Area sampled × replicates	Sites × years	Species recorded /m^2		Species recorded /site	
		(m^2)		mean	s.d.	(m^2)		mean	s.d.	mean	s.d.
Macina	BT	1 600 × 4	1	9	–	–	–	–	–	–	–
	DS	1 600 × 4	4	8.5	2.5	–	–	–	–	–	–
Gourma	BT	312.5/2 500 × 4	3	7.7	0.5	1 × 12	9	7.7	0.9	22.5	3
	DS	2 500 × 4	3	15	2.2	1 × 12	10	9	1.1	23.2	1.4
Fakara	BT	312.5/1 250 × 4	2	8.5	0.5	1 × 12	2	6.7	2.5	22.5	1.5
	DS	625 × 4	2	5.5	0.5	1 × 12	4	7.8	1.3	26.5	5.8

Table IV. Contribution of herbaceous species grouped by life-type and palatability classes to the herbage mass of the structural units of 'brousse tigrée' compared to the diffuse scrub (Macina sites, Mali).

Grasses and forbs palatibility	'Brousse tigrée'						Diffuse scrub
	Thicket				Impluvium	Total 'brousse tigrée'	
	Upstream edge	Core	Downstream edge	Total thicket			
Area (%)	17	17	16	50	50	100	100
Good	3.3	1.8	4.4	2.8	10.4	6.6	2.3
Mediocre	3.6	5.2	8.8	5.2	5.2	5.2	3.7
Poor	10.7	1.8	1.1	3.9	26.8	15.4	6
Total grasses	**17.6**	**7.8**	**14.3**	**11.9**	**42.4**	**27.1**	**12**
Good	0.4	0	1.1	0.4	35.3	17.9	59.7
Mediocre	77.9	80.4	70.3	77.6	10.5	44	16.5
Poor	4.1	10.8	14.3	10.1	11.8	10.9	11.8
Total forbs	**82.4**	**91.2**	**86.7**	**88.1**	**57.6**	**72.8**	**88**
Herbage yield (kg DM·ha^{-1})	2 618	430	332	952	25	489	1 194

As illustrated by the Macina site data (*table IV*), the species composition of the herbaceous layer of 'brousse tigrée' was generally dominated by dicotyledons, especially in the thicket where they were better adapted to dense shade. Among the grasses, most of the species were found at the upstream edge of the thicket and were adapted to temporary soil water logging. The feed quality and palatability of the herbage was usually low with the exception of a few plants that colonize the sandy deposits such as *Zornia glochidiata*, an annual legume promoted by heavy grazing, *Schoenefeldia gracilis* and *Brachiaria xantholeuca*, annual grasses, or *Andropogon gayanus*, a perennial grass.

3.5. Woody plant production

The patterned structure of 'brousse tigrée' translated into contrasting densities and composition of woody plants between impluvium and thicket, and also between the upstream edge, core and downstream edge of the thicket (*table V*). Compared to neighbouring diffuse scrub, the high density of the woody plants in the thicket approximately compensated for the very low density in the impluvium. With the exception of

Table V. Density of woody plant species per structural units of the 'brousse tigrée' compared to diffuse scrub (Macina sites, Mali).

Woody species	Density of woody plants in 'brousse tigrée' (ha^{-1})						Density in diffuse scrub (ha^{-1})
	Thicket				Impluvium	Total 'brousse tigrée'	
	Upstream edge	Core	Dowstream edge	Total thicket			
area (%)	17	17	16	50	50	100	100
Pterocarpus lucens	206	439	150	308	38	173	250
Combretum micranthum	219	811	925	691	8	350	281
Boscia senegalensis	156	321	325	281	39	160	200
Dichrostachys glomerata	31	–	–	8	–	4	12
Grewia flavescens	–	–	25	6	–	3	50
Acacia ataxacantha	6	–	50	14	–	7	19
Guiera senegalensis	656	473	25	407	15	211	–
Grewia tenax	25	–	–	6	–	3	–
All species	**1 300**	**2 044**	**1 500**	**1 721**	**81**	**901**	**812**

Table VI. Woody plant density, foliage and wood masses of ‘brousse tigrée' (BT) and diffuse scrub (DS) sites in three regions of the Sahel.

Study zone	Vegetation type	Component facies	Area (%)	Woody plant density (ha^{-1})	Wood mass (kg DM ha^{-1})	Leaf mass (kg DM·ha^{-1})
Macina	BT	thicket	50	1 721	11 095	1 402
		impluvium	50	81	68	8
		all	**100**	**901**	**5 030**	**705**
	DS	–	100	812	11 621	1 263
Gourma	BT	thicket	13	2 091	47 366	4 213
		impluvium	87	210	143	11
		all	**100**	**207**	**4 388**	**389**
	DS	–	100	220	1 938	123
Fakara	BT	thicket	30	4 519	53 820	4 109
		impluvium	70	151	572	79
		all	**100**	**2 335**	**27 196**	**2 094**
	DS	–	100	2 243	6 037	2 221

the Macina site, foliage and wood masses were higher in the 'brousse tigrée' than in diffuse scrub even at lower density of woody plants (*table VI*). The larger size of individual plants and longer span of the growing season allowed by the spatial concentration of resources in the thicket, could explain the superiority of 'brousse tigrée' foliage production and wood mass despite inferior plant density. Indeed, the partition of the wood mass per size of logs: large logs from the trunks and main branches, and small wood from branches, showed a higher proportion of large logs in 'brousse tigrée' than in associated diffuse scrubs. 'Brousse tigrée' and related diffuse scrub rank among the more productive vegetation types in the Sahel in term of woody plant products. In the studied 'brousse tigrée' sites, woody plant production spanned widely from 689 to 2 094 kg DM·ha^{-1}·yr^{-1} for foliage while the standing wood mass varied from 4 388 to 27 196 kg DM·ha^{-1} (*table VI*). Production in 'brousse tigrée' was not systematically superior to the production in diffuse scrub despite the close density of woody plant observed within each pair of neighbour sites. The palatable fraction of the foliage production of 'brousse tigrée' varied largely depending on species composition from 44.5 and 46.8 % palatable foliage in the Macina and Gourma, respectively, to only 1.3 % in the Fakara. The use of these browse resources was further limited by the difficulty of access for the animals, due to the height of some trees and the high density of the thickets. Standing wood in 'brousse tigrée' was composed of about 70 % of trunks and large branches and 30 % of minor branches, and number of species such as *Pterocarpus lucens* and *Combretum* ssp. provided good quality fuel wood.

4. DISCUSSION

4.1. Flora richness and diversity

The wide array of ecological niches created by the spatial concentration of water, nutrients and shade could explain the relatively rich herbaceous flora recorded in the 'brousse tigrée' and diffuse scrub sites (hyp. 1 validated). However, the larger contrasts between niches in 'brousse tigrée' compared to diffuse scrub did not result in a richer flora (hyp. 1 invalidated), perhaps because of the high fragmentation of the herbaceous layer in 'brousse tigrée'. The lower mean number of species per quadrat in 'brousse tigrée' supports this argumentation but the edaphic specialization of each niche (xeric in the bare soil impluvium; hydromorphic at the upstream edge of the thicket; sciaphyllous within thicket) could also contribute to explain the limited number of species recorded per quadrat. The same principles should apply to the woody plants. However, the woody flora was relatively poor whatever the pattern of the vegetation (hyp. 1 invalidated). This could indicate that niche diversification is less effective for woody plants, perhaps because competition is more severe as plant size increases [1].

4.2. Herbage and woody plant yields

Large extent of bare soils in the impluvium is the main reason for low herbage yields in 'brousse tigrée' compared to neighbouring diffuse scrubs (hyp. 2 invalidated). The impluvium is very hostile to plant development because of the shallowness of the top soil, associated to surface crusting. This causes sheet

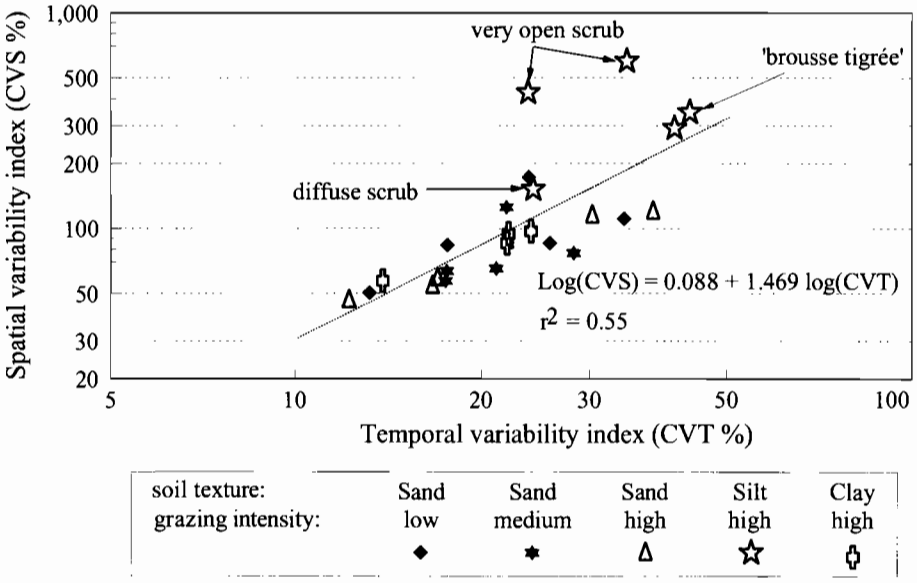

Figure 5. Relationship between spatial heterogeneity and temporal variability in herbage mass for 24 Sahelian sites (Gourma, Mali). The regression is established between the logarithm of average coefficient of variation of annual mean herbage mass (CVS) and the logarithm of the coefficient of variation of the 10 years interannual mean of the herbage mass (CVT).

run-off to redistribute most rainfall downstream to the detriment of the impluvium soil moisture [25]. In addition, the herbaceous layer is very sparse in the core of the thicket because of the dense shade. The spatial redistribution of water and nutrients benefits perennial plants, especially woody plants, allowing for the development of dense and multi-layered forest islands instead of a diffuse scrub. Annual wood production has not been measured, however; only annual foliage production compensated for inferior herbage yields in 'brousse tigrée' (hyp. 2 validated). The standing wood mass was superior in 'brousse tigrée' than in the neighbouring diffuse scrub in the Gourma and Fakara sites as observed in another site in western Niger [19], but not in the Macina site (hyp. 2 partially validated). The concentration of resources on a portion of the area extends the duration of the growing season in that spot to the benefit of the productivity of long-cycle plants and reduces the risk of plant mortality in that niche [21]. On the other hand, redistribution of resources may also increase losses through run-off spill over out of the patterned vegetation unit during large rain events or through deep percolation and leaching under the thickets [13]. The effect of patterning on the overall vegetation productivity will depend on trade-offs between productivity benefits for the woody plants in the thicket and resource losses by run-off and deep percolation.

4.3. Vegetation stability

Contrary to expectations, the high spatial heterogeneity and species diversity of the herbaceous layer of 'brousse tigrée' did not attenuate the interannual variation in herbage yield despite much lower average yields (hyp. 3 invalidated). The coefficient of variation of the 10-year mean herbage yield was consistently higher for 'brousse tigrée' than diffuse scrub found in the same climatic zone. Moreover, considering the 24 range sites monitored for 10 years in the Gourma, there was a positive linear regression between this coefficient of variation which is an indicator of the interannual variability and the average coefficient of variation of annual mean herbage mass which is an indicator of spatial heterogeneity (*figure 5*). Therefore, it appears that the higher the spatial heterogeneity of the vegetation pattern, the larger the susceptibility of the herbaceous layer production to vary from year to year [16].

4.4. The origin of 'brousse tigrée'

The transformation of two 'brousse tigrée' sites into very open scrubs following two decades of poor rains in a region that receives between 300 and 200 mm of rain annually on average confirms the climatic limit of 'brousse tigrée'. The very open scrub that resulted from these changes cannot be considered part of 'brousse tigrée' any longer because of the mutation in species composition, vegetation pattern and, above all, the change in the mode of water redistribution from sheet run-off to concentrated run-off [9]. The well-defined climatic, and also soil and topographic situations under which the 'brousse tigrée' occurs irrespective of population density [2, 10] does not support the anthropic origin of that vegetation pattern although it

does totally exclude influences of grazing, selective wood cutting or burning practices on the onset of the pattern and its dynamics.

4.5. The degradation of 'brousse tigrée'

Grazing by livestock and wood cutting or clearing for cropping are often implicated in the set-up of the patchy pattern of 'brousse tigrée' as well as in its degradation [4]. Indeed, selective and intensive grazing of annual herbs during the growing season help the dominance of woody plants (hyp. 5 validated). In addition, the patchiness of the vegetation cover reduces the risk of fire which could have balanced the influence of grazing in the competition between herbs and woody plants. However, except for species composition of the herb layer [29], no evidence was found of an influence of a long history of grazing by transhumant livestock on the structure of vegetation across grazing pressure gradients established from livestock concentration points such as water points, cattle paths or resting sites (hyp. 5 invalidated). This was confirmed by the narrow limits of the influence of livestock along major transhumance tracks such as the Diafarabé track that connect the Macina flood plains to the upland rangelands 600 km away in southern Mauritania [5]. Centuries of seasonal heavy grazing and trampling along the path only affected the pattern of the 'brousse tigrée' and that of neighbouring diffuse scrubs within 200 m from the central axis of the track (*figure 4*). On the contrary, the thicket clearing and subsequent cropping, because wood cutting, tillage and weeding maintain the soil loose and denudated during the wet season, affects the spatial redistribution of water which drives the pattern and functioning of 'brousse tigrée' [22]. The concentration of run-off, gully formation and mobilization of the sand deposits rapidly led to severe soil erosion which threatens the resilience of the 'brousse tigrée' (hyp. 5 validated) as observed in two sites in Niger (*table II*).

5. CONCLUSION: IMPLICATIONS FOR NATURAL RESOURCE MANAGEMENT

The pastoral value of 'brousse tigrée' is limited by low herbage yields and feed quality with the exception of the patches found on the thin sandy deposits which exist in some of the dryer or degraded 'brousse tigrée' [20]. However, depending on the species composition of the woody vegetation, browse could provide an important animal feed resources [24]. Selective cutting that would favour the growth of selected best-value browse species, such as *Pterocarpus lucens* and *Ziziphus mauritiana* is one option for improved management. Planting best-value species could even be envisaged in the poorest stands.

The main production of 'brousse tigrée' is forestry [23]. Because of the spatial concentration of water and nutrients, the ecological conditions in the thicket are appropriate for a forest system to develop despite limited rainfall and long lasting dry season. Based on the annual foliage production, the productivity of this discontinuous forest at least equals the productivity of neighbouring diffuse scrubs, and it yields a larger proportion of higher value timbers [19]. Forestry management should aim at maintaining this productivity in organizing selective cutting of live wood, chiefly as building material and fuel, although fuel wood harvest in the Sahel consist mainly in collecting dead wood [3] which has limited impact on the ecosystem.

The increasing practice of thicket clearing for shifting crop of sorghum, in southern Sahel, and millet, in northern Sahel, puts the 'brousse tigrée' at risk as it affects the spatial redistribution of water which drives the pattern and functioning of that biome. The concentration of run-off that result from clearing for cropping rapidly aggravates erosion on poorly permeable soils and increases water flows outside the 'brousse tigrée'. This causes sudden floods that threaten downstream cropping lands and may further justify costly reclamation operation on degraded 'brousse tigrée' [27].

Acknowledgments

This study was supported by the International Livestock Research Institute (ILRI) and carried out at the Sahelian Center of ICRISAT, Sadoré (Niger). The data from Mali emanate from collaborative research projects between the Malian 'Institut d'économie rurale' (IER) and the International Livestock Center for Africa (ILCA). The authors are grateful to A. Kalilou, A. Haïdara, Y. Maïga who contributed to field data collection and thank A. Buerkert, B. Hiernaux, S. Fernández-Rivera and T.O. Williams for their contributions. Critical comments from two anonymous referees were also appreciated.

REFERENCES

[1] Abrams P.A., Monotonic or unimodal diversity productivity gradients: what does competition theory predict?, Ecology 76 (1995) 2019–2027.

[2] Ambouta K., Contribution à l'édaphologie de la brousse tigrée de l'Ouest nigérien, thèse, Nancy, France, 1984, 116 p.

[3] Benjaminsen T.A., Fuelwood and desertification: Sahel orthodoxies discussed on the basis of field data from the Gourma region of Mali, Geoforum 24 (1993) 397–409.

[4] Boudet G., Désertification de l'Afrique tropicale sèche, Adansonia ser. 2 12 (1972) 505–524.

[5] Breman H., Diallo A., Traoré G., Djiteye M.M., The ecology of the annual migrations of cattle in the Sahel, in: Proc. First Int. Rangeland Congress, American Soc. Range Manag., Denver, USA, 1978, pp. 592–595.

[6] Cissé M.I., Production fourragère de quelques arbres sahéliens : relations entre la biomasse foliaire maximale et divers paramètres physiques, in: Le Houerou H.N. (Ed.), Browse in Africa, the Current Stage of Knowledge, International Livestock Centre in Africa (ILCA), Addis Ababa, Ethiopia, 1980, pp. 203–208.

[7] Cook C.W., Stubbendieck J., Range research: basic problems and techniques, Society for Range Management, Denver, USA, 1986, pp. 215–250.

[8] Coughenour M.B., Coppock D.L., Ellis J.E., Herbaceous forage variability in an arid pastoral region of Kenya: importance of topographic and rainfall gradients, J. Arid Environ. 19 (1990) 147–159.

[9] d'Herbès J.M., Valentin C., Surface condition in the Niamey region (Niger): spatial distribution, ecological and hydrological implications, J. Hydrol. 188 (1997) 18–42.

[10] d'Herbès J.M., Valentin C., Thiéry J., La brousse tigrée au Niger : synthèse des connaissances acquises. Hypothèses sur la génèse et les facteurs déterminant les différentes structures contractées, in: d'Herbès J.M., Ambouta J.M.K., Peltier R. (Eds.), Fonctionnement et gestion des écosystèmes forestiers contractés sahéliens, John Libbey Eurotext, Paris, 1997, pp. 131–152.

[11] de Leeuw P.N., Diarra L., Hiernaux P., An analysis of feed demand and supply for pastoral livestock: the Gourma region of Mali, in: Behnke Jr R.H., Scoones I., Kerven C. (Eds.), Range Ecology at Disequilibrium, ODI, London, 1993, pp. 136–152.

[12] Forman R.T.T., Godron M., Patches and structural components for a landscape ecology, Bioscience 31 (1981) 733–740.

[13] Galle S., Seghieri J., Mounkaila H., Fonctionnement hydrologique et biologique à l'échelle locale. Cas d'une brousse tigrée au Niger, in: d'Herbès J.M., Ambouta J.M.K., Peltier R. (Eds.), Fonctionnement et gestion des écosystèmes forestiers contractés sahéliens, John Libbey Eurotext, Paris, 1997, pp. 105–108.

[14] Gérard B., Utilisation des systèmes d'information géographiques et des photographies aériennes prises à basse altitude pour une meilleure gestion des stations de recherche agronomique, in: Nutall C. (Ed.), Travaux d'Africagis'95, UNITAR, Genève, 1995, pp. 357–362.

[15] Hiernaux P., L'inventaire du potentiel fourrager des arbres et arbustes d'une région du Sahel malien. Méthodes et premiers résultats, in: Le Houerou H.N. (Ed.), Browse in Africa, the Current Stage of Knowledge, International Livestock Centre in Africa (ILCA), Addis Ababa, Ethiopia, 1980, pp. 195–202.

[16] Hiernaux P., Spatial heterogeneity in Sahelian rangelands and resilience to drought and grazing, in: West N.E. (Ed.), Rangelands in a Sustainable Biosphere, Proc. Fifth Int. Rangeland Congress, vol. 2, American Soc. of Range Manag., Denver, USA, 1996, pp. 232–233.

[17] Hiernaux P., Coulibaly M., Diarra L., Recherche d'une solution aux problèmes de l'élevage dans le delta intérieur du Niger au Mali, vol. 1, Les pâturages de la zone d'étude, ODEM/CIPEA, Bamako, Mali, 1983, 133 p.

[18] Hiernaux P., Cissé M.I., Diarra L., de Leeuw P.N., Fluctuations saisonnières de la feuillaison des arbres et des buissons sahéliens. Conséquences pour la quantification des resources fourragères, Rev. Elev. Méd. Vét. Pays Trop. 47 (1994) 117–125.

[19] Ichaou A., d'Herbès J.M., Productivité comparée des formations structurées et non structurées dans le Sahel nigérien. Conséquences pour la gestion forestière, in: d'Herbès J.M., Ambouta J.M.K., Peltier R. (Eds.), Fonctionnement et gestion des écosystèmes forestiers contractés sahéliens, John Libbey Eurotext, Paris, 1997, pp. 119–130.

[20] Leprun J.C., Étude de quelques brousses tigrées sahéliennes : structure, dynamique, écologie, in: Le Floc'h E., Grouzis M., Cornet A., Bille J.C. (Eds.), L'aridité une contrainte au développement, Éditions de l'Orstom, Paris, 1992, pp. 221–244.

[21] Ludwig J.A., Tongway D.J., Spatial organisation of landscape and its function semi-arid woodlands, Australia, Landsc. Ecol. 10 (1995) 51–63.

[22] Mauchamp A., Rambal S., Lepart J., Simulating the dynamics of a vegetation mosaic: a spatialized functional model, Ecol. Model. 71 (1994) 107–130.

[23] Montagne P., Les marchés ruraux de bois-énergie au Niger. Outils de développement rural local, in: d'Herbès J.M., Ambouta J.M.K., Peltier R. (Eds.), Fonctionnement et gestion des écosystèmes forestiers contractés sahéliens, John Libbey Eurotext, Paris, 1997, pp. 185–202.

[24] Piot J., Nebout J.P., Nanot R., Toutain B., Utilisation des ligneux sahéliens par les herbivores domestiques. Étude quantitative dans la zone sud de la mare d'Oursi, GERDAT, Paris, 1980, 213 p.

[25] Seghieri J., Floret C., Pontanier R., Plant phenology in relation to water availability. Herbaceous and woody species in the savannas of Northern Cameroon, J. Trop. Ecol. 11 (1995) 237–254.

[26] Tilman D., Downing J.A., Biodiversity and stability in grasslands, Nature 367 (1994) 363–365.

[27] Torrekens P., Brouwer J., Hiernaux P., Évolution de la végétation spontanée sur plateaux latéritiques aménagés par des ouvrages anti-érosifs dans le département de Dosso (Niger), in: d'Herbès J.M., Ambouta J.M.K., Peltier R. (Eds.), Fonctionnement et gestion des écosystèmes forestiers contractés sahéliens, John Libbey Eurotext, Paris, 1997, pp. 235–246.

[28] Touré A.S., Grandtner M.M., Hiernaux P., Équations de prédiction et dynamique saisonnière de la masse foliaire de quatre ligneux du Moyen-Bani-Niger (Mali), Ann. ACFAS 59 (1991) 265–291.

[29] Turner M., Life on the margin: Fulbé herding practices and the relationship between economy and ecology in the inland delta of Mali, Ph.D. thesis, University of California, Berkeley, 1992, 469 p.

[30] Vetaas O.R., Effect of spatial arrangement of environmental variables on ordination results from a disturbed humidity gradient in northeastern Sudan, Coenose 8 (1993) 27–37.

[31] Wilson R.T., de Leeuw P.N., de Haan C. (Eds.), Recherches sur les systèmes des zones arides du Mali : résultats préliminaires, International Livestock Centre in African ILCA, Research Report 5, Addis Ababa, Ethiopia, 1983, 177 p.

Acta Oecologica **20** (3) (1999) 159–170 / © Elsevier, Paris

Distribution and floristics of moss- and lichen-dominated soil crusts in a patterned *Callitris glaucophylla* woodland in eastern Australia

David J. Eldridge

Centre for Natural Resources, Department of Land and Water Conservation, c/- School of Geography, University of New South Wales, Sydney NSW, 2052, Australia. (fax: +61 2 9313 7878; e-mail: d.eldridge@unsw.edu.au)

Received April 1, 1997; revised November 19, 1998; accepted November 27, 1998

Abstract — The distribution and abundance of soil crust lichens and bryophytes was examined in a patterned *Callitris glaucophylla* woodland in eastern Australia. Twenty-one lichen species and 26 bryophyte species were collected within thirty quadrats along a sequence of runoff, interception and runoff zones. Crust cover was significantly greatest in the interception zones (79.0 %), followed by the runoff zones (24.0 %), and lowest in the groved, runon zones (6.6 %). Lichens and bryophytes were distributed across all geomorphic zones, and, although there were significantly more moss species in the interception zones (mean = 9.1) compared with either the runoff (4.2) or runon (3.2) zones, the number of lichen species did not vary between zones. Ordination of a reduced data set of 32 species revealed a separation of taxa into distinct groups corresponding to the three geomorphic zones. Canonical correspondence analysis (CCA) of the 32 species and thirteen environmental variables revealed that the most important factors associated with the distribution of species were sheet and scarp erosion, soil stability and coherence, litter cover and crust cover. Surface cracking, microtopography and plant cover were of intermediate importance. The CCA biplot revealed that the timbered runon zones (groves) were dominated by 'shade-tolerant' mosses *Fissidens vittatus* and *Barbula hornschuchiana*, whilst the heavily eroded runoff zones supported sparse populations of 'erosion tolerant' lichens (*Endocarpon rogersii)* and mosses *(Bryum argenteum* and *Didymodon torquatus*). Interception zones supported a rich suite of 'crust forming' mosses and lichens capable of tolerating moderate inundation by overland flow. Two other groups of taxa were identified by this analysis: the 'pioneer' group, comprising mainly nitrogen-fixing lichens which occupy the zone of active erosion at the lower edge of the groves, and the 'opportunists' dominated by liverworts, occupying the shallow depressions or bays at the margins of the groves and the interception zones. This study confirms that the non-vascular lichens and bryophytes in these arid soil crusts, are, like the vascular plants, strongly patterned according to geomorphic zone, being most strongly associated with soil surface and erosional features. © Elsevier, Paris

Lichens / bryophytes / soil crusts / correspondence analysis / patterned landscapes

1. INTRODUCTION

Patterned landscapes, where the dominant vegetation has a regular banded appearance with alternating zones of bare soil and vegetation, have been described as 'brousse tigrée', tiger bush, banded vegetation, gilgaid desert pavements or grove-intergrove in Africa, Mexico and Australia [1, 7, 10, 28, 36, 37, 40, 46, 54, 58]. These landscapes are characterised by dense, usually perennial vascular vegetation aligned on the contour, separated from more or less unvegetated soil. This vegetated section acts as a sink area, sequestering soil sediments, water and nutrients shed from the bare source area immediately above it in the landscape. Runoff generated on the source zones is trapped on the upslope areas of the sink zones where infiltration proceeds. At the same time, erosion and decay of the lower surface of the vegetated zone occurs so that the vegetated band gradually moves upslope [52].

Water availability is the driving force in patterned landscapes, controlling the structure and the dynamics of the vegetation. Surface biota such as mosses, lichens, liverworts, fungi and cyanobacteria are strongly influenced by water availability, and themselves influence critical soil and ecological processes through their effect on infiltration, soil physical and chemical properties, nutrient cycling, decomposition and germination, and establishment [2, 8, 17, 22, 35]. Thus soil biota are likely to play a major role in the dynamics of patterned systems.

Despite the importance of these organisms to ecosystem function and stability, there has been little attempt to examine how they are distributed throughout patterned landscapes and their roles in the genesis and persistence of patterning. This is not surprising, given their small size, the difficulties involved in their identification, and problems of nomenclature, even to the level of genus. The more conspicuous components of soil crusts, i.e. lichens and bryophytes (mosses and liverworts), have largely been neglected from studies of vegetation dynamics in semi-arid regions in general, and patterned landscapes in particular [22]. Most studies have been conducted at a provincial [15, 23, 44, 45] or regional [14, 20] level, or have concentrated on sites of special interest such as National Parks and Nature Reserves [9, 43, 59]. One study, conducted in a patterned woodland in eastern Australia [11] demonstrated that soil crust biota were important components of bare microterraces formed on low slopes after wildfire. On these microterraces, the lichens *Heterodea muelleri* and *Cladia aggregata*, and various mosses and algae played a significant role in stabilising bare slopes and therefore contributing to slope stability.

Anecdotal evidence suggests that soil crusts in patterned landscapes are generally species poor and often occupy a small proportion of the soil surface. For example, crusts in 'brousse tigrée' landscapes are usually dominated by only a few cyanobacteria [56]. Similarly in patterned shrub-steppe in eastern Australia [10], crusts support only isolated lichens and mosses which are typically found on hummocks beneath perennial shrubs such as *Atriplex vesicaria* [22]. At Lake Mere, although crusts supported a moderate diversity of lichen and bryophyte species (Eldridge and Tozer unpubl. data), cover levels of lichens and bryophytes are typically less than 10 % [4, 55] though cyanobacterial cover may be substantially greater.

Extensive areas of soil crust supporting a floristically rich suit of lichens, bryophytes, cyanobacteria and algae are common in wooded ecosystems on the margins of the agricultural and pastoral regions in eastern Australia in areas of 350–500 mm average annual rainfall. Within this zone, a large area of cypress pine (*Callitris glaucophylla*) woodland exhibiting a strongly patterned sequence of runoff and runon zones, and a well-developed soil crust, provided an ideal opportunity to study the distribution and floristics of soil crust lichens and bryophytes in relation to patterning.

This paper reports an investigation of the distribution and floristics of lichens and bryophytes in soil crusts in relation to patterning in a *Callitris glaucophylla* woodland using correspondence analysis (CA) and canonical correspondence analyses (CCA). No attempt was made to study cyanobacteria or algae. Correspondence analysis was used to examine the distribution of lichen and bryophyte (moss and liverwort) species across the three geomorphic zones. Similarly, CCA was used to examine how species were distributed within the three zones in relation to a range of environmental variables.

2. METHODS

2.1. Site description

The study was conducted at 'Coan Downs', approximately 140 km south-west of Cobar, in central-western NSW Australia (145°35' E, 32°56' S). The climate is semi-arid with a low and unreliable rainfall averaging 350 mm per annum. Rainfall is evenly distributed throughout the year, and average diurnal temperatures range from a maximum of 35 °C in January to 3 °C in July. Annual evaporation at Cobar is approximately 2 575 mm [5].

The site was located on the plains unit of Yackerboon Land System [33]. 'Coan Downs' is a grazing property running Merino ewes principally for wool production. It is typical of properties in the general area which have been operating as grazing properties for over a century.

2.2. Soils and vegetation of the zones

The landscape comprised a strongly patterned open woodland on a plain with slopes up to 3 %. It is characterised by zones of water-deposited sediments supporting dense bands of cypress pine (*Callitris glaucophylla*) with band width to 16 m (*table I*). These groved, runon zones were separated by unvegetated, stony runoff zones up to 20 m across. A narrow interception zone to 3 m wide commonly occurred on the upslope edge of the groves (*figure 1*).

The *Callitris glaucophylla* groves represent zones of resource accumulation, receiving water-borne sediments from upslope by water erosion and overland flow. Consequently, ponded infiltration rates were significantly higher in the groves compared with the runoff zones [13]. The soil type at the site is a red earth [49] or Typic Haplargid [48]. A description of some physical properties of the surface soils from two depths, 0–20 and 20–40 mm from the runoff and runon (grove) zones is given in *table I*. Analyses of soil physical properties indicates higher levels of organic carbon in these zones compared with runoff zones (*table I*). Electrical conductivity was significantly

Table I. Description of the soils and vegetation of the three geomorphic zones at 'Coan Downs'. [1] Data represent the means of eight soil samples; [2] no significant differences in particle size analyses between the runoff and runon zones. Different letters within a row are significant at $P < 0.05$. n.d., Not determined.

	Runoff	Interception	Runon
Zone width (m)			
Mean (+ SEM)	10.6 (1.72)	2.50 (0.22)	8.13 (1.31)
Range	6–12	1–3	4–12
No. of zones examined	16	16	15
Soil physical properties[1]			
Organic carbon (%)			
0–20 mm	0.55[a] (0.03)	n.d.	0.90[b] (0.05)
20–40 mm	0.50[a] (0.04)	n.d.	0.62[b] (0.04)
Elect. conductivity (dSm^{-1})			
0–20 mm	0.17[a] (0.06)	n.d.	0.29[b] (0.03)
20–40 mm	0.20[a] (0.07)	n.d.	0.35[b] (0.02)
pH (water 1:5)			
0–20 mm	6.18 [a] (0.14)	n.d.	6.36[b] (0.08)
20–40 mm	5.78[a] (0.11)	n.d.	6.38[b] (0.08)
Particle size analysis (%)[2]			
0.2–2.0 mm			
0–20 mm	19 (1.1)	n.d.	18 (0.08)
20–40 mm	17 (0.7)	n.d.	19 (1.2)
0.02–0.2 mm			
0–20 mm	43 (0.7)	n.d.	42 (0.9)
20–40 mm	42 (1.1)	n.d.	42 (0.2)
0.002–0.2 mm			
0–20 mm	14 (0.5)	n.d.	14 (1.4)
20–40 mm	14 (0.8)	n.d.	12 (1.1)
< 0.002 mm			
0–20 mm	24 (0.8)	n.d.	26 (1.7)
20–40 mm	27 (0.5)	n.d.	27 (0.5)

higher in the runon zones compared with the runoff zones (*table I*).

The vascular plant community at the site is characterised by a patterned open woodland dominated by white cypress pine (*Callitris glaucophylla*). Understorey pastures were dominated by a sparse cover of speargrasses (*Stipa* spp.), wiregrasses (*Aristida* spp.) and various annual forbs.

2.3. Field measurements

A 400-m transect was positioned from a *Callitris glaucophylla* grove at the bottom of the slope to a runoff zone at the top of a ridge consistent with the gradsect approach of Gillison and Brewer [25]. Along this transect, thirty 0.5-m^2 quadrats were positioned at irregular intervals so that one quadrat was placed in each of the runoff, interception and runon zones of ten different sequences from the bottom to the top of the slope. At the time of the survey (June 1995), the area had received approximately 15 mm of rainfall, so that the three zones were easily distinguished by the growth of vascular plants and by water ponding on the surface in the case of the interception zones. Enlarged black-and-white aerial photography at a scale of approximately 1:12 000 assisted the placement of the transect and quadrats within the zones. Data on soil surface characteristics, vascular and non-vascular plant cover and composition, litter cover and type and degree of erosion were collected from each of the thirty quadrats according to the methods described below and are summarised in *table II*.

2.3.1. Soil surface characteristics

Landscape position on a quadrat basis was classified as either midslope or lowerslope. Surface microtopography was defined as the vertical distance between the lowest and highest points of the soil surface within the quadrat, i.e. < 5, 5–8, 8–15, 15–25 and > 25 mm. Crust coherence gives a measure of the force required to disrupt the soil surface with an object equivalent to the diameter of a ball-point pen. This measurement assesses the degree to which the surface has the capacity to resist stress or reform after wetting [53]. Classes were ranked as sandy (single grained), self-mulching (clay aggregates), break on touch, slight pressure, significant pressure, high pressure and unbreakable. The degree of surface cracking measures the percentage of the surface covered with cracks and relates to the capacity of the surface to disintegrate and erode: 0, < 10, 10–25, 25–50 and > 50 %. Surface stability of the soil surface to raindrop impact was ranked as stable, moderately stable, unstable or very unstable. This was determined using local experience and in some cases the Emerson drop test [53]. The degree of sheet erosion caused by wind and/or water was ranked as 0, < 10, 10–25, 25–50 or > 50 %. The degree of eroded scarp erosion was ranked as 0, < 10, 10–25, 25–50 or > 50 %.

2.3.2. Vascular and non-vascular plants

Within each quadrat, vascular plant cover and litter cover were recorded as 0, < 10, 10–25, 25–50 or > 50 %. Total cover of lichens and bryophytes in the microphytic crust was estimated (crust), along with the relative contribution of lichen (lich%) and bryophytes (bryo%) to total cover.

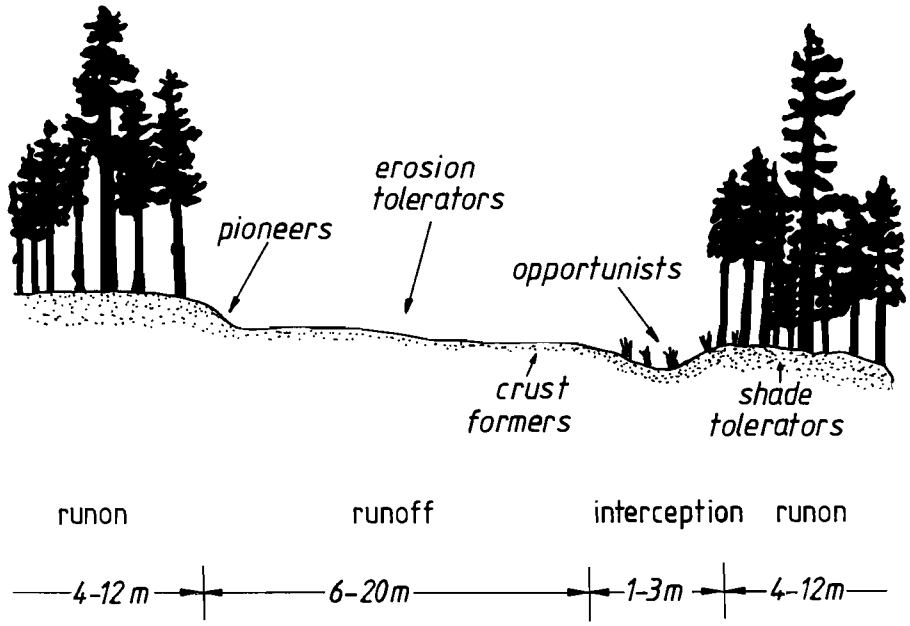

Figure 1. Diagrammatic representation of the runoff-interception-runon complex in a semi-arid *Callitris glaucophylla* woodland in semi-arid eastern Australia. The vertical distance is not to scale.

2.3.3. Crust floristics

Samples of soil crust were collected from each of the thirty quadrats, transported to the laboratory and passed through a 2-mm sieve. All bryophytes and lichens were identified, mostly to species level, using standard taxonomic keys. Nomenclature follows Streimann and Curnow [50] for mosses, Scott [44] for liverworts, McCarthy [38] for lichens, and where appropriate, more recent taxonomic revisions.

2.4. Analyses

One-way ANOVA [39] using arcsine transformed data was used to examine differences in crust cover

Table II. Environmental variables used in the canonical correspondence analysis.

Variable	Code	Range of values	Description
Microtopography	micro	1–50	< 5 mm (1) to > 25 mm (5)
Lowslope	lslo	0–1	lowslope (1) or not (0)
Midslope	mslo	0–1	midslope (1) or not (0)
Crust coherence	coher	1–7	sand (1) to unbreakable (7)
Surface cracking	crack	1–5	nil (1) to > 50 % (5) cracking
Surface stability	stab	1–4	stable (1) to very unstable (4)
Eroded sand	sand	1–5	nil (1) to > 50 % (5) eroded sand
Scarp erosion	scar	1–5	nil (1) to > 50 % (5) erosion
Plant cover	plant	1–5	nil (1) to > 50 % (5) cover
Litter cover	litt	1–5	nil (1) to > 50 % (5) litter cover
Bryophyte composition	bry%	0–100	composition (%)
Lichen composition	lic%	0–100	composition (%)
Crust cover	crust	0–100	projected foliage cover (%)

and species richness (number of species) of both lichens and bryophytes between the three geomorphic zones.

Lichen and bryophyte data were pooled to produce a data matrix of presence/absence of species within each of the ten quadrats by three geomorphic zones. Of the initial total of twenty lichens and 26 bryophytes, 'rare' species (< three total occurrences) were excluded from the matrix as their scarcity may have resulted from insufficient sampling rather than any real relationship between occurrence and geomorphic zone. It was considered that their inclusion in the data analyses may dominate and confuse the interpretations and conclusions drawn. After exclusion of these 'rare' species, the combined data matrix of sixteen lichens and sixteen bryophytes was analysed using correspondence analysis. Correspondence analysis (CA) is a graphical display ordination technique which simultaneously displays the rows (sites) and columns (species) of a data matrix in low dimensional space [27]. Row identifiers (species) plotted close together are similar in their relative profiles, and column identifiers plotted close together are correlated, enabling one to interpret not only which of the taxa are clustered, but also why they are clustered.

Canonical correspondence analysis (CCA [51]) was used to examine the relationships between the measured environmental variables and the distribution of lichens and bryophytes. Canonical correspondence analysis expresses species relationships as a linear combination of environmental variables, and combines the features of correspondence analysis ordination with canonical correlation analysis [26]. Canonical correspondence analysis ordinates species data using axes that are constrained to be linear combinations of the environmental variables. This provides a graphical representation of the relationships between species and environmental variables.

A matrix of thirty rows (quadrats) by 32 columns (species) emanated after pooling the lichen and bryophyte data across the thirty quadrats (ten per geomorphic zone). The dataset contained a large number (70 %) of zero values. The number of taxa per sample ranged from 0 to 17, and the number of samples containing any one taxa ranged from 3 to 25. Analyses were performed on the same subset matrix of 32 species by thirteen environmental variables.

3. RESULTS

3.1. Lichen and bryophyte cover

Cover of lichens and bryophytes was significantly different between all three zones ($F_{2,27} = 106.57$, $P < 0.001$), being greatest in the interception zones (mean ± SEM = 79.0 ± 4.1 %), intermediate in the runoff zones (24.0 ± 4.1 %) and least in the groves (6.6 ± 3.4 %).

3.2. Crust floristics

Sixteen lichens and sixteen bryophytes were found at the study site (*table III*). Of the bryophytes, three were liverworts from the families Aytoniaceae (*Asterella drummondii*), Ricciaceae (*Riccia* spp.) and Codoniaceae (*Fossombronia* spp.). Sixty-two percent (eight) of the remaining thirteen bryophytes comprised

Table III. Bryophyte and lichen species included in the analyses.

Code	Bryophyte
Asdm	*Asterella drummondii* (Hook. f. & Tayl.) R.M. Schuster
Baho	*Barbula hornschuchiana* Schultz
Baca	*B. calycina* Schw.
Brar	*Bryum argenteum* Hedw.
Brdi	*B. dichotomum* (Hedw.)
Brpa	*B. pachytheca* C. Muell.
Deco	*Desmatodon convolutus* (Brid.) Grout
Dito	*Didymodon torquatus* (Tayl.) Catches.
Ecpu	*Eccremidium pulchellum* (Hook. & Wils.) C. Muell.
Ecar	*E. arcuatum* (Hook. & Wils.) C. Muell.
Fivi	*Fissidens vittatus* Hook.f & Wils.
Fozz	*Fossombronia* spp. Raddi.
Fuzz	*Funaria* spp.
Gire	*Gigaspermum repens* (Hook.) Lindb.
Phro	*Phascum robustum* (Broth. ex Roth Stone) var. *robustum*
Rizz	*Riccia* spp.
Code	**Lichen**
Busu	*Buellia subcoronata* (Muell. Arg.) Malme
Cazz	*Catapyrenium* spp.
Clzz	*Cladonia* sp.
Cocz	*Collema coccophorum* Tuck.
Enpa	*Endocarpon pallidum* Ach.
Enpu	*E. pusillum* Hedwig
Enrg	*E. rogersii* McCarthy
Enro	*E. robustum* McCarthy
Ensb	*E. simplicatum* (Nyl.) Nyl. var. *bisporum* McCarthy
Ercr	*Eremastrella crystallifera* (Taylor) G. Schneider
Hebe	*Heterodea beaugelholei* R. Filson
Hede	*Heppia despreauxii* (Mont.) Tuck.
Leoc	*Lecidea ochroleuca* Pers.
Pezz	*Peltula* spp.
Psde	*Psora decipiens* (Hedw.) Hoffm.
Xabe	*Xanthoparmelia bellatula* (Kurokawa & Filson) Elix & Johnston

mosses from two families, Pottiaceae and Bryaceae. Apart from the foliose lichens *Heterodea beaugelholei* and *Xanthoparmelia bellatula*, most of the sixteen lichens were crustose or squamulose types. This is consistent with results from other semi-arid regions [42]. The genus *Endocarpon* comprised 38 % (six) of the total lichen species. The interception zones always had a greater numbers of species, genera or families compared with either the runon or runoff zones.

Only two of the thirty quadrats contained no lichens or bryophytes. Pooled across thirty quadrats, there were significantly more bryophyte species in the interception zones (mean = 7.9) compared with either the runoff (3.7) or runon (2.9) zones ($F_{2,27} = 21.35$, $P < 0.001$). There was no significant difference however in the number of lichen taxa between the three zones ($P = 0.118$). Within the intercept zone, there were significantly more bryophyte taxa (mean = 7.9) than lichen taxa (mean = 6.1; $P = 0.002$).

Ordination of the species data produced a separation of taxa (*figure 2*) which corresponded to the runoff, interception and runon zones (*figure 3*). Axis I of *figure 3* separated quadrats in the interception zones from those in the other zones, and axis II separated quadrats in the runon zones from those in the runoff and interception zones. Overlap of some quadrats near the origin indicates that these quadrats were dominated by taxa with preference profiles common to all three zones.

Lichens and bryophytes were found in all three geomorphic zones (*figures 2, 3*). Some groups of taxa however were strongly associated with a particular zone, and six distinctive groups are identified in *table IV*. Group I containing four lichens and four bryophytes is found almost exclusively in the interception zones. A second group (Group II) comprising five lichens and one bryophyte is generally associated with the interception and runon zones. Two groups (Groups III and IV, *table IV*) are generally found in all zones. The fifth group comprises those species which are found exclusively in, or have high abundances mainly in the runoff zones. The sixth group containing the two mosses *Fissidens vittatus* and *Barbula hornschuchiana*, occurs exclusively in the groved runon zones (*table IV*).

3.3. Distribution of environmental variables

The major differences in the environmental variables between the three zones are shown in *table V*. Generally, there was greater microtopography and cover of lichens and bryophytes in the interception zones, which were dominated by bryophytes. Runoff zones were characterised by smooth, eroded surfaces of sparse lichen-dominated crusts whilst the groves were uneroded, very stable and protected by an extensive and deep cover of litter.

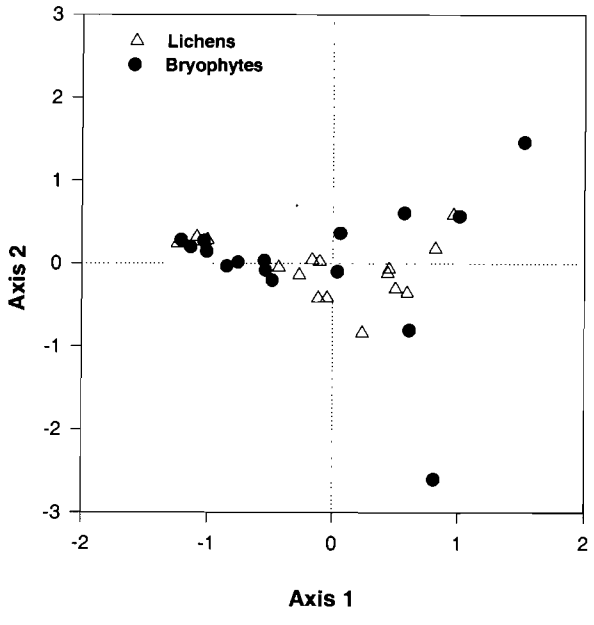

Figure 2. Correspondence analysis based on presence/absence of the 32 bryophyte and lichen species from the thirty quadrats.

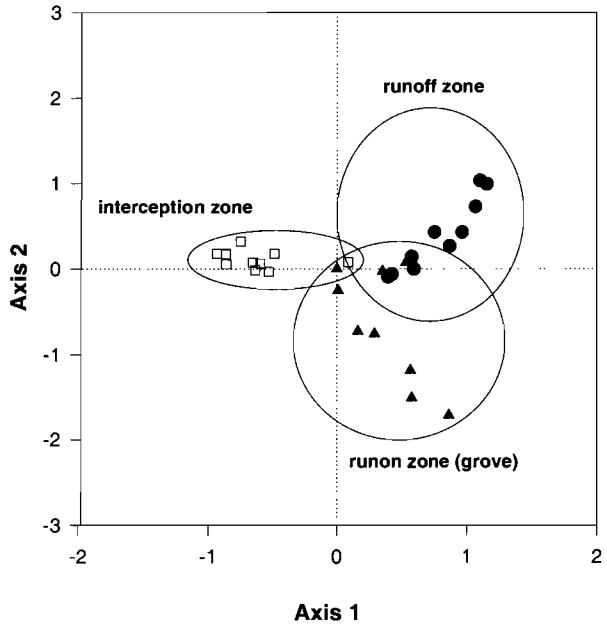

Figure 3. Correspondence analysis indicating the placement of the thirty quadrats within the runoff (circle), runon (triangle) and interception (square) zones.

Table IV. Distribution of the 32 lichen (L) and 32 bryophyte (B) species occurring in the thirty quadrats according to geomorphic zone. R, Runoff zone; I, interception zone; G, runon zone (grove). See *table III* for explanation of lichen and bryophyte codes.

	Crust Formers (Group I)								Opportunists (Group II)						Generalists (Groups III)								Pioneers (Group IV)				Erosion tolerators (Group V)				Shade tolerators (Group VI)	
	L	B	B	L	B	L	B	L	B	B	B	B	L	L	L	L	L	L	B	B	B	L	L	L	L	B	B	L	B	B	B
	XABE	ECPU	BRDI	HEBE	ECAR	PSDE	PHRO	BUSU	ASDR	FOZZ	BACA	FUZZ	PEZZ	RIZZ	CLZZ	ERCR	ENRO	CAZZ	LEOC	GIRE	BRPA	ENSB	COCZ	HEDE	ENPA	ENPU	DECO	DITO	ENRG	BRAR	FIVI	BAHO
R1																																
R2																				+			+			+	+	+				
R3																				+	+		+	+		+	+	+	+	+		+
R4																					+		+				+	+		+		
R5																					+		+				+			+		
R6																					+		+	+		+	+	+	+	+		
R7																				+	+	+	+	+	+	+	+	+		+		
R8															+			+		+	+	+	+	+		+	+	+	+			
R9																+		+	+		+	+	+				+		+			
R10														+	+			+	+	+		+	+			+	+	+				
I1			+	+	+	+			+	+	+				+	+	+		+	+	+					+		+				
I2		+		+	+	+			+	+	+				+						+	+	+					+				
I3	+	+		+			+		+	+	+			+	+			+		+	+	+										
I4	+	+	+	+	+				+	+	+			+					+		+	+	+									
I5		+	+				+		+	+	+		+	+	+			+		+	+	+	+									
I6					+	+	+		+	+	+			+		+		+		+	+	+	+	+								
I7				+	+		+	+		+	+				+	+				+	+	+	+			+		+				
I8										+	+	+	+	+			+		+		+		+	+				+	+			
I9	+	+	+		+	+	+	+	+	+		+		+		+			+	+	+	+										
I10	+				+		+	+	+	+	+	+		+	+						+	+	+	+								
G1											+								+		+	+	+				+		+			+
G2											+							+					+	+	+						+	
G3									+	+	+			+	+			+	+		+	+	+	+		+	+					+
G4																		+	+	+			+		+						+	+
G5									+	+		+			+			+	+	+	+		+	+		+	+				+	+
G6																		+					+								+	
G7													+	+					+		+	+					+					+
G8																																
G9																																
G10																+	+	+				+	+		+							+

Table V. Biophysical features of the three geomorphic zones.

Runoff	Intercept	Runon
Midslope location	lowslope	lowslope
5–8 mm microtopography	8–15 mm	5–8 mm
Very hard surface	very hard surface	crumbly surface
Moderately stable surface	moderately stable surface	very stable surface
< 10 % scarp erosion	< 10 % scarp erosion	no scarp erosion
< 10 % sheet erosion	< 10 % sheet erosion	no sheet erosion
< 10 % plant cover	< 10 % plant cover	< 10 % plant cover
< 10 % litter cover	< 10 % litter	> 50 % litter
Lichen dominant	bryophyte dominant	lichen and bryophyte co-dominant
Sparse crust cover	extensive crust cover	very sparse crust cover

3.4. Relationships between crust taxa and environmental variables

The species-environment biplot (*figure 4*) demonstrates the relationships between the 32 lichen and bryophyte species to the thirteen measured environmental variables. The length of the vectors indicates the relative importance of the variable in determining the axes, and the angle between an arrow and an axis is an inverse measure of their correlation [51]. The first three unconstrained ordination axes for the 32 lichens and bryophytes accounted for 33, 40 and 60 % respectively of the variation in species distributions.

The biplot indicates that the most important determinants of lichen and bryophyte distribution are sheeting and scarp erosion, litter cover, coherence and stability of the soil surface, and crust cover. The analysis was markedly influenced by the occurrence of the moss *Fissidens vittatus* which was strongly associated with sites of high litter cover, i.e. the *Callitris glaucophylla* groves. Examination of *table IV* reveals that it is the only one of the 32 species restricted exclusively to the runon zones (groves). The runon zones were characterised by an extensive litter cover, were uneroded, and supported *Fissidens vitattus* and *Barbula hornschuchiana*. Species restricted to the runoff zones were separated from those restricted to the intercept and runon zones by the 'scarp erosion-sheeting-% lichen cover' and 'microtopography-% plant cover' axes (*figure 4*).

4. DISCUSSION

The CCA indicates the complex organisation of environmental factors influencing the distribution of terricolous lichens and bryophytes in this patterned semi-arid woodland. The distribution of individual species was most strongly associated with cover of *Callitris* litter, stability and coherence of the soil surface, and the degree of sheeting and scarp erosion on the soil surface. Although some species clustered into neatly defined groups (*figure 4*), others showed no strong association with particular environmental variables. This is not surprising, as few of the environ-

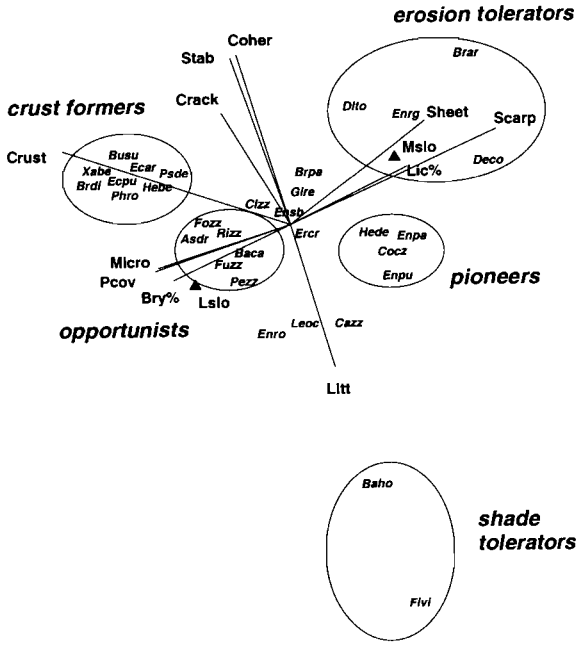

Figure 4. Species-environment biplots for axes 1 and 2 for the CCA for the combined bryophyte and lichen dataset. Vectors show the direction of maximum variation in the measured environmental variables. Closed triangles represent the centroids of the nominal variables midslope (Mslo) and lowerslope (Lslo). Species codes are given in *table III*. Explanation of environmental variables are given in *table II*.

mental variables represent simple gradients [32]. For example, although microsites under the *Callitris* trees are characterised by a dense litter layer, they also have low levels of incoming radiation, high levels of biological activity [57] and high infiltration rates [13]. Various groupings of species, responding in similar ways to the measured environmental variables, are shown in *table IV* and can be identified in *figure 4*.

4.1. Group I. The crust formers

In the upper left corner of *figure 4* are sites supporting an extensive cover of both microphytic crusts and vascular plants, and corresponding to the interception zones. Microtopography on these moderately hardsetting surfaces is up to 10 mm, and the majority of the soil surface comprises cracks up to 1 mm wide. The moderate infiltration rates in these soils [13], due to the presence of perennial grasses and their associated macropores [29], are intermediate between the runoff zones and the timbered groves. The dominant species in this zone include the mosses *Eccremidium arcuatum*, *E. pulchellum* and *Phascum robustum* var. *robustum*, and the foliose lichen *Heterodea beaugleholia*. Less abundant species are indicated in *table IV*.

As the interception zone is an area of sediment accretion, species growing in this zone must be capable of surviving frequent blanketing by deposited sediments originating upslope from the runoff zones. Consequently, taxa in the interception zone are dominated by mosses which have relatively higher growth rates compared to the slow-growing lichens. Some ubiquitous mosses are able to survive episodic burial beneath fine sediments by rapidly producing new growth from terminal shoots. Using thin section analysis, this phenomenon has been observed for *Grimmia mesopotamica*, a common moss in arid areas of Israel [8]. Soil aggregates examined by the author during laboratory identification of mosses and lichens have revealed long pieces of dead stem and attached leaves buried up to 30 mm below the soil surface [16]. Clearly then, some mosses are able to survive in this zone of accretion by growing up through successive layers of sediments using the twisting and turning movements of their leaves.

In contrast to bryophytes, lichens have extremely slow growth rates [31]. Annual growth rates of foliose lichens, measured as increases in thallus diameter, are of the order of 1–10 mm per year in more mesic areas [30]. Although there are few empirical data from semi-arid and arid regions, and none from Australia's arid zone, anecdotal evidence suggests annual growth rates of less than one millimetre per annum (J. Elix pers. comm.). Measurements of individual *Xanthoparmelia* spp. thalli at the sites indicated that some were up to 100 mm across, indicating an age of up to 100 years old. *Xanthoparmelia* spp. typically form rosettes with irregular to irregular-dichotomous lobes on the soil surface. These lichens are sensitive to fragmentation by human and animal trampling, or vehicular traffic [21]. Low levels of trampling may increase fragmentation and thus assist dispersal, but inundation is devastating. Even coverage by water during summer storms is likely to lead to the demise of these lichens as they are unable to photosynthesise when hydrated during high summer temperatures [47]. Thus individual thalli are likely to be found along the uphill edge of the interception zones where the probability of deposition is least. Furthermore, because of the risk of inundation by eroded soil, *Xanthoparmelia* spp. probably spread upslope within the interception zone as accretion proceeds from downslope, and the banded system moves upslope. This hypothesised dispersal of *Xanthoparmelia* spp. propagules upslope is yet to be tested in these patterned landscapes.

4.2. Group II. The opportunists

In the centre left of the CCA biplot (*figure 4*) is a group of six taxa associated with locally depressed bryophyte-dominated sites characterised by moderately rough surfaces with high plant cover. These sites display characteristics of both the interception zones and runon zones, and occur as an intergrade between the downslope edge of the interception zone, and the upslope edge of the vegetated groves, where the change of slope produces a series of long discontinuous depressions or bays. In patterned 'brousse tigrée' landscapes in Niger these bays have been shown to be crucially important for the establishment of annual grasses [12]. In the present study, these sites were dominated by liverworts, in particular the thallose *Riccia* group which includes *Riccia limbata*, *R. lamellosa* and *R. nigrella*, and the large *Asterella drummondii*. The *Fossombronia* group of leafy liverworts, the mosses *Barbula calycina* and *Funaria* spp., and the *Peltula* spp. group of lichens were also found in this interzone.

4.3. Group III. The generalists

In the centre of *figure 4* are the ubiquitous generalists such as *Bryum pachytheca*, *Endocarpon simplicatum* var. *bisporum* and *Gigaspermum repens* which do not appear to be strongly influenced by the measured environmental variables. Survey data from western NSW demonstrate that these three species are amongst the most common taxa associated with soil crusts [14, 20].

4.4. Group IV. The pioneers

Between the runoff and runon zones is a group of species associated with sites of sparse crust cover,

moderate levels of erosion, low levels of plant cover and relatively smooth surfaces. These sites, which have features of both the runon and runoff zones, are characterised by 'pioneer' species including filamentous cyanobacteria and the lichens *Endocarpon pallidum*, *E. pusillum*, *Collema coccophorum* and *Heppia despreauxii*. Apart from *Endocarpon pallidum*, the other species are ubiquitous throughout the world's semi-arid rangelands on a range of soil types and vegetation communities [14]. *Collema coccophorum* and *Heppia despreauxii* are cyanolichens, possessing as their photobionts cyanobacteria (blue-green algae) which are capable of nitrogen fixation. Their position as outliers on the 'crust' vector of *figure 4* suggests that they often occur as individual squamae in landscapes where crusts are poorly developed. Rogers [41] referred to these taxa as pioneers as they tended to occur early in the successional development on soil surfaces, and did not appear to be adversely affected by grazing [42]. In eastern Australia, Eldridge [14] found that the lichen *Collema coccophorum* which occurred at 65 % of 282 sites surveyed, was often found partially buried in the soil surface, suggesting that it is capable of occupying unstable microsites. In the western United States however, *Collema* spp. are known to be susceptible to animal impact [2]. As a group however, the gelatinous lichens, of which *Collema* is a member, are less susceptible to disturbance than other groups of lichens [19].

The location of this 'pioneer' group midway between the groves and runoff zones is consistent with what is known about landscape evolution in these patterned landscapes. The generally accepted view is that the vegetated bands migrate upslope by erosion downslope of the groves, sometimes referred to as the zone of senescence [52]. Erosion proceeds within this small zone of increasing slope, which is up to 30–50 cm across, gradually cutting back into the zone of senescing *Callitris* trees at the lower edge of the groves. This intermediate region would be expected to have low levels of soil nutrients, as well as high soil insolation, high runoff and high erosion. Consequently, vascular plant cover is sparse. Given the higher slopes in these bands and the relatively smooth surfaces, there is little opportunity for infiltration to occur. Cyanolichens are better suited to extreme conditions by their unique structure which makes them more efficient at water absorption and therefore extends the period over which they can photosynthesise [3, 24]. Thus pioneering cyanolichens such as *Collema coccophorum* are able to photosynthesise at higher temperatures than other green algal lichens [34]. These lichens pave the way for the 'generalist' mosses *Bryum pachytheca* and *Gigaspermum repens* as the systems' stabilisers.

4.5. Group V. The erosion tolerators

Sites characterised by relatively smooth surfaces with extensive scarp erosion, sheet erosion and loose surface sand are found in the top right corner of *figure 4*. These actively eroding runoff sites were characterised by crusts dominated by lichens, particularly *Endocarpon rogersii*, at relatively low cover levels (24 %), but also supported the mosses *Bryum argenteum*, *Didymodon torquatus* and *Desmatodon convolutus*. Although experiencing episodes of erosion in the past, active erosion only occurs in those patches where lichens are absent. Where the lichens occur, they protect the soil surface from water erosion, reducing sediment detachment and helping to trap eroding sand particles. The intimate relationship between the lichen thallus and the soil surface results in small levels of surface microtopography, generally less than 3–5 mm. These erosion tolerant mosses are ubiquitous in the arid zone of eastern Australia [20]. Furthermore, these mosses do not have strong preferences for sites of a particular condition, but are found in degraded as well as well-managed sites [18]. In particular, the cosmopolitan moss *Bryum argenteum* thrives in disturbed or inhospitable environments such as on pavements and roads [6]. Its position at the apex of the 'sheeting' vector suggests that it is able to grow in areas of active erosion. Being short and relatively stout, *Bryum argenteum* may not be able to withstand inundation in lower-lying areas or sites with greater competition from vascular plants.

4.6. Group VI. The shade tolerators

As well as the dense litter cover, the mosses *Fissidens vitattus* and *Barbula hornschuchiana* were associated with weakly coherent (non-hardsetting), non-cracking soil surfaces characteristic of surfaces beneath the *Callitris glaucophylla* canopies in the runon zones or groves. Their position away from the 'crust' cover vector suggests that these mosses do not occur as part of a well-developed soil crust, but rather as individuals. Furthermore, given the high projected foliage cover provided by the *Callitris* trees, these sites would be expected to have low levels of incoming radiation. These species could therefore be termed the 'shade tolerators'.

5. CONCLUSIONS

The measured environmental variables explained 60 % of the variation in lichen and bryophyte distribution at this patterned *Callitris glaucophylla* woodland in eastern Australia. Of the variables, litter cover, sheet and scarp erosion, soil coherence and stability were the most important. Despite this, other unmea-

sured biotic and abiotic factors may have been influential. For example, small changes in unmeasured microhabitat variables such as light intensity, soil moisture, soil fertility and micro-infiltration may have accounted for some of the unexplained variation in species distribution. Equally important might have been ecological processes such as competition, dispersal and recruitment, factors which are poorly understood in non-vascular plants.

In this patterned *Callitris glaucophylla* woodland, bryophytes and lichens were strongly patterned according to complex interactions between soil surface condition, erosion and vascular plants. Clearly defined groups of species were strongly associated with the three geomorphic zones, and looser species assemblages tended to occur at the intergrades between these zones. These results increase our understanding of the relationships between individual soil crust components and geomorphic processes such as erosion and deposition. Their predominance in terms of cover and biodiversity on some of these landscapes is clearly central to the functioning of these important patterned environments.

Acknowledgments

Merrin Tozer assisted with field data collection and identification of lichens and bryophytes. Terry Koen and Bob Gittins provided advice on analysis of the data using correspondence and canonical correspondence analyses, and Jayne Belnap provided useful comments on an early draft. This work was financed by the Land and Water Resources Research and Development Corporation and is publication No. CNR98.034 of the Centre for Natural Resources.

REFERENCES

[1] Ambouta K., Contribution à l'édaphologie de la Brousse tigrée de l'Ouest nigerien, thèse de Docteur-Ingenieur, université Nancy-I, 1984, 116 p.

[2] Belnap J., Surface disturbances: their role in accelerating desertification, Environ. Monitor. Assess. 37 (1995) 39–57.

[3] Blum O.B., Water relations, in: Ahmadjian V., Hale M.E. (Eds.), The Lichens, Academic Press, New York, London, 1973, pp. 381–400.

[4] Bryannah M., The use of ants as bioindicators of ecosystem health under grazing use in a patterned semi-arid mulga (*Acacia aneura*) woodland in eastern Australia, B.Sc (Hons.) thesis, Australian National University, Canberra, 1995.

[5] Bureau Of Meteorology, Selected tables of Australian rainfall and related data, Bureau of Meteorology, Melbourne, Victoria, Australia, 1961.

[6] Catcheside D.G., Mosses of South Australia, D.J. Woolman, Government Printer, South Australia, 1980, 364 p.

[7] Cornet A.F., Montana C., Delhoume J.P., Lopez-Portillo J., Water flows and the dynamics of desert vegetation stripes, in: Hansen A.J., di Castri F. (Eds.), Landscape Boundaries Consequences for Biotic Diversity and Ecological Flows, Ecological Studies, Springer Verlag, New York, 1992, pp. 327–345.

[8] Danin A., Gaynor E., Trapping of airborne dust by mosses in the Negev Desert, Israel, Earth Surf. Process. Landf. 16 (1991) 153–162.

[9] Downing A.J., Selkirk P.M., Bryophytes on the calcareous soils of Mungo National Park, and arid area of southern central Australia, Great Basin Nat. 53 (1993) 13–23.

[10] Dunkerley D.L., Brown K.J., Runoff and runon areas in a patterned chenopod shrubland, arid western New South Wales, Australia: characteristics and origin, J. Arid Environ. 30 (1995) 41–55.

[11] Eddy J., Humphreys G.S., Hart D.M., Mitchell P.B., Fanning P.C., Vegetation arcs and litter dams: similarities and differences, Abstract, Banded Vegetation Patterning in Arid and Semi-Arid Environments: Ecological Processes and Consequences for Management, April 1996, Paris, France, 1996, pp. 95.

[12] Ehrmann M., Galle S., Seghieri J., Valentin C., Patterning and pioneer processes of a herbaceous front in a tiger bush, Abstract, Banded Vegetation Patterning in Arid and Semi-Arid Environments: Ecological Processes and Consequences for Management, April 1996, Paris, France, 1996, pp. 27–28.

[13] Eldridge D.J., Cryptogam cover and soil surface condition: effects on hydrology on a semi-arid woodland soil, Arid Soil Res. Rehab. 7 (1993) 203–217.

[14] Eldridge D.J., Distribution and floristics of terricolous lichens in soil crusts in arid and semi-arid New South Wales, Australia, Aust. J. Bot. 44 (1996) 581–599.

[15] Eldridge D.J., Soil crust lichens and mosses on calcrete-dominant soils at Maralinga in arid South Australia, J. Adelaide Bot. Gardens 18 (1998) 9–24.

[16] Eldridge D.J., Trampling of microphytic crusts on calcareous soils and its impact on erosion under rain-impacted flow, Catena 33 (1998) 221–239.

[17] Eldridge D.J., Greene R.S.B., Assessment of sediment yield from a semi-arid red earth with varying cover of cryptogams, J. Arid Environ. 26 (1994) 221–232.

[18] Eldridge D.J., Koen T.B., Cover and floristics of microphytic soil crusts in relation to indices of landscape health, Plant Ecol. 137 (1998) 101–114.

[19] Eldridge D.J., Rosentreter R., Morphological groups: a framework for monitoring microphytic crusts in arid landscapes, J. Arid Environ. 41 (1999) 11–25.

[20] Eldridge D.J., Tozer M.E., Distribution and floristics of bryophytes in soil crusts in semi-arid and arid eastern Australia, Aust. J. Bot. 44 (1996) 223–247.

[21] Eldridge D.J., Tozer M.E., Soil crust *Xanthoparmeliae*: key indicators of rangeland health in semi-arid New South Wales, Aust. Lichenol. Newslett. 38 (1996) 19–20.

[22] Eldridge D.J., Lepage M., Bryannah M.A., Ouedraogo P., Soil biota in patterned landscapes, in: Valentin C., Tongway D.J., d'Herbes J.M., Seghieri J. (Eds.), Banded Vegetation Patterning in Arid and Semi-Arid Environments: Ecological Processes and Consequences for Management, Springer-Verlag, 1999, in press.

[23] Filson R.B., Rogers R.W., Lichens of South Australia, Government Printer, South Australia, 1979.

[24] Galun M., Bubrick P., Garty J., Structural and metabolic diversity of two desert-lichen populations, J. Hattori Bot. Lab. 53 (1982) 321–324.
[25] Gillison A.N., Brewer K.R.W., The use of gradient directed transects or gradsects in natural resource surveys, J. Environ. Manag. 20 (1985) 103–127.
[26] Gittins R., Canonical Analysis. A Review with Applications in Ecology, Springer-Verlag, Berlin, 1985.
[27] Greenacre M.J., Theory and Applications of Correspondence Analysis, Academic Press, London, 1984.
[28] Greene R.S.B., Soil physical properties of three geomorphic zones in a semi-arid mulga woodland, Aust. J. Soil Res. 30 (1992) 55–69.
[29] Greene R.S.B., Kinnell P.I.A., Wood J.T., Role of plant cover and stock trampling on runoff and soil erosion from semi-arid wooded rangelands, Aust. J. Soil Res. 32 (1994) 953–973.
[30] Hale M.E., The Biology of Lichens, 2nd ed., Edward Arnold, London, 1974.
[31] Hawksworth D.L., Hill D.J., The Lichen-Forming Fungi, Blackie, Glasgow, 1984.
[32] John E., Dale M.R.T., Environmental correlates of species distribution in a saxicolous lichen community, J. Veg. Sci. 1 (1990) 385–392.
[33] Johnston D., Milthorpe P.L., Land Systems Series Sheet SI55-2 Nymagee, Soil Conservation Service of NSW, Australia, 1984.
[34] Lange O.L., Kidron G.J., Budel B., Meyer A., Kilian E., Abeliovitch A., Taxonomic composition and photosynthetic characteristics of the biological soil crusts covering sand dunes in the western Negev Desert, Funct. Ecol. 6 (1992) 519–527.
[35] Longton R.E., The role of bryophytes and lichens in terrestrial ecosystems, in: Bates J.W., Farmer A.M. (Eds.), Bryophytes and Lichens in a Changing Environment, Cambridge Press, Oxford, 1992, pp. 32–76.
[36] Ludwig J.A., Tongway D.J., Monitoring the condition of Australian arid lands: linked plant-soil indicators, in: McKenzie D.H., Hyatt D.E., McDonald V.J. (Eds.), Ecological Indicators, Elsevier Applied Science No. 1, 1993, pp. 765–772.
[37] Mabbutt J.A., Fanning P.C., Vegetation banding in arid Western Australia, J. Arid Environ. 12 (1987) 243–250.
[38] McCarthy P.M., Checklist of Australian Lichens, 4th ed., National Herbarium of Victoria, Melbourne, 1991.
[39] Minitab, MINITAB Reference Manual, Release 8, Minitab Inc., State College, Pennsylvania, 1991.
[40] Montana C., The colonisation of bare areas in two-phase mosaics of an arid ecosystem, J. Ecol. 80 (1992) 315–327.
[41] Rogers R.W., Lichens from the T.G.B. Osborn vegetation reserve at Koonamore in arid South Australia, Trans. R. Soc. Sth. Aust. 98 (1974) 113–124.
[42] Rogers R.W., Lange R.T., Soil surface lichens in arid and sub-arid south-eastern Australia, I., Introduction and floristics, Aust. J. Bot. 20 (1972) 197–230.
[43] Scott G.A.M., Desert bryophytes, in: Smith A.J.E. (Ed.), Bryophyte Ecology, Chapman and Hall, London, 1982, pp. 105–122.
[44] Scott G.A.M., Southern Australian Liverworts, Aust. Govt. Publ. House, Canberra, ACT, 1985.
[45] Scott G.A.M., Stone I.G., The Mosses of South Australia, Academic Press, London. 1976.
[46] Serpantie G., Tezenus du Montcel L., Valentin C., La dynamique des états de surface d'un territoire agropastoral soudano-sahélien sous aridification climatique : conséquences et propositions, in: Le Floc'h E., Grouzis M., Bille J.C. (Eds.), L'aridité, une contrainte au développement, Orstom édition, Collection didactiques, Paris, 1991, pp. 419–448.
[47] Shirazi A.M., Muir P.S., McCune B., Environmental factors influencing the distribution of *Lobaria oregana* and *L. Pulmonaria,* Bryologist 99 (1996) 12–18.
[48] Soil Survey Staff, Soil taxonomy: a basic system of soil taxonomy for making and interpreting soil survey, USDA Agric. Handbook No. 436, Govt. Printer, Washington DC, 1975.
[49] Stace H.C.T., Hubble G.D., Brewer R., Northcote K.H., Sleeman J.R., Mulcahy M.J., Hallsworth E.G., A Handbook of Australian Soils, Rellim Technical Publications, South Australia, 1968.
[50] Streimann H., Curnow J., Catalogue of Mosses of Australia and its External Territories, Australian Government Publishing Service, Canberra, 1989.
[51] ter Braak C.J.F., Canonical correspondence analysis: a new eigenvector technique for multivariate direct gradient analysis, Ecology 67 (1986) 1167–1179.
[52] Thiery J.M., d'Herbes J.M., Valentin C., A model simulating the genesis of banded vegetation patterns in Niger, J. Ecol. 83 (1995) 497–507.
[53] Tongway D.J., Rangeland Soil Condition Assessment Manual, CSIRO, Melbourne, 1993.
[54] Tongway D.J., Ludwig J.A., Vegetation and soil patterning in semi-arid mulga lands of eastern Australia, Aust. J. Ecol. 15 (1990) 23–34.
[55] Tongway D.J., Ludwig J.A., Small-scale resource heterogeneity in semi-arid landscapes, Pac. Conserv. Biol. 1 (1994) 201–208.
[56] Valentin C., Sealing, crusting and hardsetting soils in Sahelian agriculture, in: So H.B., Smith G.D., Raine S.R., Schafer B.M., Loch R.J. (Eds.), Sealing, Crusting and Hardsetting Soils: Productivity and Conservation, Aust. Soc. Soil Sci. Inc. (Qld. Branch), Brisbane, 1995, pp. 53–76.
[57] Whitford W.G., The importance of the biodiversity of soil biota in arid ecosystems, Biol. Conserv. 5 (1996) 185–195.
[58] Wickens G.E., Collier F.W., Some vegetation patterns in the Republic of the Sudan, Geoderma 6 (1971) 43–59.
[59] Willis J.H., The vegetation of Hattah Lakes National Park, National Parks Authority, Victoria, 1970.

Acta Oecologica **20** (3) (1999) 171–183 / © Elsevier, Paris

Short range co-operativity competing with long range inhibition explains vegetation patterns

Olivier Lejeune [a], Pierre Couteron [b], René Lefever [a*]

[a] *Faculté des Sciences, CP 231, Université Libre de Bruxelles, B-1050 Bruxelles, Belgium.*
[b] *École nationale du génie rural des eaux et forêts (ENGREF), B.P. 5093, 34033 Montpellier cedex 01, France.*
* *Corresponding author (fax: +32 2 650 57 67; e-mail: rlefever@ulb.ac.be)*

Received March 17, 1997; revised February 10, 1999; accepted March 15, 1999

Abstract — We model the non-local dynamics of vegetation communities and interpret the formation of vegetation patterns as a spatial instability of intrinsic origin: the wavelength of the patterns predicted within the framework of this approach is determined by the parameters governing the dynamics rather than by boundary conditions and/or geometrical constraints. The spatial periodicity results from an interplay between short-range co-operative interactions and long-range self-inhibitory interactions inside the vegetation community. The influence of environmental anisotropies on pattern symmetry and orientation is discussed. As a case study, the approach is applied to a system of vegetation bands situated in the north-west of Burkina Faso. The parameters describing the co-operative and inhibitory interactions at the origin of the patterns are evaluated. © Elsevier, Paris

Tiger bush / vegetation dynamics / non-local interactions / intrinsic symmetry breaking / instability / effects of anisotropy

1. INTRODUCTION

In many uninhabited arid regions of the African, American and Australian continents, one finds vast territories where the vegetation is distributed non-uniformly with a spatial periodicity in the order of 10 to 500 m (see *table I*). Generically, these large botanical and ecological structures are called 'vegetation patterns'. They have also been given more specific names, such as vegetation arcs, bands, stripes, lanes, groves, tiger bush, spotted bush and pearled bush, which describe different modes of patterning. The differences in aspect, symmetry, or orientation existing between these modes are phenotypical rather than fundamental. They represent various manifestations of a general botanical phenomenon. The following observations have been made concerning its occurrence:

– Influence of aridity: Vegetation patterns are a characteristic landscape in arid regions where rainfalls are intense, rare and of short duration. Such climatic conditions prevail over one third of the earth's surface [34, 43]. These patterns are not specific to particular plants or soils. They may consist of herbs and grasses as well as shrubs and trees; they have been observed on soils which range from sandy and silty to clayey [2, 15, 22, 23, 33, 38, 41, 44, 45, 46, 47]. Comparing patterns consisting of the same vegetation shows that, on average, vegetation density diminishes as aridity increases. Simultaneously, the size of the spatial periodicities increases. Typically, the vegetated bands of tiger bush (also often called vegetation stripes), become less densely populated while, at the same time, the sum of the vegetated band width and of the bare inter-band width, i.e. the pattern wavelength, increases [11, 16, 42].

– Influence of environmental anisotropy: As most ecological systems, vegetation patterns are subjected to environmental factors, such as the direction of dominant winds, the sun's course in the sky, the slope of the ground surface, etc., which break the isotropy of space. But none of these 'extrinsic anisotropies' displays a spatial periodicity which per se can impose the emergence of a well-defined wavelength in the organisation of vegetal communities. They can however determine the symmetry properties and/or pattern orientation. In this respect, numerous evidences indicate that the existence of a small slope, on which water flows without forming drainage channels, orients veg-

Table I. General characteristics of vegetation patterns in different geographic regions. h, Height; w, width; s, spacing; l, length.

Region	Type of vegetation	Patterns	Slope, orientation	Authors
British Somaliland	acacias, bushes and trees (h: 6–10 m)	arcs w: 30–40 m s: 120–130 m l: 0.5–1 km	1:400, perpendicular	[23]
		lanes w: 80–100 m s: 80–400 m l: 3–4 km	parallel	
Sudan	grass	stripes w: 8–12 m s: 20–30 m	1:160 to 1:300, perpendicular	[45]
	trees (h: 4–5 m)	arcs w: 40–50 m s: 50–60 m l: 150–300 m	1:200 to 1:50	[44]
Western Australia	tall shrubland, low woodland dominated by *Acacia aneura* (h: 2–7.5 m)	bands w: 10–40 m s: 15–120 m l: 1–3 km	1:50 to 1:500, perpendicular	[21]
South Africa	thorny wooded shrub, grassland (h: 3–5)	stripes w: 20–50 m s: 20–50 m	less than 1:100	[38]
Mexico	grassland (h: 15–60 cm)	stripes w: 20–70 m s: 60–280 m l: 100–300 m	1:100 to 1:400, perpendicular	[6]
	shrub (h: 1–2.5 m)			
Jordan	shrub	arcs and lines w: 5 m s: 25–100 m l: 300–800 m	almost flat parallel and perpendicular	[41]
Southern Niger	*Combretum* woodland (h: 4 m)	stripes w: 20–40 m s: 35–150 m	less than 1:100, perpendicular	[42]

etation stripes [4, 13, 21, 28]. The orientation adopted by the stripes can be either orthogonal to the ground slope, i.e. parallel to the contour lines, or parallel to the ground slope [3, 13, 23, 41]. In the former case, an up-slope migration of the stripes has been observed for grass patterns [45]. This invalidates the hypothesis that an underlying soil pattern causes the formation of vegetation stripes: it is unrealistic to think that a soil's property moves upward and drives the stripe migration. Up-slope motion has also been advocated with trees and bushes, but on a much slower time scale [6, 13, 27, 36], whilst several other authors remained sceptical [42, 44].

In this paper, we discuss how vegetation patterns can occur as a consequence of processes which are totally 'intrinsic' to the vegetation dynamics and which are at work even in an isotropic environment imposing no oriented constraint or boundary condition upon the vegetation. We show that the pattern's wavelength is determined by the kinetic parameters associated with the plant's life cycle and by the parameters controlling inter-plant interactions. The principal ingredients explaining the patterning phenomenon are the aridity of the environment and the existence of co-operative and inhibitory interactions operating over different ranges. Remarkably, this ex-

planation works without requiring the involvement of a ground slope. It contrasts with the point of view, often expressed [10, 13, 14, 20, 45], that a slope is of primary importance for the formation of patterns. We also bring some clarification concerning the role of environmental anisotropy as a 'mechanism of pattern selection'; the switching between organisations exhibiting different symmetry properties, e.g. hexagonal symmetry versus stripes, is exemplified. We find that the orientation of the patterns with respect to a direction of anisotropy depends on whether this anisotropy influences co-operative or inhibitory interactions.

We base our discussion on an extension to botanical ecosystems of the logistic equation initially introduced by Verhulst in 1848 and used since then in various biological and non biological contexts (for reviews, see e.g. [9, 17, 25, 30]). In the next section, we briefly recall the assumptions underlying our approach. Subsequently, we discuss its properties under isotropic and anisotropic environmental conditions. As a case study in section 4, the approach is applied to a system of vegetation bands situated in the north-west of Burkina Faso.

2. A GENERALISED VERHULST EQUATION: THE π-MODEL

2.1. Formulation of the model

As a starting point for studying the mechanisms of pattern formation of vegetal communities, we consider a logistic equation of the form [18]:

$$\frac{\partial \rho(\mathbf{r}, t)}{\partial t} = F_1 \times F_2 - F_3$$

$$= \left[\int d\mathbf{r}' w_1(\mathbf{r}', L_1) f_1(\rho(\mathbf{r} + \mathbf{r}', t)) \right] \times$$

$$\left[\int d\mathbf{r}' w_2(\mathbf{r}', L_2) f_2(\rho(\mathbf{r} + \mathbf{r}', t)) \right] -$$

$$f_3(\rho(\mathbf{r}, t)) \qquad (1)$$

where $\rho(\mathbf{r}, t)$, $\rho(\mathbf{r} + \mathbf{r}', t)$ represent the epigeneous phytomass density (units: kg·m^{-2}) at time t, at space points $\mathbf{r}$ and $\mathbf{r} + \mathbf{r}'$. This density is defined as the plant total phytomass (including the necromass) per unit area. Considering a global variable, ρ, including all vegetal species present, is justified for patterns formed by a one-species pure strand and in all cases where genotypic differences and age classes can be neglected. When several species are present, it amounts to assuming that the dominant species imposes its spatial distribution [14]. We do not describe explicitly the inter-species dynamics. A less global treatment of the space-time behaviour of vegetal communities, based on a discrete cellular automata model, has been proposed recently by Mauchamp et al. [24] and Thiéry et al. [35].

The term $F_1 \times F_2$ models vegetation propagation and maturation; the term F_3 models vegetation death. Writing the former term as a product of two functions accounts for the fact that vegetation development involves processes fulfilling different biological functions, depending upon different plant structures and influenced by different systemic agents. The major distinction we make here is between processes the activation of which increases the phytomass density, which we associate with the 'propagation distribution function' F_1 (units: kg·m^{-2}·s^{-1}), and processes which, on the contrary, limit the phytomass density, which we associate with the (dimensionless) 'inhibition distribution function' F_2. The first processes mostly involve plant aerial structures, such as the canopy. They correspond to reproduction, seed dissemination, germination and the maturation of new plants. The second processes mostly involve the root system and the uptake of nutrients. They rely on the availability of free soil, which new vegetation may colonise, and on soil resources which are in limited supply. The time-evolution of ρ at point $\mathbf{r}$ depends at least in part on the plants living within the neighbourhood of the point $\mathbf{r}$ considered, e.g. at $\mathbf{r} + \mathbf{r}'$. Adopting a mean field approach, continuous in time and in space, we associate to each point of the vector field $\mathbf{r}' + \mathbf{r}$ the propagation and inhibition densities, $w_1(\mathbf{r}', L_1)$ $f_1(\rho(\mathbf{r} + \mathbf{r}', t))$ (units: kg·m^{-4}·s^{-1}) and $w_2(\mathbf{r}', L_2)$ $f_2(\rho(\mathbf{r} + \mathbf{r}', t))$ (units: m^{-2}) which introduce the weighting functions $w_1(\mathbf{r}', L_1)$ and $w_2(\mathbf{r}', L_2)$ (units: m^{-2}). The parameters L_1 and L_2 control the steepness with which the weighting functions vary. They have the dimension of a length and determine the range over which propagative and inhibitory interactions operate.

Regarding F_3 and the kinetics governing vegetation death, we suppose that plants do not kill each other at a distance or, at least, do not do so over distances comparable to L_1 and L_2. Vegetation death is modelled as a local process the rate of which is proportional to the vegetation density at the point $\mathbf{r}$:

$$F_3 = f_3(\rho(\mathbf{r}, t))$$

$$= d\,\rho(\mathbf{r}, t) \qquad (2)$$

From a biological point of view, this simplification is plausible. It is noteworthy that its validity also conditions the use of a mean field treatment [18]. The rate constant d (units: s^{-1}) represents the inverse of the vegetation lifetime. When the vegetation consists of several species, having different lifetimes, an effective $< d >$ can be defined by weighting the lifetime of each species according to its average phytomass density $< \rho_i >$:

$$<d> = \sum_i d_i \frac{<\rho_i>}{S}, \quad \text{where} \quad S = \sum_i <\rho_i> \quad (3)$$

To specify the propagation and inhibition functions f_1, and f_2, we consider their Taylor expansion in terms of the vegetation density ρ (it is superfluous to explain the space and time dependency of ρ here). The dominant terms of $f_1(\rho)$ read (prime $'$ denotes derivation with respect to ρ):

$$f_1(\rho) = f_1(0) + f_1'(0)\,\rho + \frac{1}{2} f_1''(0)\,\rho^2$$
$$= \rho\left[f_1'(0) + \frac{1}{2} f_1''(0)\,\rho\right] \quad (4)$$

By definition, the propagation distribution function F_1 vanishes in the absence of vegetation which implies that $f_1(0) = 0$ in equation (4); $f_1'(0)$ determines the rate at which phytomass increases when its density is small. The term quadratic in the density, $\frac{1}{2} f_1''(0)\,\rho^2$, amounts to a feedback effect of the vegetation on its propagation rate. Clearly, this feedback is co-operative (anti-co-operative) if $f_1''(0)$ is positive (negative). The dominant terms in the Taylor expansion of $f_2(\rho)$ read

$$f_2(\rho) = f_2(0) + f_2'(0)\,\rho \quad (5)$$

By definition, the inhibion distribution function F_2 is positive and decreases with ρ. The inequalities $f_2(0) > 0$ and $f_2'(0) < 0$ must hold, so that vegetation development is turned off as the phytomass density gets high and approaches the ratio

$$K = -\frac{f_2(0)}{f_2'(0)} \quad (6)$$

which has the dimensions of a vegetation density, and represents the territory's carrying capacity. The notion of carrying capacity expresses that environmental resources put an upper bound on the phytomass density. The very fact that mature plants have a size and thus need a minimum of physical space puts an upper bound to their density. K is the 'close packed density' of a fully occupied territory.

In practice, the quantities introduced in equations (4–6) can be estimated as follows. Knowing the average mass m and average area σ occupied by an isolated adult plant one has that

$$K = \frac{m}{\sigma}$$

The product $f_1'(0)\,f_2(0)$, the units of which are the inverse of a time, determines the vegetation reproduction-maturation time scale. Setting

$$f_1'(0)\,f_2(0) = \frac{\ln 2}{t_{1/2}} \quad (7)$$

where $t_{1/2}$ is the phytomass density doubling time, provides an estimate of it. Alternatively, $t_{1/2}$ could be identified with the time it takes for the vegetation density to recover its usual level after having been halved by some external cause, such as e.g. the action of man, grazing, fire, unusual drought, etc.

Taking equation (7) as unit of time, the inhibition range L_2 as unit of length and the carrying capacity K as unit of vegetation density, we redefine time, space, vegetation density and vegetation inverse life time by setting

$$\{t, \mathbf{r}, \rho, d\} = \left\{\frac{t_{1/2}}{\ln 2}\,\tau, \tilde{\mathbf{r}}\,L_2, \tilde{\rho}\,K, \frac{\ln 2}{t_{1/2}}\,\mu\right\} \quad (8)$$

As a measure of (anti-)co-operative feedbacks and of the range of interactions, we introduce the dimensionless parameters

$$\Lambda = \frac{f_1''(0)}{2 f_1'(0)} K \quad \text{and} \quad L = \frac{L_1}{L_2} \quad (9)$$

At this stage, one can already guess that within the framework of equation (1), the emergence of periodic patterns characterised by a well-defined wavelength arises from the competition between propagative and inhibitory interactions operating over different ranges. We shall therefore call equation (1) the 'propagator-inhibitor model', or in brief, the π-model.

2.2. Isotropic version of the π-model

For the model to be operational, the propagation and inhibition densities as well as their weighting functions must be specified. This requires that environmental conditions and vegetation kinetics be further specified. To begin with, we consider the ideal situation of an environment having no structure of its own. Space is then isotropic, meaning that all space points and

directions are equivalent. Consequently, the weighting functions are invariant under rotation. In first approximation, it is reasonable to assume that they are Gaussian normalised decreasing functions of the distance $|\mathbf{r}'|$ separating the points $\mathbf{r}' + \mathbf{r}$ and $\mathbf{r}$:

$$w_i(\mathbf{r}', L_i) = \frac{1}{2\pi L_i^2} \exp(-|\mathbf{r}'|^2 / 2L_i^2), \quad i = 1, 2 \qquad (10)$$

Placing equations (2–10) in equation (1) yields the isotropic version of the π-model:

$$\frac{\partial \rho(\mathbf{r}, \tau)}{\partial \tau} = \left[\frac{1}{2\pi L^2} \int d\mathbf{r}' e^{-\frac{|\mathbf{r}'|^2}{2L^2}} \rho(\mathbf{r} + \mathbf{r}', \tau) \cdot (1 + \Lambda \rho(\mathbf{r} + \mathbf{r}', \tau)) \right] \times \left[1 - \frac{1}{2\pi} \int d\mathbf{r}' e^{-\frac{|r'|^2}{2}} \rho(\mathbf{r} + \mathbf{r}', \tau) \right] - \mu \rho(\mathbf{r}, \tau) \qquad (1')$$

which allows us to study the mechanism governing pattern formation in botanical ecological systems in terms of only three, basic parameters: μ which is related to the aridity of the environment, Λ which determines the intrinsic co-operativity of the vegetation and L which controls the range of spatial interactions. To simplify notations, we have dropped the tildes over $\tilde{\mathbf{r}}$ and $\tilde{\rho}$ in equation (1').

We shall discuss later how the values of L_1, L_2 and Λ can be deduced from experimental observations. Before that, it is appropriate to examine the properties of the uniform stationary distributions predicted by equation (1').

2.3. Uniform stationary distributions

When the phyto-density is uniform, i.e. when ρ is a function of the normalised time τ only, equation (1') is reduced to the ordinary differential equation:

$$\frac{d\rho(\tau)}{d\tau} = \rho(\tau)\,[1 + \Lambda \rho(\tau)] \times [1 - \rho(\tau)] - \mu \rho(\tau) \qquad (11)$$

which for $\Lambda = 0$, is the classical Verhulst logistic equation. By definition, μ is non-negative ($\mu \in [0,\infty]$). Its increase amounts to a decrease of the plants life span relative to the time they need to reproduce and mature, which clearly models the effect of an increasingly arid environment. Hence, the most favourable environmental conditions is obviously $\mu = 0$, meaning that phytomass losses are negligible. The right hand side of equation (11) models a 'pure birth' process the rate of which vanishes only if no vegetation is present (the territory is a complete desert), i.e. if

$$\rho(\tau) = \rho_0 = 0 \qquad (12)$$

or if the vegetation density has reached its maximum value, i.e. if

$$\rho(\tau) = \begin{cases} -\frac{1}{\Lambda} & \text{for } \Lambda < -1 \\ 1 & \text{for } -1 \le \Lambda \end{cases} \qquad (13)$$

Thus, when $\mu = 0$, any $\rho(\tau)$, initially close to zero, monotonously increases in the course of time until asymptotically, for $\tau \to \infty$, it reaches the most densely populated state, i.e. either $-1/\Lambda$ or 1 depending on whether Λ is less or greater than -1. The trivial state ρ_0 is then unstable while the most densely populated states are stable. For $\mu > 0$ and $\tau \to \infty$, a vegetal population can only survive, if the non-trivial roots,

$$\rho_{\pm} = \frac{\Lambda - 1 \pm \sqrt{(\Lambda - 1)^2 + 4\Lambda(1 - \mu)}}{2\Lambda} \qquad (14)$$

of equation (11) are real and positive. They represent a homogeneous stationary state situation such that, at each point of the territory, the vegetation reproduction and death are exactly balanced. Depending on Λ and μ, two cases are possible.

2.3.1. Case 1: feedback effects are co-operative ($\Lambda > 0$)

When co-operativity is weak ($0 < \Lambda \le 1$), only the uniform branch of stationary solutions ρ_+ (curves drawn in full line in *figure 1*) is meaningful[1] in so far as $0 \le \mu \le 1$. When aridity (μ) increases, the vegetal population becomes sparser: ρ_+ monotonously decreases till zero which is reached for $\mu = 1$. At this point, ρ_+ intersects the trivial branch ρ_0. Subsequently, for $\mu > 1$, the trivial state ρ_0 is stable and remains the only stationary solution possible of equation (11). Vegetation survival is then impossible; the vegetation density can only tend to zero for $\tau \to \infty$. When co-operative interactions are strong ($\Lambda > 1$), the branch of solutions ρ_+ extends beyond $\mu = 1$, up to the turning point (μ^*, ρ^*) given by

$$\mu^* = \frac{(1 + \Lambda)^2}{4\Lambda}, \quad \rho^* = \frac{\Lambda - 1}{2\Lambda} \qquad (15)$$

[1] i.e. corresponds to real, non-negative values.

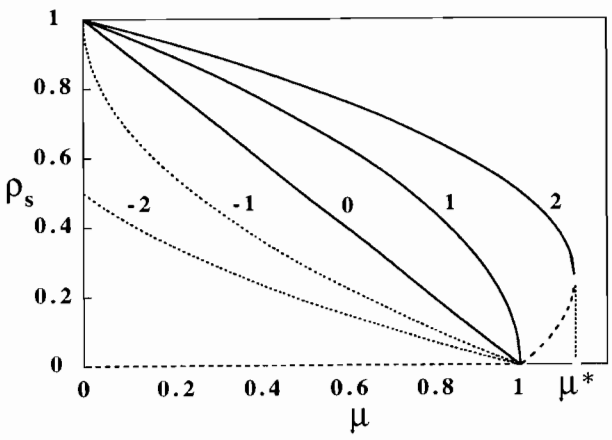

Figure 1. Uniform stationary distributions of vegetation ρ_s as a function of environmental aridity measured by μ, for different values of the vegetation feedback constant Λ (indicated on the curves). For $\Lambda = 0$, the stationary solution is simply the straight line $\rho_s = 1 - \mu$. The trivial uniform distribution, $\rho_0 = 0$, is always a solution of equation (11); it is unstable (dashed line) for $0 \leq \mu < 1$ and stable otherwise (full line). Strong inter-plant co-operative interactions ($\Lambda > 1$) give rise to a hysteresis loop allowing the survival of a stable vegetal population under environmental conditions harsher than those corresponding to $\mu = 1$.

Consequently, for $1 \leq \mu \leq \mu^*$, an hysteresis loop and a bistability phenomenon appear: both ρ_0 and ρ_+ are stable while ρ_-, which takes values in between these states (dashed curve in *figure 1*), is unstable. When $\mu > \mu^*$, only the trivial state ρ_0 is possible.

2.3.2. Case 2: feedback effects are anti-co-operative ($\Lambda < 0$)

For

$$-\infty < \Lambda < 0 \quad \text{and} \quad 0 \leq \mu \leq 1 \tag{16}$$

only the uniform stationary distributions given by ρ_+ are stable and meaningful. They correspond in general to a decrease of the average uniform vegetation density (dotted curves in *figure 1*). No hysteresis loop is possible; the stationary branch of solutions ρ_- (not drawn because unphysical) is unstable.

2.3.3. In conclusion

Within the framework of this model, the parameters μ and Λ suffice for completely unfolding the properties of uniform stationary vegetation distributions. The first one measures the degree of aridity of the environment: it controls the switching of the trivial state $\rho_0 = 0$ from instability (for $0 \leq \mu < 1$) to stability (for $\mu \geq 1$). In agreement with our assumption that non-local effects can be neglected in the kinetics governing vegetation death (cf. section 2.1) and its definition given by equation (8), μ can be estimated by using the relationship

$$\mu = \frac{<d>\, t_{1/2}}{\ln 2} \tag{17}$$

The switching point $\mu = 1$ then corresponds simply to the situation where the vegetation average lifetime and average maturation time are equal.

The second parameter upon which the uniform stationary distributions depend, Λ, controls the range of μ-values for which a vegetation population can survive at densities given by ρ_+. A crude estimation of Λ can be made by reasoning as follows (we shall indicate later a more reliable method of determination based on the spatial characteristics of the patterns themselves). First, we note that patterning can be viewed as a phenomenon of redistribution of the vegetation over space. In other words, the value of ρ_+, uniform stationary solution of equation (11), is likely to approximate the average density obtained by redistributing the pattern's vegetation over the entire territory, i.e.

$$\rho_+ \approx <\rho> = \frac{1}{A}\int d\mathbf{r}\, \rho(\mathbf{r}, \tau) \tag{18}$$

where A is the territory's surface. Next, we remember that vegetation patterns are typical of arid climates. We thus expect that their existence generally corresponds to values of μ close to 1, which suggests considering the Taylor expansion of ρ_+ in the neighbourhood of the switching point $\mu = 1$. Taking equation (18) into account, and limiting the expansion to the dominant term, this yields

$$<\rho> = \begin{cases} \dfrac{1-\mu}{1-\Lambda}, & \text{if } 0 \leq \Lambda < 1 \\ \dfrac{\Lambda - 1}{\Lambda}, & \text{if } 1 < \Lambda \end{cases} \tag{19}$$

which predicts, in the strongly co-operative case where Λ is greater than 1, the existence of a quite simple relationship between Λ and $<\rho>$:

$$\Lambda = \frac{1}{1 - <\rho>} \tag{20}$$

In the weakly co-operative case where Λ is less than 1, equation (19) predicts that $<\rho>$ should decrease like $-1/(1-\Lambda)$ as the aridity of the environment (μ) increases. When data on the behaviour of a given kind of vegetation under different aridity conditions are available, this relationship may serve for an approximate determination of Λ.

We demonstrate in section 3 that in the absence of co-operative feedback, vegetation patterns cannot form. Therefore, we are not interested here in investigating further the properties of uniform stationary state distributions corresponding to $\Lambda \leq 0$.

3. VEGETATION PATTERN FORMATION VIA A SYMMETRY BREAKING INSTABILITY

3.1. Isotropic environments

We now come back to equation (1') and the problem of pattern formation in isotropic environments to which this equation applies. The phenomena of symmetry breaking taking place under those conditions can only be of 'intrinsic origin', i.e. independent from the geometrical factors or boundary conditions imposed by the environments.

We study the stability of the uniform stationary distribution $\rho \equiv \{\rho_+,\rho_-\}$with respect to arbitrary, non-uniform perturbations $\delta\rho(\mathbf{r},\tau)$. In terms of two-dimensional Fourier modes one has

$$\delta\rho(\mathbf{r},\tau) = \frac{1}{2\pi}\int d\mathbf{k}\,\delta\tilde{\rho}(\mathbf{k},\tau)\,e^{i\mathbf{k}\cdot\mathbf{r}} \qquad (21)$$

where $\delta\tilde{\rho}(\mathbf{k},\tau) = e^{\omega_k\tau}\,\delta\tilde{\rho}(\mathbf{k},0)$ is the amplitude of the Fourier mode of wave vector $\mathbf{k}$, or equivalently, of wavelength $\lambda = 2\pi/k$, $k = |\mathbf{k}|$ being the modulus of $\mathbf{k}$. By placing equation (21) in equation (1') and linearising this equation, furnishes the dispersion relation

$$\omega_k = (1-\rho_s)(1+2\Lambda\rho_s)\,e^{-\frac{L^2k^2}{2}} - \rho_s(1+\Lambda\rho_s)\,e^{-\frac{k^2}{2}} - \mu \qquad (22)$$

The mode $\mathbf{k}$ is (un)stable if the sign of ω_k is (positive) negative. We look for conditions under which equation (22) admits a finite band of unstable wavenumbers k from which are excluded both the large modes, corresponding to spatial periodicities of the size of the plants themselves ($k \to \infty$), and the mode corresponding to spatially uniform perturbations ($k = 0$). This pattern formation mechanism, via a symmetry breaking instability, is the botanical analogue of the Turing instability which has been extensively studied in the field of chemical morphogenesis and reaction-diffusion systems [26, 30, 32, 37]. As is well-known, the so-called Turing critical point at which the instability appears is met when simultaneously:

$$(\omega_k)_{k=k_c} = 0\,, \quad \left(\frac{d\omega_k}{dk}\right)_{k=k_c} = 0 \quad \text{and} \quad \left(\frac{d^2\omega_k}{dk^2}\right)_{k=k_c} < 0 \qquad (23)$$

It is easy to show that these conditions can never be fulfilled in the anti-co-operative case where Λ is negative. Indeed: using the stationary state condition $\mu = (1-\rho_s)(1+\Lambda\rho_s)$, we may rewrite equation (22) as

$$\omega_k = -(1-\rho_s)(1+\Lambda\rho_s)\left(1-e^{-\frac{L^2k^2}{2}}\right) + \Lambda\rho_s(1-\rho_s)\,e^{-\frac{L^2k^2}{2}} - \rho_s(1+\Lambda\rho_s)\,e^{-\frac{k^2}{2}} \qquad (24)$$

Noting then that for $\Lambda < 0$, the non-trivial uniform stationary distributions are given by $\rho_s = \rho_+$ and that the inequality $0 < 1+\rho_+$ holds (cf. *figure 1*), one immediately finds that each term in equation (24) is negative. Thus, ω_k can never be equal to zero. Similarly, in the absence of feedback ($\Lambda = 0$), one immediately sees that a symmetry breaking instability is impossible.

For $\Lambda > 0$, the branch of stationary states ρ_+ is the extension for $\mu > 0$ of the stable state $\rho_s = 1$. Let us show that vegetation patterns may appear via a Turing instability of this branch when: (i) the co-operativity parameter Λ is strictly positive, and (ii) the propagation distribution function F_1 operates effectively over a shorter range than the inhibition distribution function F_2, i.e. the inequality $L = L_1/L_2 < 1$ holds. Since we are interested in periodicities corresponding to large wavelengths (small wave numbers), compared to the size of plants, it is appropriate to study the critical conditions (equation (23)) within the framework of the weak gradient limit[2] obtained by expanding equation (24) up

[2] For a more general treatment and a discussion of the consistency of this approximation see Lefever and Lejeune [18].

to $O(k^4)$. This transforms the dispersion relation ω_k into the polynomial expression

$$\omega_k = -\frac{1}{8}\rho_+(1+\Lambda\rho_+)k^4 + \frac{1}{2}[\rho_+(1+\Lambda\rho_+) - (1-\rho_+)(1+2\Lambda\rho_+)L^2]k^2 - \rho_+(1-\Lambda+2\Lambda\rho_+) \quad (25)$$

from which we straightforwardly derive, using the first two conditions of equation (23), that at the Turing critical point, the wave number k_c of the first mode becoming unstable and the corresponding value L_c of L read:

$$k_c = \left[8\frac{1-\Lambda+2\Lambda\rho_+}{1+\Lambda\rho_+}\right]^{(1/4)} \quad (26)$$

$$L_c = \sqrt{\frac{\left(1+\Lambda\rho_+ - \sqrt{2(1+\Lambda\rho_+)(1-\Lambda+2\Lambda\rho_+)}\right)\rho_+}{(1+\rho_+)(1+2\Lambda\rho_+)}} \quad (27)$$

The analysis of equations (25–27) demonstrates that:

(i) L_c is less than one for all physically acceptable values of Λ and ρ_+.

(ii) The values of ρ_+ close to one, as well as the values close to zero, are excluded from the domain of existence of the instability.

(iii) In agreement with experimental observations, the wavelength of the patterns (predicted as first approximation by the critical wavelength $\lambda_c = 2\pi/k_c$) increases as the aridity of the environment increases, i.e. for ρ_+ decreasing (μ increasing) and Λ constant.

(iv) As *figure 2* exemplifies, decreasing L, for fixed values of μ and Λ, in general destabilises the system and broadens the band of unstable modes.

(v) Different symmetries are possible for the patterns establishing themselves in the course of time (for $\tau \to \infty$) when ρ_+ becomes unstable. *Figure 3* reports a typical example showing that for a small variation in the parameter values, the patterns may switch from stripes to hexagonal symmetry.

The prediction that flat territories can support vegetation stripes steps aside from the traditional theory that a ground slope is a necessary factor for the formation of tiger bush [13, 14, 45]. The second kind of pattern, consisting of densely vegetated spots arranged on an hexagonal lattice, could be related to spotted [5] or pearly bush [3]. More recently, this kind of symmetry has been unambiguously identified by Couteron [7] in Burkina-Faso. We shall illustrate further the predictions of the model in the next section where we shall use it to analyse the tiger bush patterns studied by one of us (P. Couteron) in Burkina Faso. Before, we will very briefly indicate some results which clarify the 'pattern selection role' of environmental anisotropies.

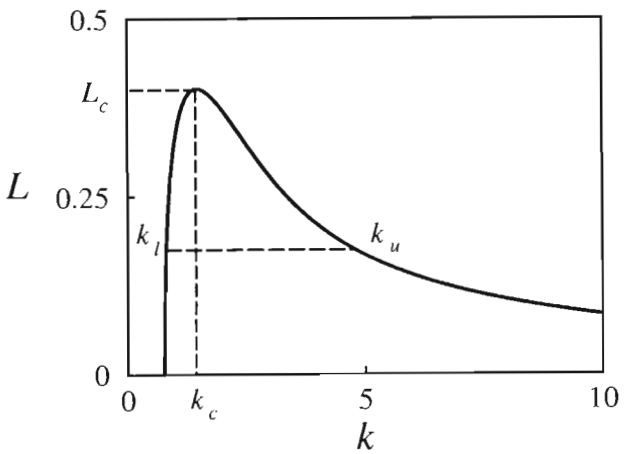

Figure 2. Band of unstable modes k as a function of L for $\mu = 1.1$ and $\Lambda = 2$. For $L > L_c$, all modes are stable; $L = L_c$, is the critical value at which $\omega_k = 0$ for $k = k_c$; when $L < L_c$, the modes between k_l and k_u are unstable. Vanishingly small modes and arbitrarily large modes are always stable for $L \neq 0$. When the ratio of reproduction and inhibition ranges, L tends to zero, k_l decreases to a finite value different from zero but k_u diverges. The case $L = 0$ needs a specific treatment and will not be considered here.

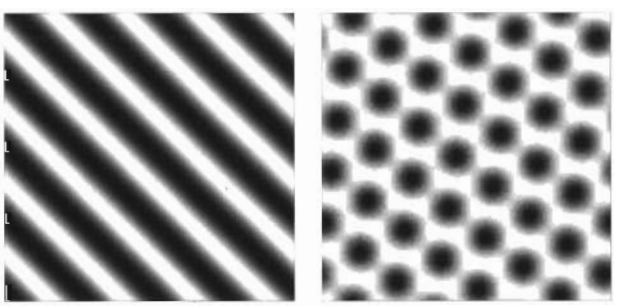

Figure 3. Patterns obtained by integrating the isotropic π-model (1′) for $\mu = 0.95$, $L = 0.1$ and two values of Λ. The integration domain is a square-shaped territory subjected to periodic boundary conditions. The initial condition is a slightly perturbed uniform stationary state distribution ρ_+ (Gaussian perturbations of zero mean and 1 % variance). The model predicts a pattern of stripes if $\Lambda = 1$ and a pattern of hexagonal symmetry if $\Lambda = 0.8$. As a consequence of the isotropy of space, the orientation finally adopted by the stripes and hexagons is determined by the random initial condition. Black corresponds to the highest phyto-density.

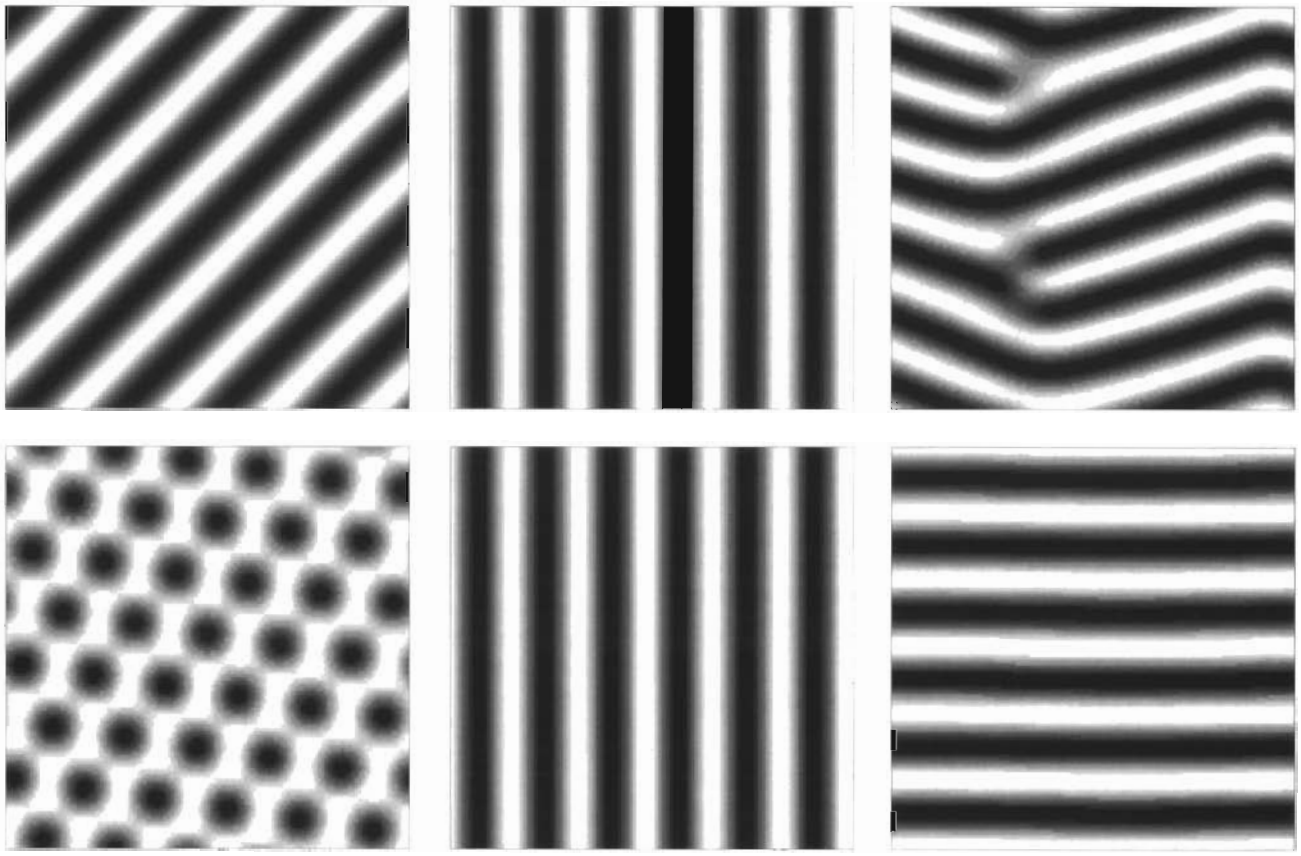

Figure 4. Influence of an anisotropic environmental factor oriented in the y-direction. The values of μ, Λ and L are the same as in the isotropic case described in *figure 3*; the patterns obtained for an isotropic environment are represented again on the left hand side of the figure (randomly oriented stripes and hexagons). The patterns in the middle and on the right hand side report the effect of anisotropy respectively on the propagator function ($t_1 = 1, t_2 = 0$) and on the inhibitor function ($t_1 = 0, t_2 = 1$). In the first case, both the randomly oriented stripes and the hexagons transform into vegetation stripes parallel to the anisotropy direction y; in the second case, the patterns transform into more or less wavy stripes orthogonal to the anisotropy direction y. Stripes parallel to the direction of anisotropy are globally static whereas orthogonal stripes migrate upward (in the positive y-direction).

3.2. Anisotropic environments

The influence of anisotropy on the symmetry breaking instability of the isotropic π-model is best seen by investigating the two situations where an environmental source of spatial anisotropy affects either only the propagation distribution function F_1 or the inhibition distribution function F_2. We have proposed a simple treatment permitting to deal with these situations [18]. It consists in introducing a bias in the weighting functions w_1, w_2 which fixes their mean to a non-zero value, respectively t_1 and t_2 for one of the plane directions, say the y-direction; in the x-direction, as before, no bias is introduced. The evolution equation for the epigeneous phytomass then becomes:

$$\partial_\tau \rho(r, \tau) = \left[\frac{1}{2\pi L^2} \int d\mathbf{r}' e^{-\frac{x'^2 + (y' - t_1)^2}{2L^2}} \rho(\mathbf{r} + \mathbf{r}', \tau) \cdot (1 + \Lambda\rho(\mathbf{r} + \mathbf{r}', \tau)) \right] \times \left[1 - \frac{1}{2\pi} \int d\mathbf{r}' e^{-\frac{x'^2 + (y' - t_2)^2}{2}} \rho(\mathbf{r} + \mathbf{r}', \tau) \right] - \mu\rho(\mathbf{r}, \tau) \quad (28)$$

Integrating this equation for the same values of μ, Λ, L as in the isotropic case considered above, but for two choices of values of t_1 and t_2, we obtain the results reported in *figure 4*. Remarkably, they demonstrate not

only that the presence of anisotropic factors determines the orientation of the patterns and their symmetry properties (stripes replace hexagons) but also that the orientation selected is either parallel or orthogonal to the direction of anisotropy depending on whether the latter affects propagation or inhibition.

On the other hand, the model also predicts that when the anisotropy affecting inhibition increases further, arc-shaped patterns perpendicular to the direction of anisotropy appear [18]. Vegetation arcs, the main axis of which is orthogonal to a ground slope, have been described by Greenwood [13] and Boaler and Hodge [3, 4]. A curvature of the ground surface is usually invoked in order to explain the origin of these structures. In contrast with widespread opinion, the model predicts that arcuate vegetation patterns can appear even if the ground gradient is constant. Finally, we may still mention that vegetation stripes parallel to the anisotropy direction are static whereas bands and arcs oriented at right angle to that direction move upward (at least for the sets of parameters considered in the simulations made so far (unpubl. results)).

4. A CASE STUDY: TIGER BUSH IN BURKINA FASO

The vegetation pattern represented in *figure 5* is located at and around 14°10' N and 2°28' W in the north-west part of Burkina Faso. Climate is tropical semi-arid; mean rainfall amounts to 490 mm·year^{-1} and potential evapotranspiration (Penman) is slightly under 2 000 mm·year^{-1} [8]. The vegetation under investigation grows on a gentle slope (around 1 %) located on Paleozoic sandstones. Soils are shallow (between 10 and 20 cm), and poorly developed on ferruginised sandstone debris, overtopping the unweathered sandstone (encountered around 60–80 cm depth). Vegetation belongs to the Sahel transition zone with most species related to the Sudanian centre of endemism [40]; it consists mainly of multistemmed shrubs/trees and of annual grasses. Dominant woody species are *Combretum micranthum* G. Don, and *Pterocarpus lucens* Lepr., which account respectively for 50 and 30 % of the total basal area. Average height of woody individuals is around 3 m [7]. The site experiences a low grazing pressure (mainly goats) but neither wood-cutting nor cultivation.

The aerial photograph was obtained on October 10, 1995 around 10h30 (U.T.), i.e. with a zenithal solar angle of about 38°. Pictures were taken from an elevation of 750 m with a Pentax ILX camera (50 mm focus and 35 mm lens). The film (Kodak Gold 100 ASA) was machine-processed into coloured

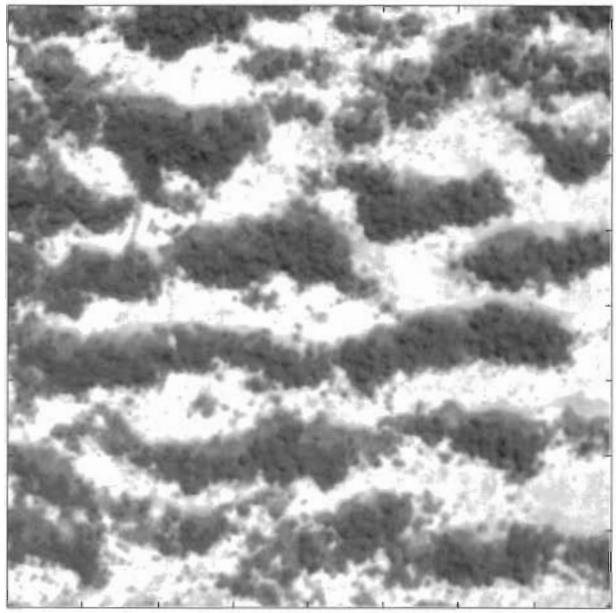

Figure 5. Banded system under investigation. The picture is oriented according to the main slope, with vegetation bands roughly following the contour. Note that herbaceous vegetation (intermediate grey tones), is mainly observed up-slope the woody thickets (dark grey).

7.5 × 5 cm printed outlooks, which have been numerised (grey-scale values in the range 0–255) at a resolution of 300 dots per inch (DPI) through a HP Scanjet scanner (pixel side equivalent to 0.8 m in the field). A square window of 400 × 400 pixels (i.e. 320 × 320 m in the field) was extracted for analysis (*figure 5*). On the picture, bright pixels correspond to bare soils, whereas dark ones are dominated by woody vegetation; intermediate grey-scale values can mainly be interpreted as being dense grass cover. Since continuous grass and woody vegetation have respective epigeneous phytomass averaging 1 500 kg·ha^{-1} and 2·10^4 kg·ha^{-1} ([19]; Couteron unpubl. data), grey-scale values can be seen as a monotonous function of the phytomass.

Fourier coefficients have been computed from the mean-corrected values z_{jk} contained in the digital image as:

$$a_{pq} = \frac{1}{n^2} \sum_{j,k}^{n} z_{jk} \cos\left[2\pi\left(\frac{pj}{n} + \frac{qk}{n}\right)\right]$$

$$b_{pq} = \frac{1}{n^2} \sum_{j,k}^{n} z_{jk} \sin\left[2\pi\left(\frac{pj}{n} + \frac{qk}{n}\right)\right] \quad \text{with} \quad n = 400$$

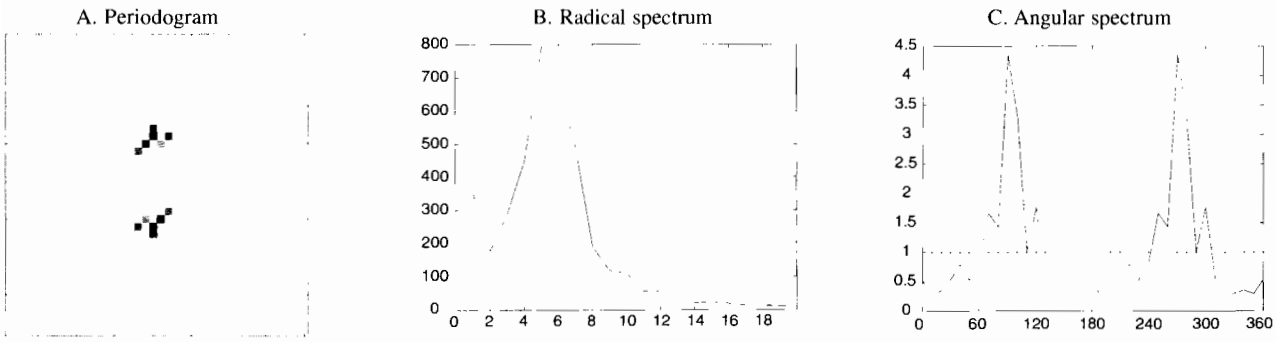

Figure 6. Spectral analysis of the tiger bush represented in *figure 5*.

The periodogram values (sample spectrum) were calculated as $I_{pq} = n^2(a^2_{pq} + b^2_{pq})$. In *figure 6A*, we display the I_{pq}-values as a $n \times n$ grey-tone image (with rescaling in the range 0–255), for which the centre corresponds to $p = q = 0$. (I_{00} is set to zero by prior subtraction of the mean). Such a picture displays a symmetry with respect to the centre since $I_{p,-q} = I_{-p,q}$. $I_{p',q'}/n^2$ represents the portion of the variance of the image accounted for by the cosine wave C_{jk} with frequency (p', q'), i.e. $C_{jk} = \cos[2\pi(p'j/n + q'k/n)]$. A periodogram with a spike at the point $p = +/-p'$ and $q = +/-q'$ ($I_{pq} = 0$ for all other values of p and q) is associated to a digital image consisting solely of such a wave (i.e. a pattern constituted of bands), whose travel direction is $\theta = \tan^{-1}(p'/q')$, while the associated wavenumber is $r = \sqrt{p^2 + q^2}$. Hence I_{pq} can also be expressed as $G_{r\theta}$. For a simple banded pattern, the dominant entry of the periodogram should indicate a direction θ perpendicular to the bands (i.e. accounting for the heterogeneity of the image) and a periodicity r corresponding to the number of bands within the window. To enhance the interpretability of the results, polar spectra [29] have also been computed by binning $G_{r\theta}$ values into polar segments, as $-5° < \theta \leq 5°$, ..., $345° < \theta \leq 355°$ and $0 < r \leq 1$, $1 < r \leq 2$, etc.

The banded pattern under consideration yielded a periodogram dominated by two groups of entries (*figure 6A*). A spike in the radial spectrum (*figure 6B*) for wave numbers 4 and 5 revealed a dominant wavelength ranging between 64 (i.e. 320/5) and 70 m. A main orientation between 90° and 100° was deduced from the angular spectra (*figure 6C*; dotted line corresponds to the isotropic situation). The average phytomass density $<\rho>$ evaluated by redistributing the vegetation uniformly over the territory gives for ρ_+ an approximate value of 0.3. In summary, the spectral analysis of *figure 5* allows us to conclude that the vegetation pattern corresponds to

$$\lambda = 70\ m \quad \text{and} \quad \rho_+ \approx <\rho> \approx 0.3 \qquad (29)$$

Using these values we may now evaluate the propagator and inhibitor ranges L_1 and L_2 of the vegetation, as well as its co-operativity Λ. Transforming equations (26) and (27) to real space, we rewrite them as

$$\frac{L_2}{\lambda_c} = \frac{1}{\pi}\left[\frac{1}{2}\frac{1 - \Lambda + 2\Lambda\rho_+}{1 + \Lambda\rho_+}\right]^{1/4} \qquad (30)$$

$$\frac{L_1}{L_2} = \sqrt{\frac{\left(1 + \Lambda\rho_+ - \sqrt{2(1 + \Lambda\rho_+)(1 - \Lambda + 2\Lambda\rho_+)}\right)\rho_+}{(1 - \rho_+)(1 + 2\Lambda\rho_+)}} \qquad (31)$$

where λ_c is now expressed in physical space units. Since the value of ρ_+ is fixed by the spectral analysis, cf. equation (29), the right hand sides of these expressions is a function of Λ only. Furthermore, in equation (30), we may equate λ_c to the measured wavelength λ given by equation (29). This procedure is exact at the Turing critical point. Below this point, when a finite band of unstable modes (for $L < L_c$) exists, the value of λ_c is generally close to that of the fastest growing mode and the relationship $\lambda = \lambda_c$ remains, even then, a good fit. On the other hand, the existence on the terrain of a small ground slope means that in reality the environment is anisotropic. The influence on the pattern wavelength of this anisotropy, as *figure 4* suggests[3], can be neglected in a first approach such as the

[3] Passing from the isotropic situation to the cases where the propagation and inhibition densities are markedly anisotropic produces no significant variation of the pattern wavelength.

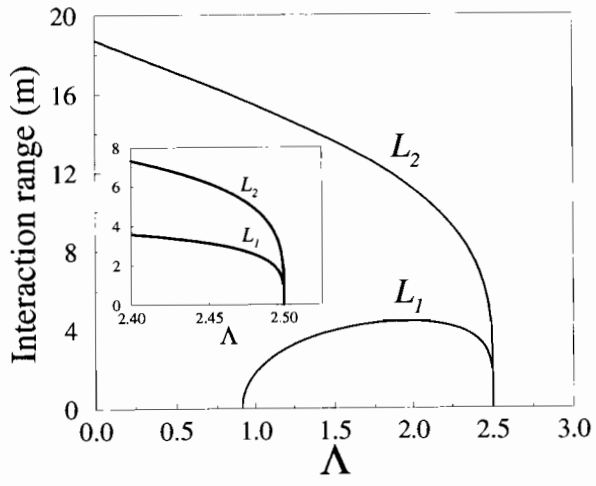

Figure 7. Range of interactions L_1 and L_2 as a function of Λ for $<\rho>=0.3$ and $\lambda = 70$ m. The inset is a blow-up showing the behaviour near $\Lambda = 2.5$.

one presented here. This point will be discussed in a forthcoming publication. Hence, by setting in equations (30) and (31), $\rho_+ = 0.3$, $\lambda_c = 70$ m, we solve these equations for L_1 and L_2 in terms of Λ. *Figure 7* reports the values of L_1 and L_2 obtained in this manner. One finds that the values of Λ and L_1 for which the model predicts the existence of patterns are given by the inequalities

$$\frac{10}{11} < \Lambda < 2.5 \quad \text{and} \quad 0\ \text{m} < L_1 < 4\ \text{m} \qquad (32)$$

In agreement with the general discussion presented above, in this domain L_2 ranges between 0 and 18 m and the inequality $L_2 > L_1$ always holds. One also sees that for a fixed value of L_1, *figure 7* predicts the possible existence of two distinct values for Λ, and hence for L_2.

The value of L_1 and L_2 can be further discussed in light of the field data. In semi-arid and arid situations, short-range co-operativity is likely to result from the favourable influence exerted by the crown of a mature woody individual on the surrounding vegetation. Such influences have been extensively studied with respect to herbaceous vegetation (see [39] for a review), but the results are likely to also hold for woody seedlings. On the other hand, long-range inhibition may result from adverse influences exerted by the root system of a pre-existing mature individual. Data regarding root systems are scarce, but it is well established that lateral roots do extend far beyond the limit of the crown [12, 31]. Furthermore, having lateral roots extending outside the crown (i.e. $L_2 > L_1$) may be an outcome of aridity [1], a recording that may explain why periodic vegetation patterns are so frequent in arid and semi-arid zones.

On our field site, we found an average value of 1.2 m for the radius of the crown of mature *C. micranthum* (the dominant species), and 1.3 m for all mature individuals, irrespective of species [7]. Since favourable influences are supposed to extend significantly up to $2L_1$ due to the properties of the Gaussian distribution, it is reasonable to consider $L_1 < 1$ m. Such a range of values yields two contrasting sets of solutions for Λ and L_2, which correspond either to low ($\Lambda < 1$) or to high ($\Lambda \approx 2.5$) co-operativity. Low co-operativity determines high values for L_2, around 15 m, whilst high co-operativity imply $L_2 < 4$ m. In the first case, the range of significant inhibition, $2L_2$, and hence of lateral root extension, should extend up to 30 m. So a large extension, though not impossible, is not reported in the literature, even for more arid conditions [12], whilst a lateral root extension between 2 m and 8 m is fully consistent with most published results. As a consequence, the high co-operativity situation appears more realistic in the light of the available data.

Acknowledgments

The support of the 'Instituts Internationaux de Physique et de Chimie', Solvay, and of the Centre for Nonlinear Phenomena and Complex Systems (U.L.B.) is gratefully acknowledged.

REFERENCES

[1] Belsky A.J., Influence of trees on savanna productivity: tests of shade, nutrients, and tree-grass competition, Ecology 75 (1994) 922–932.

[2] Bernd J., The problem of vegetation stripes in semi-arid Africa, Plant Res. Dev. 8 (1978) 37–50.

[3] Boaler S.B., Hodge C.A.H., Vegetation stripes in Somaliland, J. Ecol. 50 (1962) 465–474.

[4] Boaler S.B., Hodge C.A.H., Observations on vegetation arcs in the northern region, Somali Republic, J. Ecol. 52 (1964) 511–544.

[5] Clos-Arceduc M., Étude sur photographies aériennes d'une formation végétale sahélienne : La brousse tigrée, Bull. Inst. Afr. noire Sér. A 18 (1956) 677–684.

[6] Cornet A.F., Delhoume J.P., Montaña C., Dynamics of striped vegetation patterns and water balance in the Chihuahuan desert, in: During H.J., Werger M.J.A., Willems J.H. (Eds.), Diversity and Pattern in Plant Communities, SPB Academic Publishing, The Hague, 1988, pp. 221–231.

[7] Couteron P., Relations spatiales entre individus et structure d'ensemble dans des peuplements ligneux soudano-sahéliens au nord-ouest du Burkina Faso, Ph.D. thesis, University of Toulouse, France, 1998, 223 p.

[8] Couteron P., Kokou K., Woody vegetation spatial patterns in a semi-arid savanna of Burkina Faso, West Africa, Plant Ecol. 132 (1997) 211–227.

[9] Fife P.C., Mathematical Aspects of Reacting and Diffusing Systems. Lecture Notes in Biomathematics 28, Springer-Verlag, Berlin, 1979.
[10] Galle S., Seghieri J., Dynamics of soil water content in relation to annual vegetation: the tiger bush in the Sahelian Niger, Ann. Geophys. 12 (suppl. II) (1994) C443.
[11] Gavaud M., Étude pédologique du Niger Occidental, Éditions de l'Orstom, Dakkar-Hann, 1966.
[12] Glover P.E., The root systems of some British-Somaliland plants-IV, East Afr. Agr. J. 17 (1951) 38–50.
[13] Greenwood J.E.G.W., The development of vegetation in Somaliland Protectorate, Geogr. J. 123 (1957) 465–473.
[14] Greig-Smith P., Pattern in vegetation, J. Ecol. 67 (1979) 755–779.
[15] Hemming C.F., Vegetation arcs in Somaliland, J. Ecol. 53 (1965) 57–67.
[16] d'Herbès J.M., Valentin C., Thiéry J.M., La brousse tigrée au Niger : synthèse des connaissances acquises. Hypothèse sur la genèse et les facteurs déterminant les différentes structures contractées, in: d'Herbès J.M., Ambouta J.M.K., Peltier R. (Eds.), Fonctionnement et gestion des écosystèmes contractés sahéliens, John Libbey Eurotext, Paris, 1997, pp. 131–152.
[17] Hoppensteadt F.C., Peskin C.S., Mathematics in Medicine and the Life Sciences. Texts in Applied Mathematics 10, Springer-Verlag, Berlin, 1992.
[18] Lefever R., Lejeune O., On the origin of tiger bush, Bull. Math. Biol. 59 (1997) 263–294.
[19] Le Houerou H.N., The Grazing Land Ecosystems of the African Sahel, Springer-Verlag, Berlin, 1989, 282 p.
[20] Litchfield W.H., Mabbutt J.A., Hardpan in soils of semi-arid Western Australia, J. Soil Sci. 13 (1962) 148–159.
[21] Mabbutt J.A., Fanning P.C., Vegetation banding in arid Western Australia, J. Arid Environ. 12 (1987) 41–59.
[22] Macfadyen W.A., Soil and vegetation in British Somaliland, Nature 165 (1950) 121.
[23] Macfadyen W.A., Vegetation patterns in the semi-desert plains of British Somaliland, Geogr. J. 116 (1950) 199–211.
[24] Mauchamp A., Rambal S., Lepart J., Simulating the dynamics of a vegetation mosaic: a spatialized functional model, Ecol. Model. 71 (1994) 107–130.
[25] May R.M., Stability and Complexity in Model Ecosystems, Princeton University Press, New Jersey, 1973.
[26] Meinhardt H., Models of Biological Pattern Formation, Academic Press, New York, 1982.
[27] Montaña C., The colonization of bare areas in two-phase mosaics of an arid ecosystem, J. Ecol. 80 (1992) 315–327.
[28] Montaña C., Lopez-Portillo J., Mauchamp A., The response of two woody species to the conditions created by a shifting ecotone in an arid ecosystem, J. Ecol. 78 (1990) 789–798.
[29] Mugglestone M.A., Renshaw E., Detection of geological lineations on aerial photographs using two-dimensional spectral analysis, Comput. Geosc. 24 (1998) 771–784.
[30] Murray J.D., Mathematical Biology. Biomathematics Texts 19, Springer-Verlag, Berlin/New York, 1989.
[31] Poupon H., Structure et dynamique de la strate ligneuse d'une steppe sahélienne au nord du Sénégal, Orstom, Paris, 1980, 351 p.
[32] Prigogine I., Structure, dissipation and life, in: Marois M. (Ed.), Theoretical Physics and Biology, North-Holland, Amsterdam, 1969.
[33] Ruxton B.P., Berry L., The Butana grass patterns, J. Soil Sci. 11 (1960) 61–62.
[34] Schlesinger W.H., Reynolds J.F., Cunningham G.L., Huenneke L.F., Jarrell W.M., Virginia R.A., Whitford W.G., Biological feedbacks in global desertification, Science 247 (1990) 1043–1048.
[35] Thiéry J.M., d'Herbès J.M., Valentin C., A model simulating the genesis of banded vegetation patterns in Niger, J. Ecol. 83 (1995) 497–507.
[36] Tongway D.J., Ludwig J.A., Vegetation and soil patterning in semi-arid mulga lands of Eastern Australia, Aust. J. Ecol. 15 (1990) 23–34.
[37] Turing A.M., The chemical basis of morphogenesis, Philos. Trans. R. Soc. Lond. Ser. B 237 (1952) 37–72.
[38] Van Der Meulen F., Morris J.W., Striped vegetation patterns in a Transvaal savanna, Geo. Eco. Trop. 3 (1979) 253–266.
[39] Vetaas O.R., Micro-site effects of trees and shrubs in dry savannas, J. Veg. Sci. 3 (1992) 337–344.
[40] White F., The Vegetation of Africa. A Descriptive Memoir to Accompany the Unesco/AEFTAT/UNSO Vegetation Map, Unesco/AEFTAT/UNSO, Paris, 1983, 356 p.
[41] White L.P., Vegetation arcs in Jordan, J. Ecol. 57 (1969) 461–464.
[42] White L.P., *Brousses tigrées* patterns in southern Niger, J. Ecol. 58 (1970) 549–553.
[43] White L.P., Vegetation stripes on sheet wash surfaces, J. Ecol. 59 (1971) 615–622.
[44] Wickens G.E., Collier F.W., Some vegetation patterns in the Republic of the Sudan, Geoderma 6 (1971) 43–59.
[45] Worrall G.A., The Butana grass patterns, J. Soil Sci. 10 (1959) 34–53.
[46] Worrall G.A., Patchiness in vegetation in the northern Sudan, J. Ecol. 48 (1960) 107–115.
[47] Worrall G.A., Tree patterns in the Sudan, J. Soil Sci. 11 (1960) 63–67.

Acta Oecologica **20** (3) (1999) 185–195 / © Elsevier, Paris

Soil organic matter dynamics in tiger bush (Niamey, Niger). Preliminary results

Karine Guillaume [a]*, Luc Abbadie [a], André Mariotti [b], Hassan Nacro [a]

[a] *Laboratoire d'écologie, CNRS UMR 7625, École normale supérieure, 46, rue d'Ulm, 75230 Paris cedex 05, France.*
[b] *Laboratoire de biogéochimie isotopique, INRA-CNRS, URA 196, université Pierre-et-Marie-Curie, 4, place Jussieu, 75252 Paris cedex 05, France.*

* *Corresponding author (fax: +33 1 44 32 38 85; e-mail: kguillau@biologie.ens.fr)*

Received April 1, 1997; revised December 1, 1998; accepted December 16, 1998

Abstract — Some typical features of soil organic matter dynamics and soil texture were studied to discuss the particular spatial pattern of tiger bush in Niger and its dynamics. The soil texture through silt and clay contents showed a high variability in the vegetation arc as well as in the bare area. These variations were clearly linked to water/wind erosion and termite activity. Tiger bush soils showed a high capacity to store soil organic matter despite a moderate primary production, even in the bare area where the input of plant debris has been nil for many decades. The carbon content was higher within the vegetation arc (0.93 %) than within the bare area (0.45 %). Additionally, potential carbon mineralisation significantly varied in relation to the total carbon content and thus to primary production. Then, the vegetation arcs can be viewed as 'fertility islands' as in many arid ecosystems. The measurements of $\delta^{13}C$ showed a dominant contribution of C_3 plants to the soil organic matter pool. Nevertheless, the contribution of C_4 plants was not negligible. Two hypotheses could be proposed: a different mineralisation rate between C_3 and C_4 plants; or (ii) a better physical protection of C_4 compounds against biodegradation. The soil variables depending totally or partly on biological factors, such as carbon and nitrogen contents, carbon isotopic composition, carbon potential mineralisation, did not show any symmetry in their variations along the studied transects. It was expected in the vegetation arc because the vegetation cover does not show symmetry in its specific composition and spatial structure. In the bare area, a clear asymmetry was observed on some of the variables: carbon content, fine material content and natural abundance of ^{13}C. This supports the hypothesis that the vegetation arcs move upslope, and weakens the hypothesis of the alternance of contraction and spreading periods of the vegetation cover. © Elsevier, Paris

Total organic carbon / organic matter dynamics / mineralisation / tiger bush / Niger / Sahel

1. INTRODUCTION

The term 'brousse tigrée' or 'tiger bush' was used for the first time in 1956 [11] in relation to aerial photographs of some areas in Niger. Inside these areas, vegetation was described as alternating bands of vegetation and bare soil, strongly suggesting tiger (or zebra) skin. This vegetation pattern is not restricted to Niger. Similar structures have also been described in other arid and semi-arid regions such as Mauritania, Mali and Burkina-Faso [28], Somaliland [9, 20, 31], Sudan [46], Australia [30], USA [23], Mexico [34] and Jordan [44].

In Niger, the tiger bush vegetation occurs in the Sahelian zone extending from 13° N to 15° N [2]. Vegetation is concentrated in bands of ca. 25 m wide, perpendicular to the slope, separated by ca. 50 m wide zone of bare soil. The origin of such a vegetation pattern is still in discussion. Some authors hypothesised previously that the vegetation was continually distributed but contracted into patches after an increase in aridity [11]. Others hypothesised a continuous upward movement of the vegetation arcs due to a particular pattern of water infiltration in the soil [2, 4, 28, 46]. Some authors proposed the following mechanism: the water running on the bare area would be stopped by grasses at the upslope boundary of the vegetation arc, enter the soil, and then be supplied to grasses and trees, allowing an upward extension of plant cover [2, 4, 28, 46]. At the downslope boundary of the vegetation arc, plants would lack water and die, leading to woody vegetation regression. Some simulation models have been recently proposed, linking the observed vegetation pattern to the primary succession

Table I. Review of available data on soil organic matter and carbon contents (expressed in %) in some banded vegetation around the world.

Site	Latitude	Annual rainfall (mm)	Average annual temperature	Number of dry months	Depths (cm)	% Organic matter					References
N'Daki (Mali)	15°34' N	300				Bare ground		Herbaceous zone	Living woody		
					0–20	1.0		0.7	2.0		[28]
								Upper edge of arc	Centre of arc		
Baran (Somaliland)	08°15' N to 47°12' E	150			0–5			2.6			[20]
					0–23				1.0		
						% Carbon					
						Vegetated area					
Chihuahan desert (Mexico)	26°29' to 26°52' N	264	20.8 °C	~7	0–3	0.55	1.96				[13]
					6–14	0.45	0.53				
					25–33	0.30	0.31				
					48–58		0.23				
							Settling zone	Annual herbaceous	Living woody	Dead woody	
Goguezé	13°37' N	600	30 °C	> 7	Crust		0.41	0.42			
Koara (Niger)					A_1				0.71	0.51	[2]
					A_{11}	0.19	0.17	0.47			
					A_{12}	0.29	0.30	0.42			
					BC	0.34	0.29	0.30	0.39	0.43	

process [35, 36] or to the competitive interactions between neighbours for water uptake [41].

Little attention has been paid to organic matter and nutrient cycling in tiger bush. Only few data, listed in *tables I* and *II*, are available on soil organic matter pools [2, 13, 20, 28] and chemical characteristics of soil [2]. However, soil organic matter cycling and nutrient availability act as strong constraints on plant functioning [19]. In many arid ecosystems, nitrogen, after water, is the major factor controlling the rate and level of primary production [39]. More generally, nutrient availability influences many vegetation characteristics such as growth rate, plant distribution and spatial occupation. Nutrient distribution and availability partly regulate plant competition intensity, and thus plant colonisation ability.

Tiger bush provides an attractive opportunity to study how plant communities control soil organic matter storage, quality, distribution and mineralisation. Indeed, several vegetation types are concentrated on small areas, on soils with similar physical characteristics (texture), and under the same macroclimatic conditions. Vegetation types follow each other, in time and space, and differ by plant functional types (perennials vs. annuals; trees vs. grasses; C_3 vs. C_4), architecture (root distribution) and chemical composition. Tiger bush also provides a good opportunity to study soil organic matter turnover since the effects of the plant succession on soil organic matter dynamics can be understood through the simultaneous study of all stages. In addition, some large areas are completely devoid of vegetation where the input of organic matter into soil is stopped for many years and soil organic matter is only driven by the mineralisation process.

The purpose of this paper is to give some general information on soil organic matter dynamics in the tiger bush system. We have measured the quantities and spatial distribution of soil organic matter in the different zones of the vegetation arc and the bare area. Potential soil respiration was determined in order to evaluate the ability of soil to produce mineral nutrients. We also assessed its origins (grass/tree) through the measurements of ^{13}C natural abundance in the soil of the vegetation arc and the bare area. A comparison

Table II. Review of available data on nitrogen content (expressed in %), in some banded vegetation around the world.

Site	Latitude	Annual rainfall (mm)	Average annual temperature	Number of dry months	Depths (cm)	% Nitrogen					References
						Bare ground	Vegetated area				
Chihuahan desert (Mexico)	26°29' to 26°52' N	264	20.8 °C	~7	0–3		0.052				[13]
					6–14		0.053				
					25–33		0.056				
					48–58		0.033				
								Herbaceous zone	Living woody		
N'Daki (Mali)	15°34' N	300			0–20	0.082		0.056	0.188		[28]
							Settling zone	Annual herbaceous	Living woody	Dead woody	
Goguezé Koara (Niger)	13°37' N	600	30 °C	> 7	Crust		0.06	0.07			
					A_1				0.07	0.03	[2]
					A_{11}	0.02	0.01	0.04			
					A_{12}	0.03	0.02	0.02			
					BC	0.02	0.02	0.02	0.03	0.03	

between the soil organic matter contents, intensity of the mineralisation process and isotopic composition of carbon, between the vegetation arc and the bare area, will be used to discuss the spatial pattern of tiger bush: contraction and decontraction of vegetation cover in response to long-term rainfall regime, or upward movement of vegetation arcs under the influence of soil water dynamics.

2. MATERIALS AND METHODS

2.1. Study site

The study site is located 60 km NE of Niamey (Niger, West Africa) in the vicinity of Banizoumbou (13°40' N; 2°48' E). The climate belongs to the Sahelo-Sudanian type [3]. Mean annual rainfall is 560 mm (1905–1989 [26]), with a short rainfall season (< 5 months, May to September) and a long dry season (> 7 months). Monthly average temperature is 26 °C. Tiger bush occurs exclusively on shallow gravely soils developed on plateaux formed by a thick lateritic cuirasse of Tertiary age [17] with gentle slopes (0–0.2 %). Soils are classified as tropical ferrugineous soils (FAO-Unesco: Acrisols).

As in many tropical areas, the main types of crusts, at the top soil, have been distinguished and classified using porosity (abundance and type) and arrangement of coarse and fine particles (related distribution pattern, orientation and distribution) [10, 43]. These crusts are colonised by blue algae, and act on run-off and water infiltration [32].

Each bare area-vegetation arc can be divided into four zones according to plant cover, crust type and run-off ability [10]: (1) the bare area characterised by a high run-off; (2) the herbaceous zone, characterised only by annual grasses with *Michrochloa indica* and *Cyanotis lanata* as the main annual dominant species; (3) the woody zone with *Combretum micranthum* and *C. nigricans* as the dominant trees; and (4) the senescent zone with dead trees (*figure 1*). Some living termite mounds occur in the herbaceous and woody zones whereas those in the senescent zone are abandoned [11].

2.2. Samples collection

Sampling was carried out in April 1995 during the dry season. Soil samples were collected along three transects through the vegetation arc in the middle of each zone defined above and, up to the 24-m transect in the upward bare area (4 m each). For each point along the transects, two depths were distinguished: 0–10 and 10–20 cm. Soils samples were immediately air-dried, sieved to 2 mm and stored for analysis.

In order to determine the plant photosynthetic pathway (C_3, C_4), litter and leaves of the two common woody species (*Guiera senegalensis* and *Combretum*

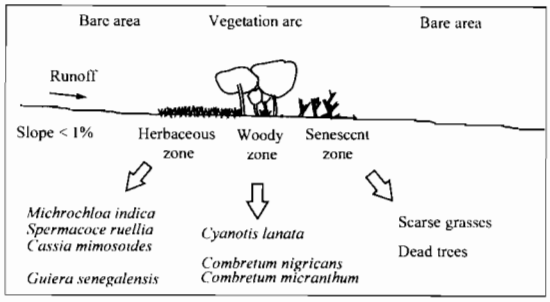

Figure 1. Schematic representation of an elementary unit (bare area - vegetation arc) of tiger bush. The vegetation arc is classically divided into three zones and characterised by the vegetation cover: herbaceous, woody and senescent zones.

micranthum) were sampled inside the vegetation arc. Litter was collected at random in five points on the soil surface and pooled in a larger sample. Leaves were collected at random in five trees of each species, and also pooled in two larger samples. Some leaves of the three main grass species (*Michrochloa indica*, *Cyanotis lanata*, *Spermacoce ruellia*) were also collected later, during the wet season, following the same protocol.

2.3. Laboratory measurements

2.3.1. Soil texture determination

Organic matter was destroyed by adding 100 mL hydrogen peroxide to 20 g soil, held at 20 °C for 6 h and then 60 °C for 16 h. Distilled water (300 mL) and 25 mL sodium hexametaphosphate (40 $g \cdot L^{-1}$) were then added to disperse the aggregates and the samples were shaken for 16 h at 175 rpm. The water suspension was sieved at 50 µm. The 0–50 µm fraction was sonicated at 100 $J \cdot mL^{-1}$ (Branson Sonifier 450) and passed through a 20-µm sieve in water in order to split microaggregates. The 0–20 µm fraction was centrifuged (Sorvall RC 3B Plus, Du Pont De Nemours) to separate the 2–20 and 0.05–2 µm fractions. Centrifugation speed and time were calculated according to Jackson and Tanner [24, 40]. The resulting six fractions were dried at 40 °C and weighed: 50–2 000 (sands), 20–50 (coarse silt), 2–20 (fine silt) and 0.05–2 µm (clay).

2.3.2. Total organic C and N

Aliquots of sieved samples (< 2 mm) were thoroughly crumbled. Total organic carbon and nitrogen were determined with an elemental analyser (NA 1500 Series 2, Fisons). The results were expressed as percentage of dry soil.

2.3.3. $\delta^{13}C$ natural abundance

Natural abundance of ^{13}C was measured on sieved and crumbled soil samples with an elemental analyser (NA 1500, Fisons) coupled with a mass spectrometer (Sira 10, Fisons), according to Girardin and Mariotti [18]. The results were expressed as $\delta^{13}C$ units:

$$\delta 13C = [(R \text{ sample}/R \text{ standard}) - 1] \times 1\,000$$

where $R = {}^{13}C/{}^{12}C$

The standard used was calibrated against NBS 19, and $\delta^{13}C$ was expressed against PDB [12].

2.3.4. Soil respiration

Aliquots of 20 g air dry soil were incubated in the dark in glass bottles with rubber stoppers at 28 °C (± 1 °C) and 80 % of the water holding capacity. After 3 d, a 250-µL aliquot of the accumulated atmosphere was removed from each flask with a gas-tight syringe and analysed by gas chromatography (DI 200 Analyser apparatus, Delsi-Nermag). Results were expressed as µg $C\text{-}CO_2$ produced by 20 g dry soil.

2.4. Statistical analysis

Data were tested using SAS® (Statistical Analysis System, SAS Institute Inc. 1990). Because of variables not normally distributed, we used two different procedures: PROC RANK and PROC GLM. We tested responses of texture (silt and clay), soil total organic carbon and nitrogen contents, $\delta^{13}C$ and $C\text{-}CO_2$ measurements along the element unit (bare area – vegetation arc), sampling point (0, 4, 8 m, etc. senescent zone) and depth (0–10, 10–20 cm). Additionally, we used PROC REG, within the bare area, because of a lack of soil sample replicates. A simple linear regression was performed to identify a relationship between total carbon, nitrogen, silt and clay contents along the bare area. The LSMEANS procedure was used to compare the least square means of variables. All tests were performed at the 0.05 significance level.

3. RESULTS AND DISCUSSION

3.1. Soil texture

Inside the whole soil (0–20 cm), silt and clay contents differed significantly between the bare area and vegetation arc ($P < 0.05$). There was no significant interaction between zone and depth ($P > 0.5$). The silt

Table III. Silt and clay contents at the two different depths inside the vegetation arc. Results are expressed in % ($n = 3$, standard error in parentheses). Statistical analysis did not show any significant effect of zonation or depth ($P > 0.5$).

	Vegetation arc					
	Herbaceous zone		Woody zone		Senescent zone	
Depth (cm)	0–10	10–20	0–10	10–20	0–10	10–20
% Silt	20 (2)	17 (1)	21 (2)	18 (3)	21 (3)	20 (5)
% Clay	18 (7)	26 (6)	25 (2)	33 (2)	24 (3)	29 (4)

content was higher inside the vegetation arc (20 ± 2.9 %) than inside the bare area (18 ± 1.2 %). On the contrary, the clay content was higher inside the bare area (29 ± 6 %) than inside the vegetation arc (24 ± 6 %).

Inside the vegetation arc, no variation was observed between the herbaceous, woody and senescent zones in silt and clay contents for the whole soil, 0–10 and 10–20 cm layers. No significant interaction existed between zonation and depth (*table III*).

Within the bare area, there was no significant relationship between silt content and distance for the whole soil, 0–10 and 10–20 cm layers ($P > 0.2$). Nevertheless, a negative linear regression was observed between clay content and distance for the whole soil and the 0–10 but not for the 10–20 cm layer: the clay content decreased from upslope to downslope and tended to be more concentrated in the 10–20 cm layer (*table IV*).

As tiger bush exclusively occurs on a gentle slope (< 1 %) and 70 % of rainfall runs off [38], an accumulation of fine particles was expected in the lower part of the bare area. In fact, we observed the opposite pattern. This pattern has already been observed by several authors [11, 28, 32, 37, 45]: the relative increase in fine particles, in the upper part of the bare area, resulted from both water and wind erosion of dead termite mounds in the senescent zone of the vegetation arc. These fine particles from the dead mounds were agglomerated in crusts which prevented most of the water infiltration [10]. Consequently, the run-off only acts on coarse particles that are intercepted by the herbaceous zone where they accumulate, decreasing even more the clay content. In the woody zone, the high fine particle content was obviously linked to the building activity of termites. They take up fine materials in the zones near the colony to built their nests [27]. This horizontal transport results in an enrichment in fine particles in the nest zone and an impoverishment in its surroundings.

3.2. Total organic C and N contents

Significant differences between the vegetation arc and bare area were observed in total organic carbon and nitrogen contents (0–20 cm) ($P > 0.05$) with a significant interaction between zone and zonation ($P > 0.05$). The carbon content was higher inside the vegetation arc (0.93 ± 0.4 %) than inside the bare area (0.45 ± 0.2 %). The nitrogen content followed the same pattern: high inside the vegetation arc (0.09 ± 0.03 %) and low inside the bare area (0.05 ± 0.02 %).

Inside the vegetation arc, there was a high significant effect of zonation on C and N contents in the whole soil (*figure 2*), but no significant effect of depth. The highest values of carbon content were measured inside the woody and senescent zones (C = 1.28 ± 0.3 %; C = 0.96 ± 0.2 %, respectively). Inside these two zones, the nitrogen contents were 0.1 % (± 0.02) and 0.09 % (± 0.02) respectively. The lowest carbon and nitrogen contents were observed in the herbaceous zone: 0.54 % (± 0.09) and 0.06 % (± 0.02) respectively. These results were expected since a

Table IV. Silt and clay contents at the two different depths inside the bare area. Results are expressed in % (individual sample values). A negative linear regression was only found between clay content and distance for the whole soil ($y = -0.39\ x + 34.07$; $r^2 = 0.29$) and the 0–10 cm layer ($y = -0.49\ x + 31.46$; $r^2 = 0.72$).

	Bare area													
	0 m		4 m		8 m		12 m		16 m		20 m		24 m	
Depth (cm)	0–10	10–20	0–10	10–20	0–10	10–20	0–10	10–20	0–10	10–20	0–10	10–20	0–10	10–20
% Silt	13	18	20	19	17	17	18	17	18	17	17	17	21	19
% Clay	30	33	34	40	25	32	23	33	26	37	21	30	20	27

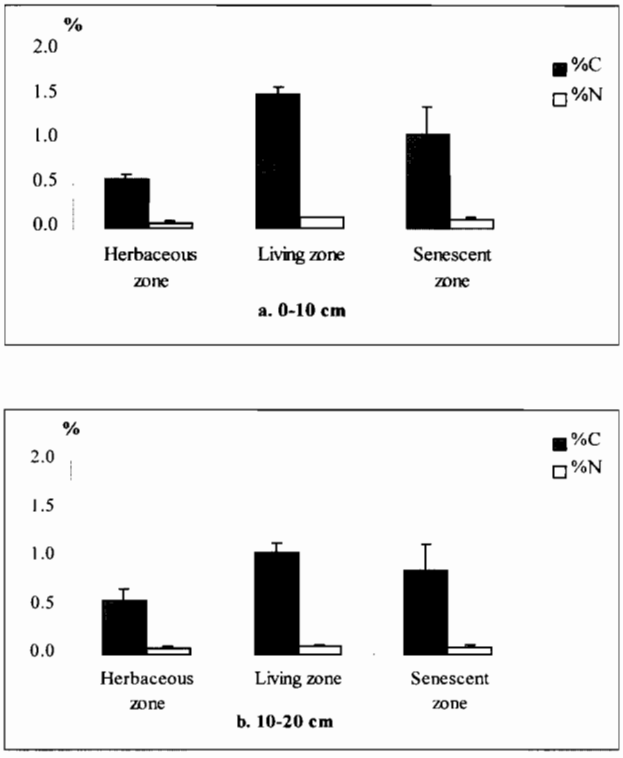

Figure 2. Total carbon and nitrogen contents inside the vegetation arc (a) at the 0–10 cm layer and (b) at the 10–20 cm layer. Results were expressed in % ($n = 3$, with standard error). Statistical analysis showed a highly significant effect of zonation for the total carbon and nitrogen contents in the 0–20 cm layer ($P < 0.001$).

positive linear relationship is often observed between net primary production and soil organic matter content in the superficial layers. Obviously, primary production is highly variable among zones in the vegetation arc. It is maximum in the woody zone, medium in the herbaceous zone, and insignificant in the senescent zone. No quantitative data about primary production are available, but the woody biomass was estimated to 27 t·ha^{-1} in the woody zone of the Banizoumbou site [22]. The herbaceous production was estimated at 952 kg dry matter·ha^{-1} in the Macina tiger bush in Mali [21]. Moreover, C and N contents were high in the senescent zone even though the primary production is insignificant which can be interpreted in two ways: (i) the organic matter stock is not yet affected by erosion; or (ii) the decomposition of soil organic matter has not yet begun [48].

Along the bare area, high variations of total carbon and nitrogen contents were observed (*figure 3*). This variability could be related to the variability of the soil texture within the bare areas [10, 43]. The highest carbon and nitrogen contents were measured upwards from the bare area: 0.75 % (± 0.04) and 0.08 % (± 0.01), respectively. Moreover, a negative linear correlation was observed between the organic carbon content and the distance only at 0–20 and 0–10 cm depth. In the majority of tropical soils, and particularly in West Africa, soil organic matter content is largely dependent on soil texture: there is a strong positive correlation between soil organic matter, clay and silt contents [15]. However, we did not observe a positive correlation between carbon and clay contents but a negative linear correlation was found between the total carbon and silt contents, in the whole soil ($y = -0.06\,x + 1.58$; $r^2 = 0.44$). Obviously, soil texture only explained a part of the carbon content variation. Generally, the size of the soil carbon pool depends both on decomposition and plant debris incorporation. In the bare area, the input of plant debris into the soil does not occur which implies that the carbon content variation can only be driven by the mineralisation process. As the carbon content is higher upslope than downslope, two hypotheses could be proposed: (i) the mineralisation rate is higher downslope than upslope; or (ii) the time elapsed since the beginning of decomposition is larger downslope than upslope, i.e. a higher proportion of carbon has been mineralised downslope than upslope. If the second hypothesis is validated, the age of the organic matter pool is higher downslope than upslope and it thus supports the hypothesis of an unidirectional movement of vegetation.

3.3. ^{13}C natural abundance

Carbon isotope fractionation associated with photosynthesis is less intensive in C_4 than in C_3 plants: $\delta^{13}C$ values of C_3 plants lie between –23 and –34 ‰ (average of –26 ‰) whereas for C_4 plants, they range from –9 to –17 ‰ (average of –12 ‰) [33]. In tiger bush, plants belong to the two photosynthetic groups: the leaves of the two major tree species, *Guiera senegalensis* ($\delta^{13}C = -27.1$ ‰) and *Combretum micranthum* ($\delta^{13}C = -27.6$ ‰) had a natural abundance of ^{13}C typical of C_3 plants, like the two grass species *Cyanotis lanata* ($\delta^{13}C = -29.3$ ‰) and *Spermacoce ruellia* ($\delta^{13}C = -28.5$ ‰). Only the grass *Michrochloa indica* ($\delta^{13}C = -13.8$ ‰) is a C_4 plant. In the tree leaf litter, the $\delta^{13}C$ was –27.5 ‰.

For the whole soil, there was a significant effect of zone on $\delta^{13}C$ values ($P < 0.0001$). Under the bare area, we observed an enrichment of soil organic matter (SOM) in ^{13}C ($\delta^{13}C = -22.4 \pm 0.9$ ‰) whereas, under the vegetation arc, SOM is impoverished in ^{13}C ($\delta^{13}C = -23.6 \pm 1.6$ ‰).

In the vegetation arc, there was a significant effect of zonation, but not of depth (*table V*). This meets previous observations by Balesdent et al. [6, 7]: the

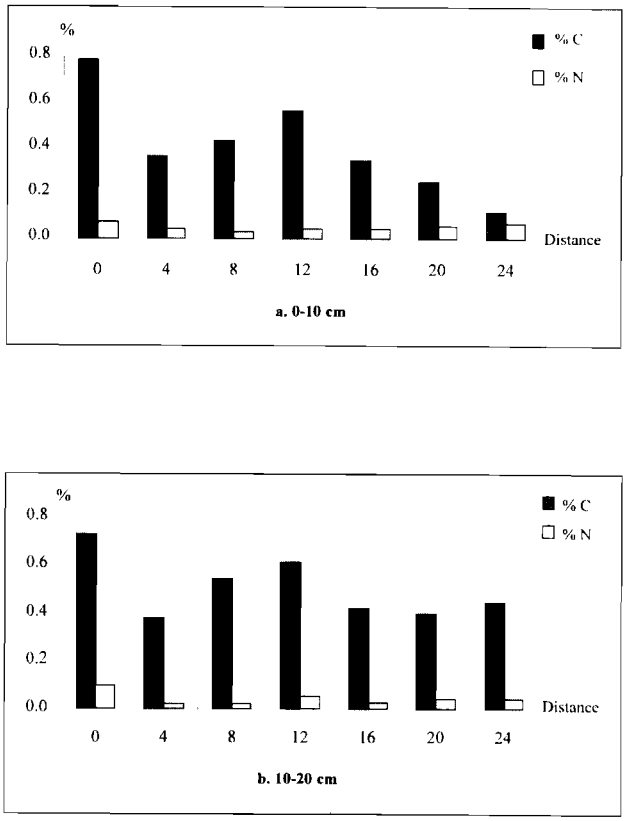

Figure 3. Total carbon and nitrogen contents inside the bare area (a) at the 0–10 cm layer and (b) at the 10–20 cm layer. Results were expressed in %. A negative linear regression was found between the total carbon content and the distance for the whole soil ($y = -0.01 \times + 0.62$; $r^2 = 0.45$) and the 0–10 cm layer ($y = -0.02 \times + 0.65$; $r^2 = 0.67$).

main source of local variations for the $\delta^{13}C$ in the soil organic matter is the photosynthetic pathway of the vegetation up to 15 ‰ [6, 7] and not the depth which can only account for small variations of 2 to 3 ‰. Under the herbaceous zone, SOM was more enriched in ^{13}C (–21.6 ± 1.4 ‰) than the SOM under the woody and senescent zones (–25 ± 0.6 and –24 ± 0.5 ‰, respectively). The isotope composition of soil carbon is in relation with the vegetation growing on the soil [33]. Under the herbaceous zone where the vegetation cover was mixed with C_3 and C_4 grasses, the ^{13}C of soil organic matter was close to –21 ‰. In contrast, under the woody and senescent zones where the vegetation cover exclusively belonged to the C_3 type, the $\delta^{13}C$ of soil organic matter was close to –24.5 ‰.

Within the bare area, the $\delta^{13}C$ measures in SOM were strongly related to the distance (*table VI*). An enrichment of ^{13}C in SOM was observed along the bare area from upslope to downslope, for the whole soil and the 0–10 cm layer. The lowest value was measured upslope (–24 ‰ in the 0–20 cm layer) and the highest downslope, near the herbaceous zone (–21.5 ‰ in the 0–20 cm layer).

From the data obtained, it was possible to estimate the relative proportion of C_3 and C_4 plant material in the SOM pool. We hypothesised that the isotopic composition of the carbon in soil depends only on both the isotopic composition of the carbon in the C_3 and C_4 plants and the proportions in which these two types of plant material were incorporated in the soil. Thus, it can be expressed by the following equation:

$$(p_{C3} \times \delta_{C3}) + (p_{C4} \times \delta_{C4}) = \delta_S$$

where p_{C3} is the proportion of C_3 plant material in the SOM pool, δ_{C3} the $\delta^{13}C$ mean value of four C_3 species, p_{C4} the proportion of C_4 plant material in the SOM pool, δ_{C4} the $\delta^{13}C$ value of one C_4 grass, δ_S the observed $\delta^{13}C$ value of the SOM pool.

As $p_{C3} + p_{C4} = 1$, we obtained:

$$p_{C3} = [(\delta_S - \delta_{C4})/(\delta_{C3} - \delta_{C4})] \times 100$$

Some important features can be noted from these calculations (shown in *tables V, VI*). There is a sur-

Table V. Natural abundance of ^{13}C ($\delta^{13}C$) and the relative contribution of C_3 and C_4 plants to the soil organic matter at the two depths inside the vegetation arc. The $\delta^{13}C$ was expressed in ‰ whereas the relative contributions were expressed in %. Statistical analysis showed a significant effect of zonation ($P < 0.001$) but not of depth ($P > 0.5$).

	Vegetation					
	Herbaceous zone		Woody zone		Senescent zone	
Depth (cm)	0–10	10–20	0–10	10–20	0–10	10–20
$\delta^{13}C$ (‰)	–21.1	–21.7	–25.2	–24.5	–24.3	–23.8
% C_3	51	55	78	75	74	70
% C_4	49	45	22	25	26	30

Table VI. Natural abundance of ^{13}C ($\delta^{13}C$) and the relative contribution of C_3 and C_4 plants to the soil organic matter at the two depths inside the bare area. The $\delta^{13}C$ was expressed in ‰ whereas the relative contributions were expressed in %. A negative linear regression was found between the $\delta^{13}C$ and the distance for the whole soil ($y = 0.09\ x - 23.49$; $r^2 = 0.66$), and the 0–10 cm layer ($y = 0.10\ x - 23.56$; $r^2 = 0.80$).

	Bare area													
	0 m		4 m		8 m		12 m		16 m		20 m		24 m	
Depth (cm)	0–10	10–20	0–10	10–20	0–10	10–20	0–10	10–20	0–10	10–20	0–10	10–20	0–10	10–20
$\delta^{13}C$ (‰)	–24.1	–23.9	–22.2	–22.1	–23.1	–23.5	–22.3	–22.5	–21.8	–21.7	–21.3	–21.4	–21.0	–22.1
% C_3	72	71	59	58	65	68	59	61	56	55	52	53	51	58
% C_4	28	29	41	42	35	32	41	39	44	45	48	47	49	42

prisingly high contribution of C_4 plants to SOM storage inside the vegetation arc, which was never below 20–25 % and can amount up to 50 %. C_4 plants, mainly represented by *Michrochloa indica*, only contribute less than 5 % of the above grass biomass (Guillaume, unpubl. data). It seems that the C_4 signal in the soil is too high when compared to the real input of C_4 plant material in the organic matter pool. The proportion of stabilised C_4 organic matter will be higher than the proportion of C_4 compounds in the incoming vegetal debris. Two hypotheses could be proposed: (i) different rate decomposition between the C_3 and C_4 plants; or (ii) a better physical protection of the C_4 plants against biodegradation. Indeed, within the bare area, the input of fresh organic matter is nil. Mineralisation is the only process controlling the output of carbon. The natural abundance of ^{13}C should not change during decomposition [5, 25, 42], except if the $\delta^{13}C$ signatures of the chemical fractions differ and decay at different rates [8]. As we observed a 2 ‰ variation of $\delta^{13}C$ natural abundance, we can hypothesise that the decomposition rates differ between the C_3 and C_4 compounds, leading to a progressive relative enrichment of the compounds of C_4 origin with time, i.e. with distance. The better physical protection of the C_4 organic matter could be the mechanism of this enrichment. The physical fractionation of soil organo-mineral particles should help to clarify these points.

3.4. Soil respiration

The quantities of CO_2 involved were significantly higher under the vegetation arc (104 ± 54 µg $C\text{-}CO_2 \cdot g^{-1}$ soil) than under the bare area (19.8 ± 6 µg $C\text{-}CO_2 \cdot g^{-1}$ soil). This is obviously due to the pattern of organic carbon distribution and quality in the landscape. The organic compounds are more abundant and more degradable (regular and fresh organic matter inputs) in the vegetation arc than in the bare soil (no material input and humified compounds): carbon mineralisation is high and thus nutrient availability more important in the vegetation arc than in the bare area.

Inside the vegetation arc (*figure 4*), there was no significant effect of depth but a significant one of zones in the whole soil. The $C\text{-}CO_2$ value was lower under the herbaceous zone (65.4 ± 15 µg $C\text{-}CO_2 \cdot g^{-1}$ soil) than those of the woody zone (165.9 ± 18 µg $C\text{-}CO_2 \cdot g^{-1}$ soil). Furthermore, a positive linear correlation was observed between the carbon dioxide production and the total organic carbon content in the whole soil, 0–10 and 10–20 cm layers (*table VII*). The intensity of potential soil respiration was mostly dependent on the quantity of organic carbon, like in other tropical ecosystems [1, 14]. Nevertheless, the accessibility of the organic matter partly controls potential soil respiration as shown by the carbon mineralisation rate (ratio $C\text{-}CO_2/C$, *figure 4*) which is much higher under the herbaceous and woody zones than under the senescent zone.

In the bare area, although SOM was low, potential respiration was not negligible (*figure 5*) in relation with the presence of cryptogamic crusts [32, 39]. CO_2 production did not vary significantly with depth or distance. Nevertheless, the highest value was measured upslope (29.1 ± 10 µg $C\text{-}CO_2 \cdot g^{-1}$ soil, 0–20 cm); whereas the lowest was measured downslope (15.6 ± 0.3 µg $C\text{-}CO_2 \cdot g^{-1}$ soil, 0–20 cm). A positive linear relationship between carbon dioxide total production and the organic carbon content was observed in the whole soil, 0–10 cm, and in 10–20 cm layers (*table VIII*) clearly indicating that the potential respi-

Table VII. Results of the linear regression between the $C\text{-}CO_2$ measurements (as dependent variable) and the total organic carbon content (as regressor) inside the vegetation arc in the 0–10, 10–20 and 0–20 cm layers.

	Parameter estimate		F-value	$P > F$	R-square
	a	b			
0–10 cm	0.99	3.59	6.61	0.03	0.48
10–20 cm	2.16	2.45	11.83	0.01	0.62
0–20 cm	1.34	3.18	17.72	0.0007	0.52

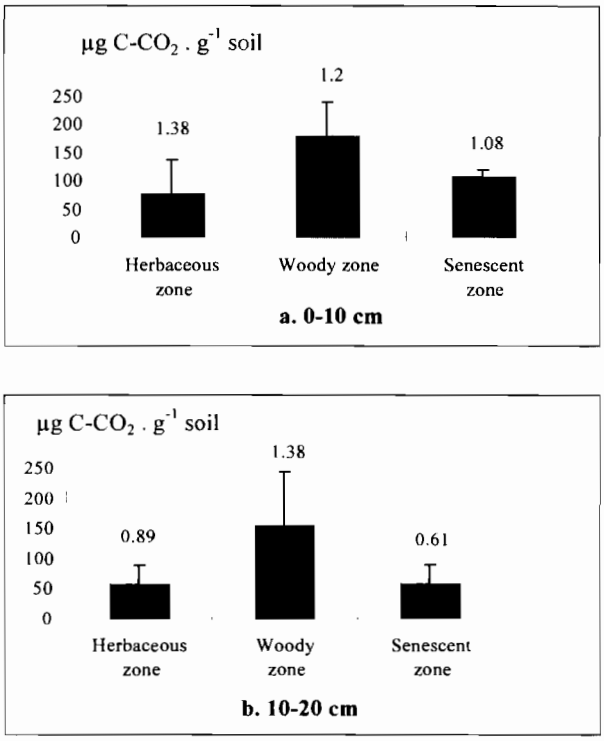

Figure 4. Potential of carbon mineralisation and mineralisation rate inside the vegetation arc (a) at the 0–10 cm layer and (b) at the 10–20 cm layer. The potential of carbon mineralisation was expressed in µg $C\text{-}CO_2 \cdot g^{-1}$ ($n = 3$). The mineralisation rate (number) was expressed in %. Statistical analysis showed a significant effect of zonation ($P < 0.02$) but not of depth ($P > 0.4$).

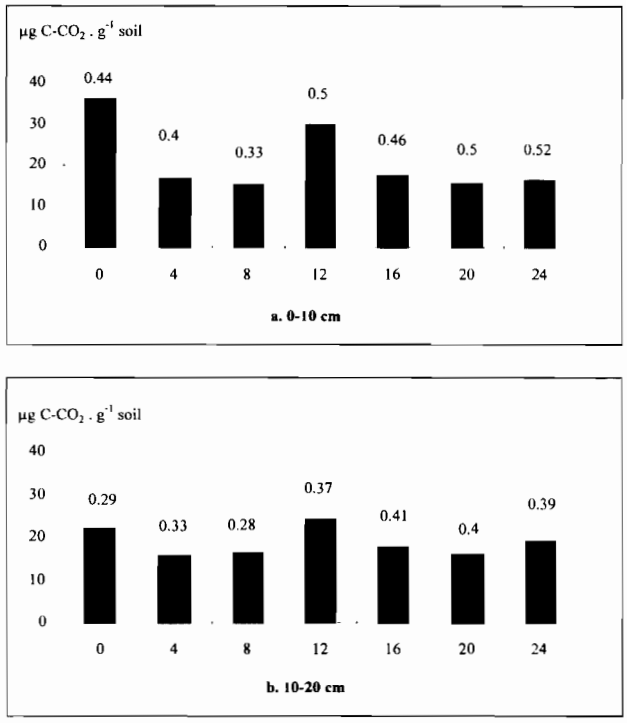

Figure 5. Potential of carbon mineralisation and mineralisation rate inside the bare area (a) at the 0–10 cm layer and (b) at the 10–20 cm layer. The potential of carbon mineralisation was expressed in µg $C\text{-}CO_2 \cdot g^{-1}$. The mineralisation rate (number) was expressed in %. No linear regression existed between the total carbon content and the distance for the whole soil, 0–10 and 10–20 cm layers ($P > 0.1$).

ration was driven more by the quantity of organic carbon than its quality. Moreover, the carbon mineralisation rate does not significantly vary with distance. This allows us to reject our hypothesis which explained the higher carbon content upslope than downslope by a difference in the mineralisation rate.

Table VIII. Results of the linear regression between the $C\text{-}CO_2$ measurements (as dependent variable) and the total organic carbon content (as regressor) inside the bare area in the 0–10, 10–20 and 0–20 cm layers.

	Parameter estimate		F-value	$P > F$	R-square
	a	b			
0–10 cm	1.42	2.4	15.04	0.01	0.75
10–20 cm	1.01	2.40	7.29	0.04	0.59
0–20 cm	1.15	2.41	16.70	0.001	0.58

4. CONCLUSIONS

The present study has revealed some typical features of soil organic matter and dynamics in the tiger bush ecosystem.

(1) A high variability in clay content was observed in the vegetation arc as well as in the bare area. In relation with water run-off and termite activity, there is a clear tendency in fine particle variations. These variations could be due to the removal of coarser material from the bare area (relative increase in fine material) which is deposited in the herbaceous zone where the fine materials relatively decrease, induced by the building activity of termites in the woody zone (absolute increase of fine material).

(2) Soil total carbon and nitrogen contents were high. Even in the bare area, organic matter content was not negligible despite the lack of plant material input for many decades. Tiger bush system showed a surprisingly high capacity of the soils to store organic

matter despite a moderate primary production level. This is likely to be related to the high soil fine particles content partly due to termite activity. An important fraction of the organic matter is probably stabilised on mineral colloids. In other words, a significant part of the organic matter stored in the soil, measured either in the vegetation arc or in the bare area, could have been produced during a previous primary production cycle by a previous vegetation arc.

(3) Measurements of $\delta^{13}C$ showed a dominant contribution of C_3 plants to the soil organic matter pool. Nevertheless, the contribution of C_4 plants, mainly the annual grass *Michrochloa indica*, was not negligible. In the bare area, the $\delta^{13}C$ values varied with distance, i.e. the relative contributions of C_3 and C_4 plants to the SOM pool varied with time, that of C_3 becoming lower and lower (lower in the downslope than in the upslope). The two types of organic matter likely differed in their relative enrichment in ^{13}C during mineralisation, i.e in their mineralisation rate. This point could be elucidated with a study of the distribution and the isotopic composition of organic carbon in different size classes of soil organo-mineral particles, obtained after a physical soil fractionation.

(4) Potential carbon mineralisation significantly varied between the vegetation arc and the bare area. It was high in the vegetation arc, but remained significant in the bare area. Nutrient availability was likely high during the wet season, as previously observed in comparable formations in Australia [29]. Vegetation arcs can be viewed as 'fertility islands' as in many arid ecosystems [16, 39, 47].

(5) The soil variables depending totally or partly on biological factors, such as carbon and nitrogen contents, isotopic composition of carbon, carbon potential mineralisation, did not show any symmetry in their variations along the studied transects. It was expected in the vegetation arc because the vegetation cover do not show symmetry in its specific composition and its spatial structure. In the bare area, a clear asymmetry was observed on some of the variables, carbon content, fine material content and natural abundance of ^{13}C. This supports the hypothesis that vegetation arcs move upslope, and weakens the hypothesis of the alternance of contraction and spreading periods of the vegetation cover.

Acknowledgments

We express our gratitude to A. Casenave, Director of Orstom Niamey for the facilities he offered us in the field. V. Parra, J.C. Lata and the two anonymous reviewers provided helpful comments on an earlier version of the manuscript. We thank Id and Hamza for their assistance in the field, and G. Guillaume, D. Benest, C. Girardin, M. Grably for their technical assistance in the laboratory. The work was supported by grants from SALT programme (CNRS and Orstom).

REFERENCES

[1] Abbadie L., Lensi R., Carbon and nitrogen mineralization and denitrification in a humid savanna of West Africa (Lamto, Côte d'Ivoire), Acta Oecol. 11 (1990) 717–728.

[2] Ambouta K., Contribution à l'édaphologie de la brousse tigrée de l'Ouest nigérien, Ph.D. thesis, université Nancy-I, 1984, 121 p.

[3] Aubréville A., Climats, forêts, et désertification de l'Afrique tropicale, Soc. Edit. Géogr. Marit. Colon., Paris, 1949, 351 p.

[4] Audry P., Rossetti C., Observations sur les sols et la végétation en Mauritanie du sud-est et sur la bordure adjacente du Mali (1959-1961), Food and Agricultural Organisation, Rome 24067/F/1, 1962.

[5] Balesdent J., Girardin C., Mariotti A., Site-related $\delta^{13}C$ of tree leaves and soil organic matter in a temperate forest, Ecology 74 (1993) 1713–1721.

[6] Balesdent J., Mariotti A., Guillet B., Natural ^{13}C abundance as a tracer for studies of soil organic matter dynamics, Soil Biol. Biochem. 19 (1987) 25–30.

[7] Balesdent J., Wagner G.H., Mariotti A., Soil organic matter turnover in long-term field experiments as revealed by Carbon-13 natural abundance, Soil Sci. Soc. Am. J. 52 (1988) 118–124.

[8] Berg B., Mc Claugherty C., Johansson M.B., Litter mass-loss rates in late stages of decomposition at some climatically and nutrionally different pines sites. Long term decomposition in a Scots pine forest, Can. J. Bot. 71 (1993) 680–692.

[9] Boaler B., Hodge C.A.H., Observations on vegetation arcs in the northern region, Somali Republic, J. Ecol. (1964) 511–544.

[10] Casenave A., Valentin C., A runoff capability classification system based on surface features criteria in semi-arid areas of West Africa, J. Hydrol. 130 (1992) 231–249.

[11] Clos-Arceduc M., Études sur photographies aériennes d'une formation végétale sahélienne : la brousse tigrée, Bull. IFAN sér. A 7 (1956) 677–684.

[12] Craig H., Isotopic standards for carbon and oxygen correction factors for mass spectrometric analysis of carbon dioxide, Geochim. Cosmochim. Acta 12 (1957) 133–149.

[13] Delhoume J.P., Distribution spatiale des sols le long d'une toposéquence représentative de la Réserve de la Biosphère de Mapimi, Estudio integrado de los recursos vegetacion, suelos y agua en la Reserva de la Biosfera de Mapimi I, Ambiente y humano Instituto de Ecologia, Mexico, 1987, 30 p.

[14] Djellali N., Billes G., Bounaga N., Lossaint P., Étude de l'activité biologique des sols de la steppe d'Alfa d'Algérie. Minéralisation du carbone et de l'azote, Oecol. Plant. 6 (1985) 289–307.

[15] Feller C., Fritsch E., Poss R., Valentin C., Effet de la texture sur le stockage et la dynamique des matières organiques dans quelques sols ferrugineux et ferralitiques (Afrique de l'Ouest, en particulier), Cah. Orstom sér. Pédol. XXVI (1991) 25–36.

[16] Garner W., Steinberger Y., A proposed mechanism for the formation of 'Fertile Islands' in the desert ecosystem, J. Arid Environ. 16 (1989) 257–262.
[17] Gavaud M., Étude pédologique du Niger occidental, 3 vol., Orstom, Paris, 1965.
[18] Girardin C., Mariotti A., Analyse isotopique du ^{13}C en abondance naturelle dans le carbone organique : un système automatique avec robot préparateur, Cah. Orstom Sér. Pédol. XXVI (1991) 371–380.
[19] Harper J.L., Population Biology of Plants, Academic Press, 1977, 892 p.
[20] Hemming C.F., Vegetation arcs in Somaliland, J. Ecol. 53 (1965) 57–67.
[21] Hiernaux P., Gérard B., The influence of vegetation pattern on the productivity, diversity and stability of the vegetation: the case of 'brousse tigrée' in the Sahel, Acta Oecol. 20 (1999) 147–158.
[22] Itchaou A., Étude de la productivité des formations forestières de brousse tigrée et de brousse diffuse : Conséquences pour la gestion et la régénération de ces formations, Mémoire d'Ingénieur spécialité eaux et forêts, 1995, 161 p.
[23] Ives R., Desert ripples, Am. J. Sci. 244 (1946) 492–501.
[24] Jackson M.L., Soil Chemical Analysis Advanced Course, 5th ed., University of Madison Press, Wisconsin, 1969, 894 p.
[25] Kingston J.D., Marino B.D., Hill A., Isotopic evidence for neogene hominid paleoenvironments in the Kenya Rift Valley, Science 264 (1994) 955–959.
[26] Lebel T., Le Barbé L., Rainfall climatology of the central Sahel during the years 1950-1990, J. Hydrol. 188-189 (Hapex Sahel Spec. Issue) (1997) 97–122.
[27] Lepage M., Abbadie L., Mariotti A., Food habits of sympatric termite species (Isoptera, Macrotermitinae) as determined by stable carbon isotope analysis in a Guinean savanna (Lamto, Côte d'Ivoire), J. Trop. Ecol. 9 (1993) 303–311.
[28] Leprun J.C., Étude de quelques brousses tigrées sahéliennes : structure, dynamique, écologie, in: Le Floc'h E., Grouzis M., Cornet A., Bille J.C. (Eds.), L'aridité, une contrainte au développement, Orstom, Paris, 1992, pp. 221–244.
[29] Ludwig J.A., Tongway D.J., Spatial organisation of landscapes and its function in semi-arid woodlands, Australia, Landsc. Ecol. 10 (1995) 51–63.
[30] Mabbut J.A., Fanning P.C., Vegetation banding in arid western Australia, J. Arid Environ. 12 (1987) 41–59.
[31] Macfayden W.A., Soil and vegetation in British Somaliland, Nature 165 (1950) 121.
[32] Malam Issa O., Premières données sur les biofilms microbiens à la surface du Niger. Résultats micropétrographiques et géochimiques, DEA, université d'Orléans, 1995, 50 p.
[33] Mariotti A., Le carbone 13 en abondance naturelle, traceur de la dynamique de la matière organique des sols et de l'évolution des paléoenvironnements continentaux, Cah. Orstom Sér. Pédol. XXVI (1991) 299–313.
[34] Mauchamp A., L'hétérogénéité spatiale, sa dynamique et ses implications dans une mosaïque de végétation en zone aride, Ph.D. thesis, université Montpellier-II, 1992, 169 p.
[35] Mauchamp A., Rambal S., Lepart J., Simulating the dynamics of a vegetation mosaic: a spatialized functional model, Ecol. Model. 71 (1994) 107–130.
[36] Montana C., The colonization of bare area in two-phase of an arid ecosystem, J. Ecol. 80 (1992) 315–327.
[37] Ouedraogo P., Rôle des termitières dans la structure et la dynamique d'une brousse tigrée soudano-sahélienne, Ph.D. thesis, université Paris-VI, 1997, 232 p.
[38] Peugeot C., Influence de l'encroûtement superficiel du sol sur le fonctionnement hydrologique d'un versant sahélien (Niger). Expérimentation in situ et modélisation, Ph.D. thesis, université Grenoble-I, 1995, 317 p.
[39] Skujins J., Nitrogen cycling in arid ecosystems, in: Clark F.E., Rosswall T. (Eds.), Terrestrial Nitrogen Cycles, Stockholm, 1981, pp. 477–491.
[40] Tanner C.B., Jackson M.L., Nomographs of sedimentation times for soil particles under gravity or centrifugal acceleration, Soil Sci. Soc. Am. J. 12 (1948) 60–65.
[41] Thiéry J.M., d'Herbès J.M., Valentin C., A model simulating the genesis of banded vegetation patterns in Niger, J. Ecol. 83 (1995) 497–507.
[42] Tieszen L.L., Bouttom T.W., Stable carbon isotopes in terrestrial ecological research, Ecol. Stud. 68 (1989) 167–195.
[43] Valentin C., Bresson L.M., Morphology, genesis and classification of surface crust in loamy and sandy soils, Geoderma 55 (1992) 225–245.
[44] White L.P., Vegetation arcs in Jordan, J. Ecol. 57 (1969) 461–464.
[45] White L.P., Vegetation stripes on sheet wash surfaces, J. Ecol. 59 (1971) 615–622.
[46] Worral G.A., The Buttana grass patterns, J. Soil Sci. 10 (1959) 34–53.
[47] Zaady E., Groffman P.M., Shachak M., Litter as a regulator of N and C dynamics in Macrophytic patches in Negev desert soils, Soil Biol. Biochem. 28 (1996) 39–46.
[48] Zanguina I., Thurow T.L., Juo A.S.R., Manu A., Soil and hydrology of a banded vegetation site in Niger and their effect on tree establishment, in: Banded Vegetation Patterning in Arid and Semi-arid Environment, Orstom, Paris, France, 1996, pp. 53–55.

Acta Oecologica **20** (3) (1999) 197–208 / © Elsevier, Paris

Spatial distribution of *Prosopis glandulosa* var. *torreyana* in vegetation stripes of the southern Chihuahuan Desert

Jorge López-Portillo*, Carlos Montaña

Instituto de Ecología, Apartado Postal 63, Xalapa 91000 Veracruz, Mexico.
** Corresponding author (fax: +52 28 18 78 09; e-mail: lopez-p@ecologia.edu.mx)*

Received March 17, 1997; revised December 8, 1998; accepted December 16, 1998

Abstract — Mosaics consisting of vegetation stripes surrounded by bare areas have been described in several arid and semiarid ecosystems. The dynamics of the system depends on the redistribution of rainwater which is preferentially stored and evapotranspired in the vegetated stripes. A process of plant 'colonization' in the upslope fringe of the stripes has been described in some cases and a consequent upslope migration of the stripes has been inferred, but not confirmed in all cases quoted in the literature. In this paper, we studied the spatial distribution of mesquite (*Prosopis glandulosa* var. *torreyana*) and the soil parameters in three vegetation stripes and their associated bare areas in the southern Chihuahuan Desert. The spatial distribution of mesquites of different sizes do not coincide with that expected under the hypothesis of an uniform upslope stripe migration, but soil data suggest that current bare areas had been vegetated some time ago. Dispersion and establishment abilities enhanced by overgrazing may explain the observed mesquite distribution, but the presence of trees with high basal diameters in any part of the stripes suggests stripe permanence at the same site and no upslope migration. These results point to the conflicting evidence on stripe migration that has been already found in other areas. The most probable scenario in our study area is that of a general long-term change of form of the stripes taking place at very variable speeds in different stripes, including the possibility that some of them remain stationary for prolonged periods, and showing different histories of colonization according to the life-history of the different species concerned. The speed and regularity of the process would show a very high temporal and spatial variability due to the interaction of climatic, geomorphologic and biotic interactions. © Elsevier, Paris

'Brousse tigrée' / Mexico / stripe migration / size distribution of woody plants

1. INTRODUCTION

Vegetation patches with long axes parallel to the slope and surrounded by bare areas have been reported in many arid and semiarid ecosystems. Such pattern has been called 'brousse tigrée' (tiger-spotted scrub) by Clos-Arceduc [13]. Other related plant associations are vegetation arcs [5, 25] and vegetation stripes [4, 45]. We will use 'vegetation stripes' as the generic term.

It has been proposed that vegetation stripes can be formed in either of two alternative ways (i.e. [22]): by the lateral extension of embryonic vegetation patches in a generally bare area; or, in a vegetated area, by the formation of gaps and the reorganization of the remaining vegetation in stripes. Once stripes are formed, there are two possibilities: stripes migrate upslope; or they remain at the same location. Researchers who infer vegetation stripe migration from their data indicate that the upslope front of the stripe can expand between 15 and 30 cm annually (e.g. [5]). Montaña [31] reported an expansion of 4 m in 5 humid years (210–412 mm annual rainfall) at the front of a vegetation stripe in Mapimí, Mexico (i.e. 80 cm per annum), but that expansion was nill in the two following dry years (168 and 199 mm annual rainfall) indicating a high temporal variability of the process.

Water arriving to the stripes may come from two sources: direct rainfall which may infiltrate; or sheet flow which results from brief and intense showers. A proportion of sheet flow gets stranded at the front and in the depressions of the stripes, while the rest runs varying distances across the stripe, depending on the amount of flow. Since in Mapimí, the probability of rains generating intense sheet flow (i.e. higher than 5 mm) is low [14], it can be suggested that sheet flow will irrigate the upslope sections of the stripes more

frequently. This suggestion agrees with the proposed association between stripe movement and a gradient of water availability decreasing downslope within the stripe [22].

A long-lived plant (e.g. a shrub or a tree) established at the upslope front of a stripe with a slopewise width of, say, 30 m, will be 50-year-old when found in the middle of the stripe and 100-year-old when in the downslope margin of this stripe (considering a 30 cm advance per year). As the stripe advances, water availability will change from (relatively) very high in the upper and middle sections of the stripe to low and very low at the downslope part and its associated bare area. As a consequence, the plant will lose part of its biomass through the death of some of its branches and decrease its growth rate. Nevertheless, basal stem diameter will remain as a record of the growth reached under optimal humidity conditions. If this dynamics is true and vegetation stripes advance in rates measurable in years, then, for long-living plants such as trees and some shrubs we can hypothesize that:

(a) There will be younger plants (smaller basal diameters) at the upslope front of the stripes, and the oldest (greater basal diameters) will be found in the downslope part and its associated bare area.

(a') Cover and height will be higher in the middle position of the stripe (where plants have reached an optimal size due to their age and to water availability) and will tend to decrease downslope.

However, the literature also contains examples of apparently stable (i.e. non-migrating) stripes. Authors suggesting this have based their conclusions on the constancy of shape and location of stripes in aerial photographs taken with a difference of 15–20 years [21, 43], or on the existence, below the stripes, of a concave layer cemented by siliceous compounds which requires a long time of stripe permanence at the same position [28, 29]. Additionally, Boaler and Hodge [5] and Mabbutt and Fanning [29] suggested that stripe migration would diminish the impluvium area which would in turn modify water availability in the stripe. If stripes are stationary in absence of a water availability gradient, we can hypothesize that:

(b) There will be no consistent trend in the distribution of long-living plants, and their age (basal diameter), height and cover distribution will not be related to their position in the stripe.

Even if stripes are stationary, a water gradient below them is possible, for reasons stated before. Such a long-term gradient would be reflected in changes in the cover, height and basal diameter of the individual trees. For this reason, if the stripes are stationary in spite of a water availability gradient we can hypothesize that:

(c) Cover, height and basal diameter of long-lived shrubs or trees will tend to diminish from the upslope to the downslope part of the stripes.

A recapitulation of the three hypotheses is shown in *table I* and is graphically represented in *figure 1*, where

Table I. Hypotheses related to the logic of distribution of long-lived woody plants in vegetation stripes. If stripes migrate and there is a resource (i.e. water availability) gradient decreasing slopewise, cases contained in hypothesis 1 are found; with no stripe migration and a resource gradient, hypothesis 2 would explain our data; finally, no stripe migration and no resource gradient would result in a logic of distribution of plant attributes best explained by hypothesis 3. It is not possible for stripes to migrate if there is no water availability gradient.

Water availability gradient	Stripe migration	
	Yes	No
Yes	Hypothesis 1	Hypothesis 2
No	Impossible	Hypothesis 3

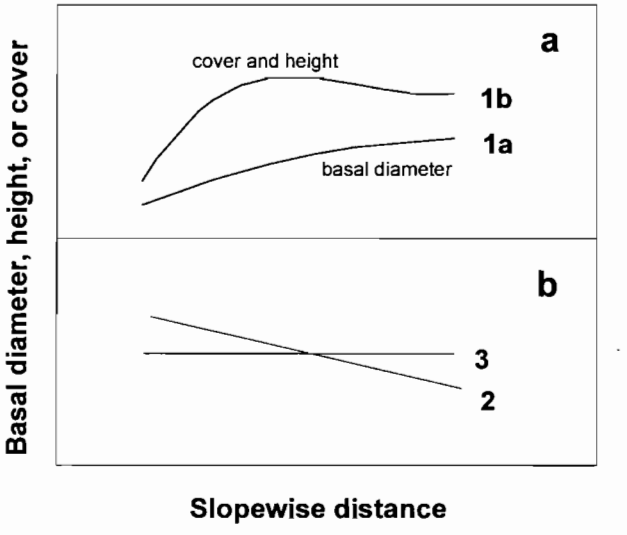

Figure 1. Expected distribution of basal diameters, height and cover of mesquite plants in vegetation stripes if the stripes migrate (a) and if the stripes remain stationary (b), under the hypotheses described in *table I*. Curve 1a shows the expected distribution of the basal diameter and curve 1b the distribution of the height and cover of the plants if the stripes migrate. Curve 2 shows the distribution of basal diameter, height and cover of mesquites if the stripes are stationary in the presence of a soil moisture gradient, while curve 3 shows the distribution of the same variables if the stripes are stationary in the absence of such gradient.

basal diameter, height and cover of shrubs or trees are related to distance along the stripe.

There are no explicit hypothesis on the relationship between plant density and stripe dynamics. However, Bush and Van Auken [12] suggested that in the savannas of Texas, the mortality of *Prosopis glandulosa* was highest in the transition from seedlings to saplings, and that once these were established, survival probability was high. For this reason, we would expect, under the stripe migration hypothesis, similar densities of the older plants in the middle and downslope (older) parts of the stripes, and a higher density of younger plants at the front of the stripes (since space has not yet been preempted), especially if there is a moisture gradient.

Soil characteristics may change in a different way if vegetation stripes migrate or remain stable as shown by Mabbutt and Fanning [29]. If plants can modify soil structure, promote lixiviation and illuviation, differences in soils beneath stable stripes and the adjacent bare areas could be expected to be due to the long-term presence of vegetation in the same site, while no differences in soil parameters will be found if the stripes migrate in the long term.

The objective of this paper was to analyze the spatial distribution of the basal diameter, height, cover and density of individuals of the honey mesquite, *Prosopis glandulosa* var. *torreyana* (Fabaceae) to test the three hypotheses stated above. We made explicit assumptions about the conditions under each of the hypotheses, and compared them with field data resulting from the census of this species in three vegetation stripes. Additionally, we measured soil properties in the same three stripes to test the hypothesis of stripe migration.

2. MATERIALS AND METHODS

2.1. Study site

The study site (26°41' N, 103°44' W, 1 170 m altitude) is located in a lower Bajada (an alluvial fan from arid environments) at the Bolsón de Mapimí, a closed basin within the Chihuahuan Desert [32]. Average annual rainfall is 264 mm, 71 % distributed mainly in summer showers of short duration. Mean annual temperature is 20.8 °C with a seasonal variation of 16.2 °C and a mean daily range of 20 °C. There is a mean number of 37 d (range: 11–58) with freezing temperatures, which occur mainly in December and January [14]. Vegetation is a xerophytic scrub [35] or Chihuahuan Desert scrub [8], but vegetation stripes (our community of interest) can be described as patches of dense grassed-scrub (i.e. an association of *Hilaria mutica* grasses and of mainly *Prosopis glandulosa* var. *torreyana* trees) surrounded by bare areas with vegetation cover lower than 10 %. Vegetation stripes, as well as other vegetation types within the study area are used for extensive cattle ranching. Cattle managers do not use fire to promote resprouting, since they fear that this kind of management would result in extensive grass killing. Only dead parts of plants are used as fuel wood, and this is collected by hand. Also, we found no evidence of natural fires due to lighting strikes in our field surveys. Soils are haplic yermosols with a clay loam texture developed on lutite facies covered by fine textured alluvial fans of variable (10–50 cm) depth [7, 16]. For the purpose of this work, we selected three vegetation stripes and their associated bare areas.

2.2. Species

The honey mesquite, *P. glandulosa* var. *torreyana* is a long-lived woody species (tree or shrub) distributed in the Chihuahuan and Sonoran deserts. This and other species of *Prosopis* can be considered as facultative phreatophytes, since their roots can take water from shallow and deep soil horizons [2, 24, 38].

2.3. Census of individuals

In each of the three vegetation stripes and their associated bare areas, we traced 50×150 m bands, with the longer axis perpendicular to contour lines. Each band was subdivided in a mesh of 10×10 m. We registered the location of each mesquite individual regardless of its size in a Cartesian coordinate system, so that its exact location could be known and graphically represented. The height, basal diameter of the widest (live or dead) branch, and the longest and shortest diameters of the canopy of every individual were annotated. The census areas inside vegetation stripes were 91×50 m for stripe 1, and 50×50 m for stripes 2 and 3, the remaining areas corresponded to the upslope and downslope bare zones.

2.4. Relief

Relief was determined with a topographer's transit, at 5-m intervals along four parallel lines equidistant from each other in each band (i.e. every 12.5 m). We calculated linear regressions between relief and distance, one for each line. All linear regressions indicated a significant association between distance and relief ($P < 0.001$). We proceeded to calculate the regression lines and their residuals. Regression coefficients indicated the mean slope (0.3–1 %), while the residuals showed variations in microtopography excluding the distance-related trend. We merged the residuals data for each stripe in order to have a three-dimensional map that could suggest lateral flow.

2.5. Size classes and density

We arbitrarily divided the censused individuals into three basal diameter (bd) categories: (a) 'small' individuals (up to 2 cm bd); (b) 'medium sized' individuals (2 to 5 cm bd); and (c) 'big' individuals (larger than 5 cm bd). To estimate density, we considered each of the points where relief was measured as the center of a 5×10 m rectangle, axis perpendicular to the slope, and assigned the number of individuals at each size class corresponding to that 50 m^2 area. Since each of the four topography lines was drawn along 31 sampling points, there were a total of 124 'density rectangles' in every vegetation stripe and its associated bare areas.

2.6. Soil sampling

Five positions were sampled in two randomly-selected transects crossing perpendicularly each one of the three vegetation stripes: upslope bare area (5 m upslope of the vegetation limit), upslope of vegetation stripe (5 m downslope of the vegetation limit), center of the vegetation stripe, downslope vegetation stripe (5 m upslope of the vegetation limit) and downslope bare area (5 m downslope from the vegetation limit). In each position, a pit was dug and one soil sample was taken every 20 cm up to 1.20 m depth (i.e. six depths per pit).

Texture [6], carbon content [42], pH, calcium carbonate, Na^+, K^+ and electrical conductivity [34] were determined in each sample.

2.7. Data analysis

To compare our plant data (height, cover, and stem basal diameter) with the a priori models stated under our three working hypotheses, we adjusted polynomial regressions by means of generalized linear models (GLM) with a normal distribution of errors. In this case, slopewise distance was considered as the only independent variable. To compare plant density, we also used GLMs, but considered errors as Poisson-distributed (i.e. a log-linear model) and used the strategies for model simplification as suggested by Aitkin et al. [1] which are equivalent to multiple comparisons once significant differences are found between factor levels. Since we calculated density for fixed areas related to the point at which every relief datum was registered, we were able to test density against three independent variables: one continuous (relief) and two categorical (vegetation stripe and position inside stripes).

We analyzed soil data by means of a double-nested ANOVA, with 'vegetation stripe' as a random variable, 'position' nested within vegetation stripe and 'depth' nested within position. In order to have an overall idea of the importance of each factor in the soil variability, an ANOVA of the scores of principal component axes of the correlation matrix of the soil variables was made. Then, to get a more precise estimation of the importance of every factor in the variability of soil parameters, a separate nested ANOVA for each soil variable was conducted. These calculations were made with the JMP software [36]. Significance levels were fixed for $P < 0.05$, unless otherwise stated.

3. RESULTS

3.1. Plant distribution in relation to microtopography

Figure 2 shows the distribution of mesquites of the three size categories as a function of a three-dimensional map of relief residuals in the three vegetation stripe segments. We divided each stripe into three positions (F, C, and B as front, center and back of the stripe, respectively) plus the two positions occupied by the upslope and downslope bare areas (U and D in *figures 2* and *5*, respectively). The range in relief residuals is around 20 cm in vegetation stripe 1 (*figure 2a*), 10 cm in stripe 2 (*figure 2b*), and 12 cm in stripe 3 (*figure 2c*). It can be seen that the three size categories are distributed in all positions inside the stripes. However, plants tend to cluster in small areas where relief is similar. The three-dimensional maps suggest there is lateral surface flow and water impoundment inside vegetation stripes as suggested by Dunkerley [18].

3.2. Density

Relative density in the three size categories was significantly associated to vegetation stripe, position in the stripe and their interaction, and not associated to relief. Following the simplification procedures for GLMs [1], we found that density of small individuals was significantly higher ($P < 0.001$) in the middle and downslope portion of vegetation stripe 3 (*figure 3a*). Density of medium-sized individuals was significantly lower ($P < 0.0001$) in the upslope and downslope positions of vegetation stripes 2 and 3 (*figure 3b*), and that density of bigger individuals was lower ($P < 0.0003$) at the downslope part of vegetation stripe 3 (*figure 3c*).

3.3. Height and cover of plants

We analyzed the plants with basal diameters ≥ 5 cm, considering them as indicators of maximum size attained at every position inside or outside the three vegetation stripes. *Figure 4* shows the height

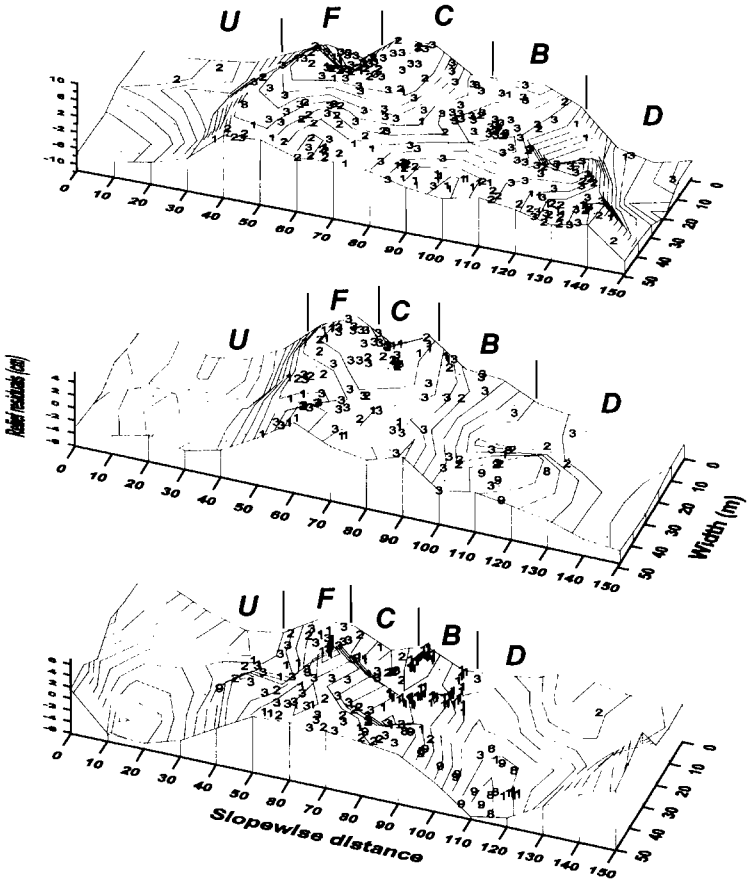

Figure 2. Spatial distribution of mesquites of different size categories in three vegetation stripes as a function of the slopewise distance and of the residuals of four linear regressions between relief and slopewise distance. Size categories are: (1) less than 2 cm of basal diameter (bd), (2) between 2 and 5 cm bd, and (3) more than 5 cm bd. Numbers 8 and 9 in the stripes indicate dead individuals corresponding to size categories 2 and 3, respectively. Positions are indicated as: (U) upslope bare area, (F, C, B) front, center and back of the stripe, and (D) downslope bare area.

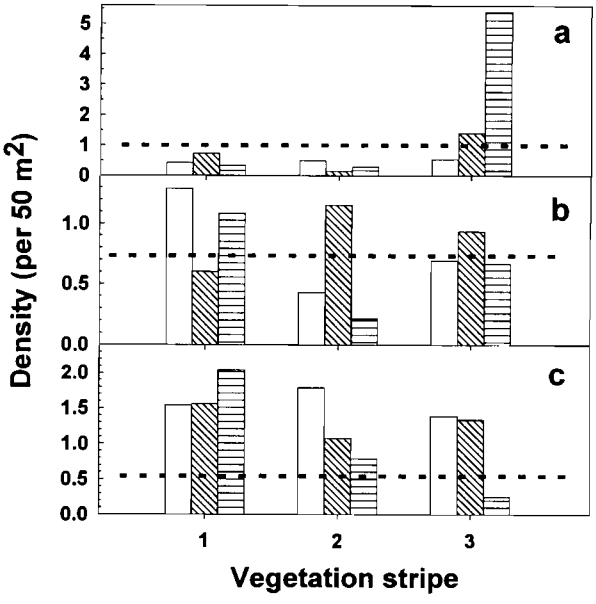

Figure 3. Density of mesquites of three size categories in three positions within three vegetation stripes. Data from each size category are shown in a separate histogram: (a) less than 2 cm of basal diameter (bd), (b) between 2 and 5 cm bd, and (c) more than 5 cm bd. Figures along the abscissa axes identify the different stripes. Each bar represents the density of plants in each position: front (white bars), medium (diagonally-hatched bars), and back (horizontally-hatched bars) of the stripes. Discontinuous lines parallel to the abscissas split density groups that are significantly different ($P < 0.05$).

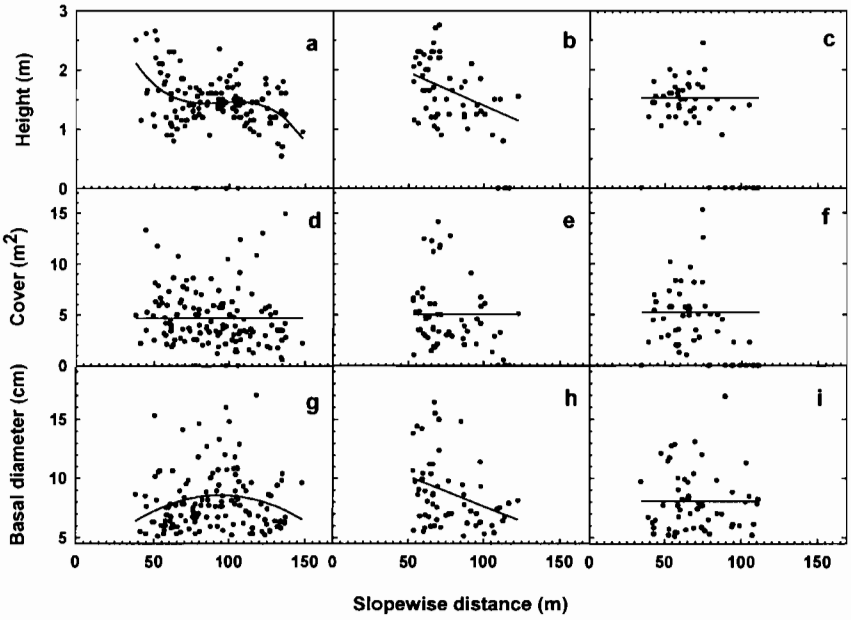

Figure 4. Plant height (a–c), cover (d–f) and basal diameter (g–i) of mesquites with basal diameters ≥ 5 cm growing in three vegetation stripes as a function of the slopewise distance. Each triad (a, d, g), (b, e, h) and (c, f, i) of scatter diagrams and their adjusted lines corresponds to one of the three sampled vegetation stripes. Stripe 1 showed a cubic (a, $r^2 = 0.16$, $P < 0.001$) and a quadratic (g, $r^2 = 0.04$, $P = 0.02$) regression, while stripe 2 showed significant linear regressions in b ($r^2 = 0.16$, $P = 0.02$) and h ($r^2 = 0.10$, P = 0.01). There were no significant regressions in stripe 3 for any plant attribute.

(*figure 4a–c*) and cover (*figure 4d–f*) in the three vegetation stripes as a function of the slopewise distance. There was a significant correlation between slopewise distance and height in two vegetation stripes (*figure 4a, b*). The slopes of the regression lines were negative, indicating that height tends to decrease downslope. We did not find significant relationships between plant cover and slopewise distance in any stripe (i.e. cover was similar along stripes).

3.4. Basal diameter

Figure 4g–i shows the basal diameter (bd) of 'older' individuals (≥ 5 cm) in the three vegetation stripes as a function of the slopewise distance. The trend in stripe 1 (*figure 4c*) was for bd to be higher at the center. A significant linear regression between bd and slopewise distance was found for stripe 2 (*figure 4h*); the slope of the regression line indicated that basal diameter tends to decrease downslope.

3.5. Soil

Soil profiles were very similar to those described by Delhoume [16] and Breimer [7]. They had a 10- to 15-cm thick A horizon extending to a more or less clayey B horizon 40- to 50-cm thick. Then a weathered lutite C horizon with a blocky structure overlaid a massive lutite bedrock. The first three principal components of the correlation matrix of soil variables (clay, silt, sand, carbonate, organic carbon, sodium and potassium content, pH and electrical conductivity) accounted for 39.4, 18.0 and 15.3 % of the total variability. The nested ANOVA of the first axis scores revealed that most of its variability (81.6 %) was accounted for by depth and that positions and stripes explained 3.7 and 4.4 %, respectively, the three effects being significant. The variability of the second axis was significantly associated to the stripe (7.1 % of the total variability explained) whereas its relationship with depth and position (37.8 and 6.9 %, respectively) was not significant. In the third axis, the most important factors were depth and stripe (35.5 and 30.4 % of variability explained) and the effect of position was non-significant (4.6 %).

Clay content varied between stripes (15.7 % of the variance explained by this factor) and between depths (51.7 % of the variance explained) but not between positions. Variation between stripes ranged from 31.3 in stripe 2 up to 41.0 % in stripe 3 (stripe 1 had an intermediate value of 37.4 %). Variation between depths ranged from 24.3 % at 20 cm depth up to nearly 40.0 % at the remaining depths (*figure 5a*). Silt and

sand content also varied between stripes (6.7 and 6.1 % of the variances explained for each respective ANOVA) but varied neither between positions nor depths. In these cases, ranges of variation were from 15.0 (stripe 3) up to 19.5 % (stripe 1) in silt content and from 43.2 (stripe 1) up to 49.6 % (stripe 2) in sand content.

pH varied between stripes (11.7 % of the variance explained by this factor) but varied neither between positions nor depths. It varied from 8.7 in stripe 3 up to 9.0 in stripe 2 (stripe 1 had an intermediate value of 8.8).

Calcium carbonate content varied between stripes (4.4 % of the variance explained by this factor) and between depths (76.4 % of the variance explained). Stripe 3 had the highest content (21.9 %) whereas stripes 1 and 2 had 19.1 and 19.4 %, respectively. It was lower at 20 cm and increased with depth (*figure 5b*).

Carbon content varied between stripes (4.5 % of the variance explained by this factor), between positions (4.7 % of the variance explained) and between depths (75.2 % of the variance explained). It was higher in stripe 3 (0.42 %) than in stripes 1 and 2 (0.31 and 0.28 %, respectively). It was also higher (0.71 %) at 20 cm than at any other depths (*figure 5c*). Finally, it was higher inside the stripes (0.38 %) than in the bare areas (around 0.27 %) (*figure 5d*). Separate analyses for each depth showed that differences between positions were only significant at the upper layer (0–20 cm, *figure 5e*).

Potassium content varied between stripes (2.7 % of variance explained) and between depths (69.9 %). It ranged from 0.55 meq·100 g^{-1} in stripe 1 up to 0.74 meq·100 g^{-1} in stripe 3, with an intermediate value of 0.70 meq·100 g^{-1} in stripe 2. In depth, it decreased from 1.4 meq·100 g^{-1} in the surface up to 0.4 meq·100 g^{-1} below 80 cm (*figure 5f*).

Sodium content varied significantly between stripes (13.7 % of the variance explained), between positions (7.7 %) and between depths (57.2 %). It ranged from 6.6 in stripe 1, to 13.9 meq·100 g^{-1} in stripe 3, with an intermediate value of 9.5 meq·100 g^{-1} in stripe 2. It increased with depth from 2.6 at the surface up to nearly 15 meq·100 g^{-1} below 80 cm (*figure 5g*). Regarding positions, it ranged from 8.2 meq·100 g^{-1} in the downslope part of the vegetation stripe up to 11.2 meq·100 g^{-1} in the upslope bare area (*figure 5h*). Aiming to elucidate whether the vertical distribution of the Na^+ content varied with positions, we calculated the interaction of position and depth (although its validity for purposes of generalization can be criticized because of the nested nature of our experimental design). This interaction was non-significant ($P = 0.9$) indicating that the eventual leaching of Na^+ did not differ between soils from stripes and bare areas. Contrariwise, the stripes by depth interaction was highly significant ($P = 0.003$). Sodium content was lower than 5 meq·100 g^{-1} up to 40 cm depth in all stripes. Between 40 and 60 cm depth, it amounted to 5.5, 8.8 and 11.9 meq·100 g^{-1} in stripes 1, 2 and 3, respectively, and below 80 cm, it increased to 9.4, 13.8 and 21.3 meq·100 g^{-1} suggesting an important difference in the sodium contained in the bedrock. Separated nested ANOVAs for each depth revealed that differences between stripes were significant below 60 cm whereas there was no differences between positions at any depth, except between 60 and 80 cm. These results suggest a high variability in the sodium contained in the bedrock and a lower variability in the allochtonous material deposited over it.

Electrical conductivity had a pattern of variability similar to that of sodium content. It varied significantly between stripes (11.4 % of the variance explained), between positions (11.9 % of the variance) and depth (59.9 % of the variance). It ranged from 2.2 in stripe 1 up to 4.4 mS·cm^{-1} in stripe 3, with an intermediate value of 2.5 mS·cm^{-1} in stripe 2. It increased with depth from 0.3 near the surface to nearly 4.6 mS·cm^{-1} below 80 cm (*figure 5i*). Regarding positions, it ranged from 2.3 in the downslope vegetation-stripe to 3.5 mS·cm^{-1} in the upslope bare area (*figure 5j*). The calculations of the interactions and of separate nested ANOVAs for each depth showed a pattern similar to sodium content.

4. DISCUSSION

4.1. Mesquite distribution

Mesquite density was not related to position inside the stripes in any of the size classes we distinguished. This suggests different histories of colonization of the vegetation stripes by this species of *Prosopis*. There is also no trend as to where younger plants were established, or where they survive and grow. It has been reported that mesquites occupy pasture lands where cover has been sensibly affected by grazing [9, 11], a very likely situation at our study site, which has been exposed to cattle grazing since the last century [20, 26]. It could then be argued that, under these conditions, seedlings may establish at any position within the stripe, and that this trend would be similar whether stripes migrated or not. Thus, the distribution of plants within stripes could be thought of as a mosaic of different patch sizes not arranged in a slopewise direction as expected if vegetation stripes migrated upslope.

We did not establish the statistical relationship between basal stem diameter and age, and are aware of

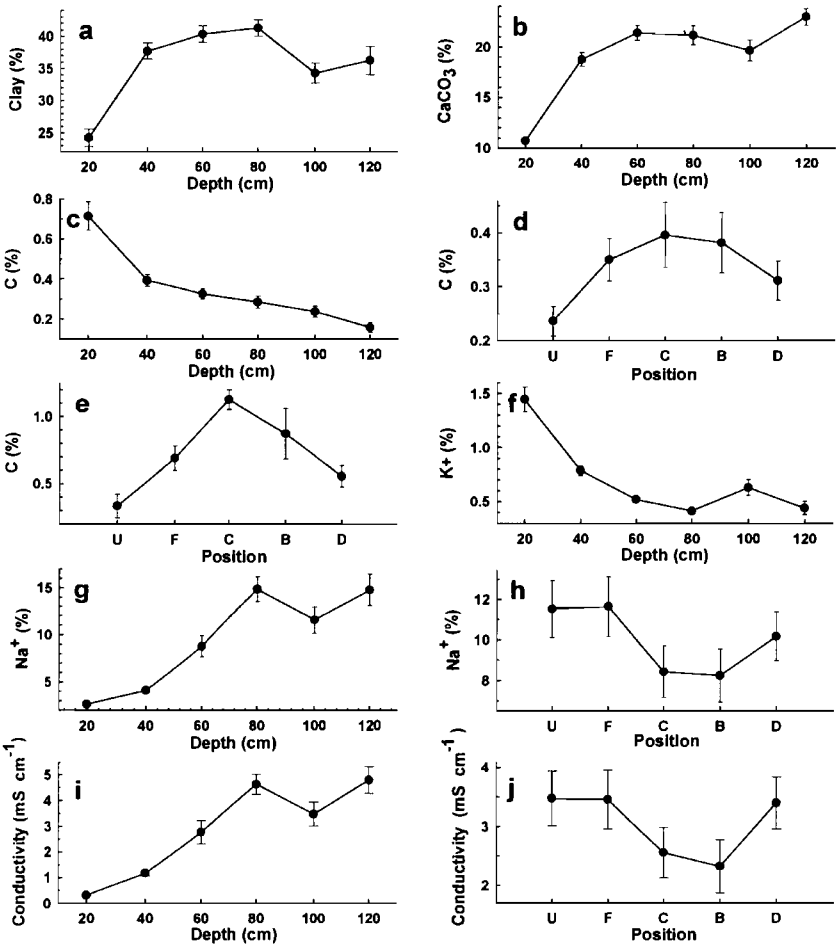

Figure 5. Soil data from three vegetation stripes merged by position along the stripes and their bare areas or by soil sampling depth. Two transects perpendicular to contour lines were sampled at five positions and six depths in three vegetation stripes. Relationship between: (a) clay content and depth; (b) calcium carbonate and depth; (c) C and depth; (d) C and position; (e) C in the 0–20 cm layer and position; (f) K^+ and depth; (g) Na^+ and depth; (h) Na^+ and position; (i) electrical conductivity and depth; and (j) electrical conductivity and position. Soils were sampled at 20-cm depth intervals; the top value of each interval is shown in the corresponding abscissas. Positions are indicated as: (U) upslope bare area, (F, C, B) front, center and back of the stripe, and (D) downslope bare area. Vertical lines represent standard errors.

this limitation [23], considering that plants are genetically different and that different growth rates could be possible even under similar water availability conditions. In addition, older stems would have died and their stumps would go unregistered; if so, we would underestimate in favor of greater basal diameters. Fires are not used as a management tool by land users, so this factor can be ruled out as a cause of mortality. Wildfires due to lighting strikes would have restricted effects due to the existence of bare areas between stripes; we found no evidence of massive mortality in the stripes we studied. Another cause of death would be wood-borers mainly in Coleoptera, but this would affect an ample range of basal diameters.

We used stems with the highest basal diameters for our analyses on plant attributes. Although an interaction between these individuals could be expected, this would be less intense than that between plants of contrasting sizes [10]. Therefore, a supposition we depend on for the validity of these analyses (in order to avoid violation of the statistical principle of independence between observations) is that such 'big' trees are relatively independent of each other.

If we were to detect a pattern in the spatial distribution of basal diameters, this should be very slight due to intraspecific and substrate variation (i.e. statistical models of slopewise distance against plant at-

tributes should explain a low proportion of their variability). No model parameters derived from our data explained more that 16 % of total variability of plant attributes. To suggest a relationship between basal diameter (bd) and age, we relied on the work of Archer [3] in a subtropical savanna of Texas concerning the growth of *Prosopis glandulosa* var. *glandulosa* trees in vegetation islands 'founded' by the tree itself. Archer [3] estimated that tree stem bd near 5 cm were around 50 years of age, and from 172 to 217 years old if bd was around 27 cm. Since there is a high density of trees with ≥ 5 cm bd at the front of the three stripes we studied, we consider this as evidence against the moving stripe hypothesis. Furthermore, all models between slopewise distance and plant height, cover or basal diameter are more akin to the stable stripe hypotheses, i.e. basal diameter tended to be greater at the middle of vegetation stripe 1, but it diminished towards the downslope part, and basal diameter (in the other stripes) and height either tended to diminish slopewise, or were similar along the stripes as was found for plant cover.

An argument that has been used to suggest stripe migration is that there are more dead trees or shrubs in the downslope limits of the stripe and its associated bare area [5, 15, 25, 27, 33, 41, 44], a result we also found in vegetation stripes 2 and 3. However, taking into consideration that we found no evidence supporting the migration of stripes, an alternative would be that some sections of the downslope part of the stripes have contracted, the rest of the area remaining stable (see last paragraph). A similar conclusion with additional elements was found and described as an 'enduring feature' by Dunkerley and Brown [19].

In conclusion, the distribution of mesquite densities suggests that colonization events were different in the three stripes under study and the results do not support the stripe migration hypothesis since (a) mesquites of the higher basal diameters tend to be distributed at the front of the stripes, or at any position within; and (b) there are no unequivocal trends between the position inside the stripes and mesquite physiognomy, and the observed trend would seem to be opposite to that expected under the stripe migration hypothesis (i.e. height tended to be higher in the upslope part of two stripes and was similar along the third stripe, and there were no differences in cover within the stripes). Finally, the presence of dead individuals downslope of the stripes (labeled as 8 and 9 in *figure 2*) could be a consequence of a partial downslope contraction of the stripes.

4.2. Soil variability

The variability between stripe vs. bare area soils seems to support the hypothesis that stripes change their positions in the long term. The results of the PCA of soil variables indicate that a very low variability could be assigned to the position of the soil samples. These results show that the most important effect on soil variability is due to depth. It explains most of the variability of the three axes analyzed (although its effect on the second axis is not significant). Between-stripe differences has a fair importance for explaining the variability of the third axis, whereas position has a very low importance significantly explaining only 3.7 % of the first axis variability. Separate ANOVAs for each soil variable showed that there were no differences between soils beneath stripes and bare areas, with the exceptions of carbon and sodium content, and electrical conductivity. Differences in carbon content were restricted to the surface horizon (the first 20 cm) and it could be argued that this is a consequence of the long-term change in the position of vegetated areas. Sodium content and electrical conductivity were lower at the center and downslope of the stripe when compared to the upslope of the stripe and the bare areas. There was no evidence of a long-term different leaching between positions as revealed by a non-significant interaction between positions and depths, but there was evidence of a strong variation in the bedrock and the original soil material. In summary, contrasting with mesquite distribution, soil data would suggest that vegetation stripes do not remain stationary in the long term. Soil profiles did not indicate any mineralogical, structural pre-existent differences or other than those produced by the presence of vegetation in the stripes. Moreover, carbon content in bare areas suggests that they were vegetated some time ago. Other studies conducted in the same area point in the same direction. Delhoume ([16, 17]; see also [15]) found that soils of stripes and bare areas were developed over fine-textured alluvial-colluvial transported material, overlying on in situ claystone (lutite), except in very small and localized pockets where they are developed over a bit coarser colluvial deposits. Soils of stripes and bare areas only differed in the surface horizons and these differences were interpreted by the authors as the consequence of differences in vegetation cover. Soils of both types presented the same succession of horizons with the same morphology. The main differences were in the carbon content of the 0–25 cm layer: bare areas had less carbon content (0.55 %; C/N ratio of 7.1) than vegetated areas (1.96 %; C/N ratio of 37.7).

4.3. Consequences for the dynamics of vegetation stripes

Regarding vegetation, Montaña et al. [33] found that most of *P. glandulosa* and *F. cernua* seedlings occurred in the upslope part of the stripes they studied, 20 km apart and under a less grazed condition than the

ones studied in the present work. Cover variation of adult plants also agreed with the hypothesis that the stripes do not remain stationary. Mauchamp et al. [30] found that the establishment of *F. cernua* seedlings is highly dependent on the conditions provided by the colonization front of the arcs. As a consequence, they proposed that *F. cernua* populations function as a metapopulation with successive establishment and local extinctions according to the development and spatial change of the grass cover as the upslope front of the stripe expands.

However, the detailed distribution of *Prosopis* saplings reported in this paper suggests that changes in the position of vegetated patches do not follow the regular and predictable pattern underlying the migration hypotheses outlined in this paper. In addition, the presence of mesquites with high basal diameter values in the upslope boundary of the stripes suggests that those boundaries have changed little since these trees were established. On one hand, it may be that differences in relief within the stripes determine differences in soil water stocking where pockets of high (or low) water storage do not follow a regular pattern across the stripes, an argument that has been considered at greater length by Dunkerley [18]. But the dispersion and establishment characteristics of *P. glandulosa* may also explain the observed patterns of distribution of saplings and juveniles. Mesquite seeds are endozoochorously dispersed by large herbivores and can be clumped in places where animals graze or rest, as we was found at the back of one of our vegetation stripes. Brown and Archer [10] concluded that rapid development of roots enhanced *P. glandulosa* var. *glandulosa* seedling survival in a Texas savanna by enabling them to access soil moisture below the layers explored by grasses. Also, their ability to develop extensive lateral root systems allow water uptake from large volumes of soil [24]. Results reported for the same species by Bush and Van Auken [11] indicate that reduced grass competition enhances seedling establishment. These characteristics of mesquite biology suggest that their populations can explosively grow in stripes under grazing conditions, different situation to that of non-endozoochorously dispersed species (e.g. *Flourensia cernua*, [30]).

In summary, our data points to the conflicting evidence on stripe migration that has been already exposed (e.g. [45, 46]). If we merge the information already discussed, we could argue that the most likely scenario for our study area is that of a general long-term (hundreds of years) change of form taking place at variable speeds in different stripes, including the possibility that they might remain stationary. This scenario could include a rearrangement of the spatial distribution of vegetation patches when their structure (or the surface of their associated water-collecting bare areas) are changed by sudden erosional events due to unusual rainstorms or periods of overgrazing. In addition to rainfall unpredictability, the variability in the speed of this rearrangement process could be attributed both to the development of the microgeomorphological processes, which ultimately determine the redistribution of sheet-flowing water, and to the population biology (seed dispersal, establishment requirements, growth rate) of the species concerned and the resulting biotic interactions (competition and facilitation between plants, granivory, secondary dispersion, and herbivory).

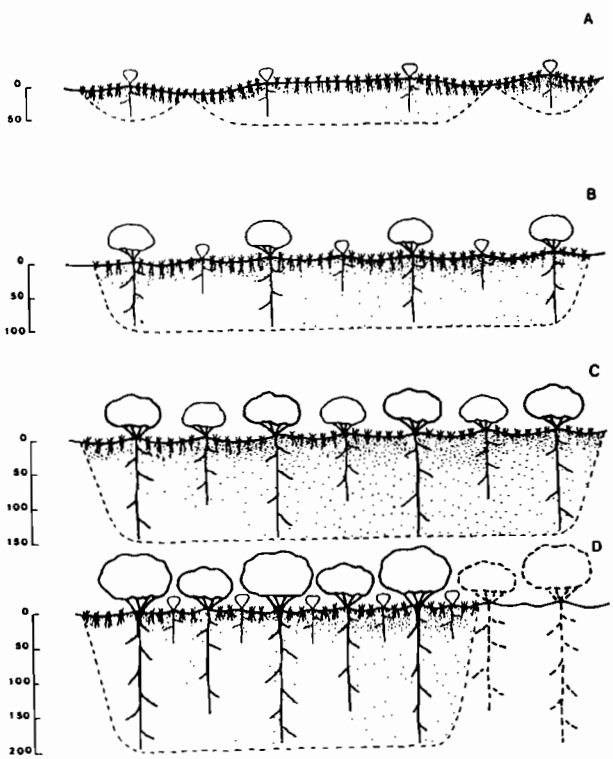

Figure 6. Four successive steps involved in the formation or reconstruction of degraded stripes. (A) Small patches of grasses and woody plants coalesce. (B) As the vegetation develops, roots explore deeper layers so the soil is modified by their activity, increasing soil water-holding capacity. Additionally, other plants are established in small bare areas within the stripes or where the grass has been grazed. (C) The full development and function of root systems further increase water infiltration. (D) Evapotranspiration demand outgrows soil water-stocking capacity. Some plants of the downslope margin of the stripes, receiving less water from sheet flow, die from water deficit. The result is a contraction of the downslope part of stripe. Vertical scales show soil depth in cm. The upslope part of the stripe is on the left.

We propose, for the formation or spatial reorganization of stripes, a dynamics compatible with our data and synthesized in four stages (*figure 6*). In the first stage, a vegetation stripe would be formed through the coalescence of smaller patches of grasses and woody plants; roots would be mostly superficial and thus the depth of the soil modified by their activity [40]. In the second stage, the aerial and subterranean parts of woody plants develop. As roots increase in depth, the soil is modified by their activity, increasing its capacity of water storage. Additionally, other plants are established in the bare areas within the stripes or where the grass has been grazed. In the third stage, development and function of roots further increase water infiltration, which may cause ion lixiviation and clay illuviation [5, 29, 41, 43, 44], until water storage capacity below the stripes is in equilibrium with the amount of water received both by direct rainfall and sheet flow, which can be up to 2.5 times the annual precipitation [15, 25]. In the fourth stage, growth and development of plants further modify soil conditions, but the water that is evapotranspired is higher than the one that can be stocked, and the plants in some sections of the downslope margin of the stripes, receiving less water from sheet flow, die as a consequence of a water deficit. This model would imply that available water is relatively homogeneous and that the main contrast is between vegetation stripes and their bare areas. Only after these four steps have been completed, do the conditions become suitable for the process of upslope colonization and migration to be set in motion, but field evidence of such process remains controversial [37, 39]. Even after that, a very high temporal and spatial variability in the speed of the process should be expected due to the interaction of climatic, geomorphologic and biotic factors. However, stripe migration does not seems to be a necessary condition for the existence of the striped vegetation pattern.

Acknowledgments

The staff of the 'Laboratorio del Desierto' gave logistic support during field work. Lourdes Cruz and Ninfa Portilla conducted the soil analyses. Financial support was granted by the 'Consejo Nacional de Ciencia y Tecnología'. We thank two anonymous referees for the critical revision of this manuscript.

REFERENCES

[1] Aitkin M., Anderson D., Francis B., Hinde J., Statistical Modelling in GLIM. Oxford Statistical Science Series, Clarendon Press, Oxford, 1990, 374 p.

[2] Ansley R.J., Jacoby P.W., Cuomo G.J., Water relations of honey mesquite following severing of lateral roots: influence of location of subsurface water, J. Range Manag. 43 (1990) 436–442.

[3] Archer S., Development and stability of grass/woody mosaics in a subtropical savanna parkland, Texas, USA, J. Biogeogr. 17 (1990) 453–462.

[4] Boaler S.B., Hodge C.A., Vegetation stripes in Somaliland, J. Ecol. 50 (1962) 465–474.

[5] Boaler S.B., Hodge C.A., Observations on vegetation arcs in the Northern region, Somali Republic, J. Ecol. 52 (1964) 511–544.

[6] Bouyoucos G.J., Hydrometer method improved for making particle size analysis of soil, Agron. J. 54 (1962) 464–465.

[7] Breimer R.F., Physiographic soil survey, in: Montaña C. (Ed.), Estudio Integrado de los Recursos Vegetación, Suelo y Agua en la Reserva de la Biósfera de Mapimí, Instituto de Ecología, México, 1988, pp. 115–134.

[8] Brown D.E., Chihuahuan Desert-scrub, Desert Plants 4 (1982) 169–179.

[9] Brown J.R., Archer S., Woody plant invasion of grasslands: establishment of honey mesquite (*Prosopis glandulosa* var. *glandulosa*) on sites differing in herbaceous biomass and grazing history, Oecologia 80 (1989) 19–26.

[10] Brown J.R., Archer S., Water relations of perennial grass and seedling vs. adult woody plants in a subtropical savanna, Texas, Oikos 57 (1990) 366–374.

[11] Bush J.K., Van Auken O.W., Growth and survival of *Prosopis glandulosa* seedlings associated with shade and herbaceous competition, Bot. Gaz. 151 (1990) 234–239.

[12] Bush J.K., Van Auken O.W., Importance of time of germination and soil depth on growth of *Prosopis glandulosa* (Leguminosae) seedlings in the presence of a C4 grass, Am. J. Bot. 78 (1991) 1732–1739.

[13] Clos-Arceduc M., Étude sur photographies aériennes d'une formation végétale sahélienne : La brousse tigrée, Bull. Inst. Fr. Afr. Noire Sér. A 18 (1956) 677–684.

[14] Cornet A., Principales caractéristiques climatiques, in: Montaña C. (Ed.), Estudio Integrado de los Recursos Vegetación, Suelo y Agua en la Reserva de la Biósfera de Mapimí, Instituto de Ecología, México, 1988, pp. 45–76.

[15] Cornet A.F., Montaña C., Delhoume J.P., López-Portillo J., Water flows and the dynamics of desert vegetation stripes, in: Hansen A.J., Di Castri F. (Eds.), Landscape Boundaries. Consequences for Biotic Diversity and Ecological Flows, Ecological Studies No. 92, Springer Verlag, Germany, 1992, pp. 327–345.

[16] Delhoume J.P., Distribution spatiale des sols le long d'une toposéquence représentative, in: Montaña C. (Ed.), Estudio Integrado de los Recursos Vegetación, Suelo y Agua en la Reserva de la Biósfera de Mapimí, Instituto de Ecología, México, 1988, pp. 135–166.

[17] Delhoume J.P., Fonctionnement hydro-pédologique d'une toposéquence de sols en milieu aride (Réserve de la Biosphère de Mapimí, nord-Mexique), thèse, université de Poitiers, France, 1996, 295 p.

[18] Dunkerley D.L., Banded vegetation: development under uniform rainfall from a simple cellular automaton model, Plant Ecol. 129 (1997) 103–111.

[19] Dunkerley D.L., Brown K.J., Runoff and runon areas in a patterned chenopod shrubland, arid western New South Wales, Australia: characteristics and origin, J. Arid Environ. 30 (1995) 41–55.

[20] Ezcurra E., Montaña C., Los recursos naturales renovables en el norte árido de México, in: Leff E. (Ed.), Medio ambiente y desarrollo en México, Centro de Investigaciones Interdisciplinarias en Humanidades, UNAM-Grupo Editorial Miguel Angel Porrúa, Mexico, 1990, pp. 297–327.
[21] Greenwood J.E.G.W., The development of vegetation patterns in Somaliland Protectorate, Geogr. J. 123 (1957) 465–473.
[22] Greig-Smith P., Pattern in vegetation, J. Ecol. 67 (1979) 755–779.
[23] Harper J.L., Population Biology of Plants, Academic Press, London, 1977, 892 p.
[24] Heitschmidt R.K., Ansley R.J., Dowhower S.L., Jacoby P.W., Price D.L., Some observations from the excavation of honey mesquite root systems, J. Range Manag. 41 (1988) 227–231.
[25] Hemming C.E., Vegetation arcs in Somaliland, J. Ecol. 53 (1965) 57–68.
[26] Hernández L., Ganado bovino asilvestrado en el Bolsón de Mapimí: sus antecedentes históricos y su papel ecológico y socio-económico en la Reserva de la Biosfera de Mapimí, Ph.D. thesis, Instituto Politécnico Nacional, México, 1995, 247 p.
[27] Janke B., Zum problem der vegetationsstreifen (Brousse-Tigrée) in semiariden Afrika, Die Erde 1 (1976) 31–46.
[28] Litchfield W.H., Mabbutt J.A., Hardpan in soils of semi-arid Western Australia, J. Soil Sci. 13 (1962) 148–159.
[29] Mabbutt J.A., Fanning P.C., Vegetation banding in arid Western Australia, J. Arid Environ. 12 (1987) 41–59.
[30] Mauchamp A., Montaña C., Lepart J., Rambal S., Ecotone dependent recruitment of a desert shrub, *Flourensia cernua*, in vegetation stripes, Oikos 68 (1993) 107–116.
[31] Montaña C., The colonization of bare areas in two-phase mosaics of an arid ecosystem, J. Ecol. 80 (1992) 315–327.
[32] Montaña C., Breimer R.F., Major vegetation and environmental units, in: Montaña C. (Ed.), Estudio integrado de los recursos vegetación, suelo y agua en la Reserva de la Biósfera de Mapimí, Instituto de Ecología, México, 1988, pp. 99–114.
[33] Montaña C., López-Portillo J., Mauchamp A., The response of two woody species to the conditions created by a shifting ecotone in an arid ecosystem, J. Ecol. 78 (1990) 789–798.
[34] Richards L.A. Diagnosis and Improvement of Saline and Alkali Soils, (Ed.), US Department of Agriculture Handbook No. 60, Washington DC, 1954, 160 p.
[35] Rzedowski J., Vegetación de México, Limusa, México, 1978, 432 p.
[36] SAS Institute, JMP User's Guide, Version 3.1, SAS Institute Inc., North Carolina, USA, 1995, 239 p.
[37] Seghieri J., Galle S., Rajot J.L., Ehrmann M., Relationships between soil moisture and growth of herbaceous plants in a natural mosaic in Niger, J. Arid Environ. 36 (1997) 87–102.
[38] Simpson B.B., Solbrig O.T., Introduction, in: Simpson B.B. (Ed.), Mesquite. Its Biology in Two Desert Scrub Ecosystems, Dowden, Hutchinson, Ross, Stroudsburg, Pennsylvania, 1977, pp. 1–25.
[39] Thiéry J.M., d'Herbès J.M., Valentin C., A model simulating the genesis of banded vegetation patterns in Niger, J. Ecol. 83 (1995) 497–507.
[40] Tiedemann A.R., Klemendson J.O., Effect of mesquite on physical and chemical properties of the soil, J. Range Manag. 26 (1973) 27–29.
[41] Tongway D.J., Ludwig J.A., Vegetation and soil patterning in semi-arid mulga lands of Eastern Australia, Aust. J. Ecol. 15 (1990) 23–34.
[42] Walkley A., Black T.A., An examination of the Degtjareff method for determining soil organic matter and a proposed modification of the chromic acid tritation method, Soil Sci. 37 (1934) 29–38.
[43] White L.P., Vegetation arcs in Jordan, J. Ecol. 57 (1969) 461–464.
[44] White L.P., Brousse tigrée patterns in southern Niger, J. Ecol. 58 (1970) 549–553.
[45] White L.P., Vegetation stripes on sheet wash surfaces, J. Ecol. 59 (1971) 615–622.
[46] Wickens G.E., Collier F.W., Some vegetation patterns in the Republic of Sudan, Geoderma 6 (1971) 43–59.

Acta Oecologica **20** (3) (1999) 209–217 / © Elsevier, Paris

Forum

Run-on contribution to a Sahelian two-phase mosaic system: Soil water regime and vegetation life cycles

Josiane Seghieri [a]*, Sylvie Galle [b]

[a] *IRD, B.P. 5045, 34032 Montpellier, France.*
[b] *LTHE, B.P. 53, 38041 Grenoble cedex 9, France.*
* *Corresponding author (fax: +33 4 67 41 62 94; e-mail: Josiane.Seghieri@impl.ird.fr)*

Received April 1, 1997; revised February 12, 1999; accepted March 16, 1999

Abstract — An experiment was carried out from 1992 to 1995, in south-western Niger on a banded vegetation pattern which dominates on a laterite-capped plateau in the region. We quantified the changes in infiltration and vegetation in a thicket from which run-on from the upslope bare soil zone was artificially divested. A concrete wall (40 m long, 60 cm high, 20 cm thick, with a foundation 25 cm deep) was constructed at its upslope boundary. Infiltration was measured to a depth of 5.4 m by a neutron probe, and densities of annual plants were monitored along transects crossing perpendicularly a control thicket and the thicket deprived of run-on. Phenological phases and leaf water potential of the two dominant shrub species were recorded from stratified sampling according to their preferred location along the water resource gradient. Results indicated that run-on contributed the most to infiltration in the central zone, but the water content available to the annual plants (layer 0–10 cm) was not affected by run-on deprivation. Significant differences were found in the water content available to the shrubs (layer 0–100 cm) both between zones (upslope and central), and between thickets after the wall was built. However, in the thicket deprived of run-on, life cycle and physiology of the shrubs were severely disturbed upslope, while much smaller effects were observed in the centre. Surprisingly, within the study interval, run-on contribution was not found to be as essential to shrubs' life cycle at the location where it contributed the most to the infiltration. © Elsevier, Paris

Banded vegetation pattern / leaf water potential / phenology / life history strategy / water resource / water flow / gradient

1. INTRODUCTION

Several hypotheses have been proposed to explain the functioning of banded vegetation pattern and most refer to the influence of overland water flow [3, 15, 16, 17]. In Niger, 4 years of monitoring soil water content and run-off demonstrated that about 70 % of heavy rain (54 % of annual rainfall) falling on bare surfaces produces sheet run-off [20]. It moved downslope to be intercepted and to pond over the thicket where the average infiltration was equal to four times the incident rainfall [8]. Seghieri et al. [21] showed that the distribution of the vegetation changed characteristically along this soil water gradient. In this study, we sought to quantify the changes in infiltration and vegetation response when no water flow reaches the thicket.

We prevented water flow into a thicket by building a concrete wall on its upslope border. We compared the soil moisture regime, the density of plants in herbaceous layer, and the phenology and leaf water potential of the two dominant species in the woody cover between a control thicket, and the thicket deprived of run-on. The leaf water potential indicated the physiological responses of the shrubs to drought periods induced by seasonal variations in water availability. It allowed us to quantify the level of shrub water stress [10, 24]. Leaf water potential represents the integration of both atmospheric stress and soil water

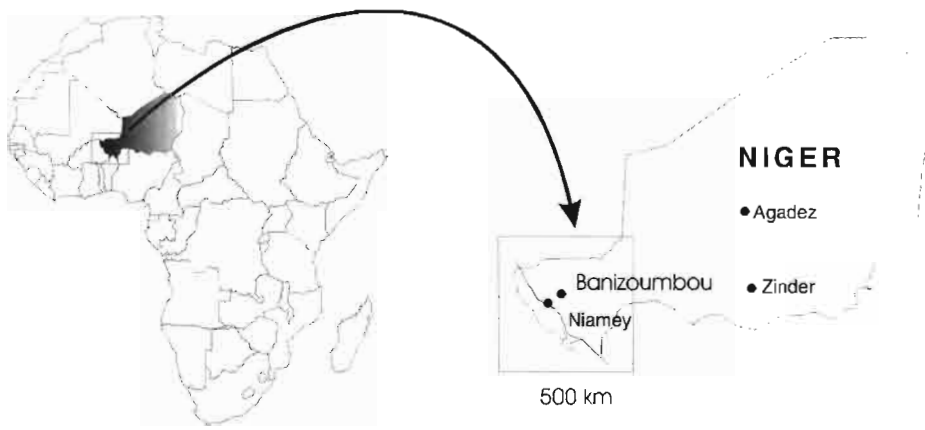

Figure 1. Geographical location of Banizoumbou site, south-western Niger.

stress in the whole rooting zone of the plants, and it is the basic measurement to which other plant functions are related [22].

2. MATERIALS AND METHODS

The nomenclature used throughout is that of Hutchinson and Dalziel [11].

2.1. Study site

The site was located in south-western Niger (13°32' N and 2°42' E) near Banizoumbou village (75 km north-east of Niamey) in the Tillabery department (*figure 1*).

Climate is semi-arid tropical with a long dry season (from October to May), alternating with a short rainy season (June to September) characterised by high intensity storms. Mean annual rainfall (1905–1989) is 560 mm [13]. A rain gauge recorder was installed at the site during the entire study period (1992–1995, *figure 2*). The study period included both relatively dry years and wet years (from –25 % to +21 % of the mean). The longest rainy season, the highest amount of rainfall and the most regular distribution of the showers occurred in 1994. 1992, 1993 and 1995 were drier and distribution of the first rains were more irregular (*figure 2*).

In Niger, banded vegetation patterns occur only on the laterite-capped plateau composed of 'continental terminal' sandstone, with a gentle slope (range 0.06–0.5 %). The shallow soil (60–110 cm thick) is underlain by ferricretes, located over a laterite gravelland, with hardening of the plinthite to ironstone. The soil is sandy clay loam (after USDA scheme) with 56 % sand and 27 % clay in 0–250 cm layer; the 250–550 cm layer is loam and more homogeneous [8, 21].

The study site showed a typical 'tiger bush' vegetation with thickets arranged in a concentric pattern (*figure 3*). They were 5 to 20 m in width while the bare zones were 25 to 80 m wide. The vegetation covered 25 % of the study area, according to an aerial photograph assessment (*figure 3*). The woody population was mainly composed of *Combretum micranthum* G. Don (60 % of total basal area) and *Guiera senegalensis* J.F. Gmel (13 % of total basal area). *Combretum micranthum* dominated the central zones of the thickets and *Guiera senegalensis* was almost the only shrub of the upslope zone. In the centre of the thickets, associated species were *Gardenia sokotensis*, *Acacia macrostachya* Reichenb., *Combretum nigricans* Lepr., *Grewia flavescens* Juss., *Commiphora africana* Engl. At the downslope boundary of the thicket, the dominance of dead stumps indicated a 'senescence zone' [1]. Only the annual species formed the herbaceous layer of which the densest part covered the upslope half of the thickets.

2.2. Methods

Two areas (50 × 40 m each) including thicket and its upslope bare soil zone were monitored from 1992 to 1995 (*figure 3*). At the upslope boundary of one thicket, a concrete wall (40 m long, 60 cm high, 20 cm thick with a foundation 25 cm deep) was built perpendicularly to the slope before the 1993 rainy season. Deflectors at its ends prevented the monitored area from receiving potential lateral water flows (*figure 3*). The boundary of the thicket was defined as the upper limit of the area colonised by the annual plants during 1992. Consequently, the 'upslope zone' dominated by

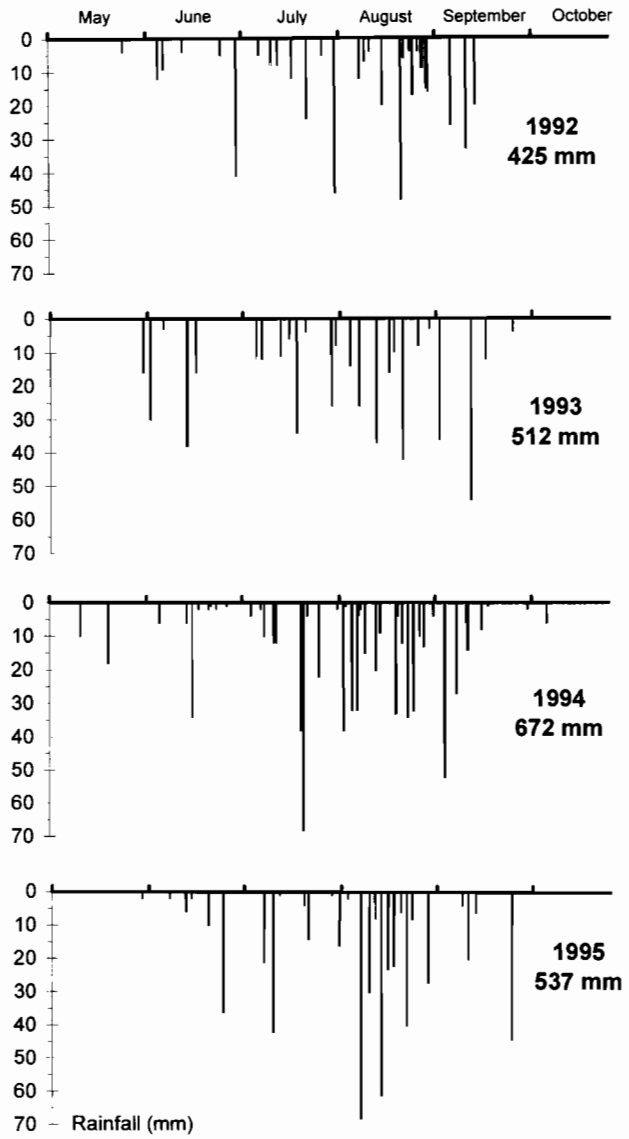

Figure 2. Rainfall distribution in Banizoumbou during the 1992, 1993, 1994 and 1995 rainy seasons.

Guiera senegalensis and annual cover, the 'central zone' dominated by *Combretum micranthum* and the 'senescence zone' of the thicket were divested of run-on. We collected data on infiltration and annual plant density before and after the wall was built, which allowed comparisons using a time control as well as a spatial control.

2.2.1. Infiltration and available moisture for vegetation

Soil moisture profiles (min. 1 m and max. 5.40 m deep) were monitored over 4 years, using Solo-25s neutron probes (Nardeux, Saint-Avertin, France). Access tubes were installed in each of the two thickets as follows: 1) one in the upslope bare zone; 2) one in the upslope zone of the thicket; 3) one in the central zone; and 4) one in the senescence zone. Soil moisture was monitored according to a rain-dependent time series, i.e. 1, 2 and 4 d after rainfall. Frequency progressively decreased to once a month during the dry season. For calibration, two soil samples, 500 g each, were used from the 0–250 and 250–550 cm layers. They were analysed using the nuclear absorption-desorption technique described in Couchat et al. [4]. The calibration equation was a function of the dry bulk density. It was measured with a gamma-ray probe (Nardeux Solo40), with values ranging from 1.65 $g \cdot cm^{-3}$ in the 0–20 cm top layer, to 1.8 $g \cdot cm^{-3}$ in deeper layers. Further details on the calibration specific to banded vegetation are available in Cuenca et al. [5].

During the dry season, deep drainage and evapotranspiration exhausted the moisture in the profile to the depth measured [8]. Whatever the previous rainy season, the driest profile observed remained the same every year. Tightly bound to the soil, this remaining water was unavailable for plants and for redistribution. The retention curve indicated that a volumetric soil water content of 12 % corresponds to a 10-MPa soil water pressure head. Unlike the minimum water profile, the maximum water profile observed depended on the rainy season. The annual range of variation of soil water content characterised the infiltration processes during each year in each zone.

In a given soil layer, the available water for the plants at any time was calculated as the difference between the measured stored soil water at this time and the minimum stored soil water (in mm). At the end of the experiment, extractions of plants from the three herbaceous groups considered below indicated that their roots were never deeper than 10 cm and generally above 5 cm. Uprooted shrubs of *Guiera senegalensis* in the upslope zone and of *Combretum micranthum* in the central zone had 90 % of their major roots above 60 and 100 cm deep, respectively. Means of stored water available for the plants were calculated over a period from July to September for each year, in upslope and in central zones of the thickets. The two soil layers considered corresponded to two rooting depths: one for annual plants (0–10 cm) and the other for woody plants (0–100 cm).

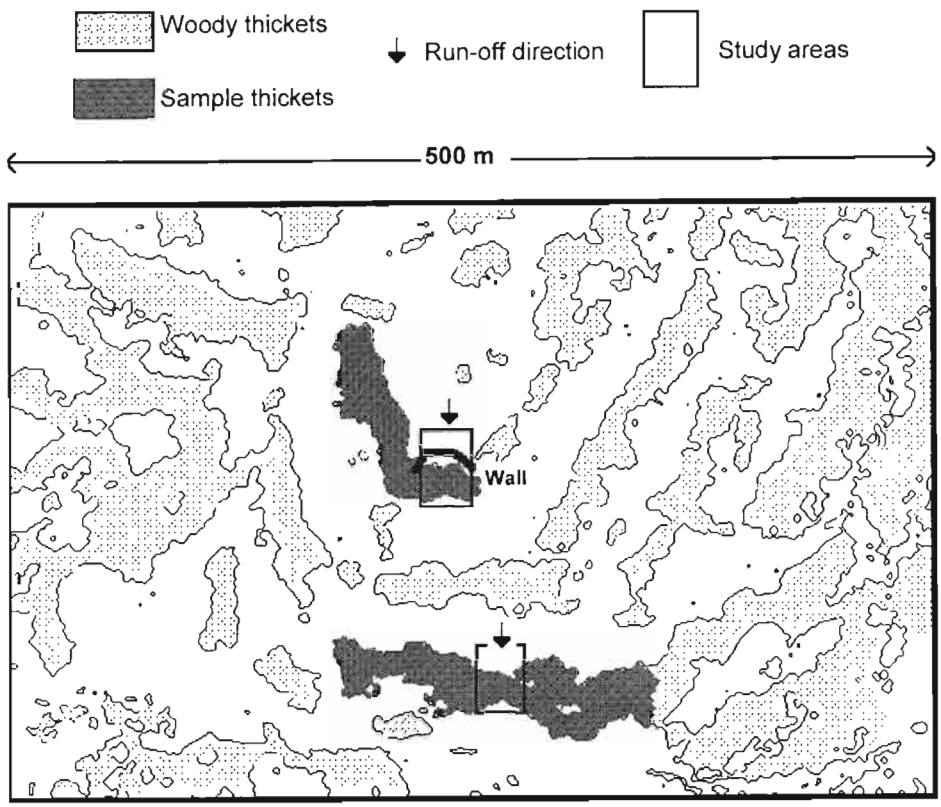

Figure 3. Experimental lay-out.

Analysis of variance (software Genstat 5, release 3.2 PC/Windows NT) was used to test the significance level of the differences observed in available water for the plants between two thickets (control and thicket deprived of run-on in 1993), two periods (before and after the wall was built), 3 years (1992, 1993 and 1994), and two zones (upslope and central).

2.2.2. Vegetation

Data on the herbaceous layer were recorded during 1992, 1993 and 1994, from upslope boundaries to the centre of the thickets, along six transects (three per thicket), 20 m long, and perpendicular to the thickets. The number of plants were counted for each species in a sliding rectangle (5 × 20 cm). Data were collected once or twice a week, from the beginning of the growth period (when seedlings became identifiable) until the plants withered. Species were divided into three groups: one group for each of the two dominant species and one group for all remaining species. The two dominant herbaceous species were identified in 1992. Among the 25 species registered, 67 % of individuals were *Microchloa indica* (L.F.) P. Beauv. (Gramineae) and 21 % were *Cyanotis lanata* Benth. (Commelinaceae). They were dominant respectively upslope and downslope of the six transects. Their spatial distributions were consistent between the two thickets on the six transects at all dates of observations [21]. For this work, mean densities of each group of plants were calculated for the two zones (upslope and central zones of the thickets) on the six transects over the period of July to September every year. Analysis of variance was used to test the significance level of the differences observed between thickets (control and thicket behind the wall), two periods (before and after the wall was built), 3 years (1992, 1993 and 1994), and two zones (upslope and central zones).

The phenology and the leaf water potential of the woody species were recorded, after the wall was built, during 1994 and 1995 for *Guiera senegalensis* and only 1995 for *Combretum micranthum*. In each

Table I. Classification of the phenological stages observed on each individual shrub sampled.

	Foliation	Flowering	Fruiting
Stage 0	Absent	Absent	Absent
Stage 1	Swelling buds, no leaf development	Floral buds only	Early setting stage
Stage 2	Leaf buds and open buds (over 10 and less than 50 % of these organs in each individual)	Floral buds and open flowers (over 10 but less than 50 %)	Development of fruits to normal size
Stage 3	Leaves mostly open	Over 50 % of organs carrying open flowers	Maturity
Stage 4	Leaves and dry leaves, or leaves which have changed colour (over 10 but less than 50 %)	Open flowers and dry flowers (over 10 and less than 50 %)	Ripe fruits and onset of dissemination (fall of fruits)
Stage 5	Over 50 % in each individual with dry leaves and falling leaves*	A majority of dry flowers and shedding of flower elements	Fruits dried and fallen

* This is a difficult stage to monitor since it may extend over several months according to the species (e.g. *Guiera senegalensis*).

thicket, ten *Guiera senegalensis* located in the upslope zone and twenty *Combretum micranthum* located in the central zone were selected. Data on phenology were collected according to the method of Grouzis and Sicot [9]. Each shrub was classified as shown in *table I* after Le Floc'h [14]. Data were collected weekly during the rainy season, and monthly during the dry season.

Among the individuals for which phenology was monitored, three *Guiera senegalensis* and five *Combretum micranthum* per thicket were sampled for the leaf water potential recordings. We used a hydraulic press (HP, Objectif K model, France) rather than conventional methods, because it was more convenient to implement in the field. Good correlations have been found between HP and conventional methods such as psychrometric and pressure chamber techniques [2, 10, 12, 23]. We measured the pressure when water was first exuded from a piece of leaf. Diurnal variation in leaf water potential of each shrub was recorded every week or every two weeks. It was measured on two leaves per shrub, every hour from predawn to the time the minimum value was overtaken. The mean water potentials were calculated from six sampled leaves per thicket for *Guiera senegalensis* and ten sampled leaves per thicket for *Combretum micranthum* at each time of measurement. For each species, seasonal courses of predawn and daily minimum means were plotted for the two thickets. Predawn leaf water potential was an indicator of the soil water availability in the rooting zone. Daily minimum potential was related to the daily maximum of both atmospheric stress and soil water stress from which the shrubs suffered.

3. RESULTS

3.1. Similarities remaining between the two thickets after construction of the wall

The increasing infiltration gradient from the bare soil zone to the centre of the thicket, and the decreasing one from the centre of the thicket to the senescence zone remained in the thicket deprived of run-on (*figure 4*). Indeed, there was a statistically significant difference in available water for the shrubs between upslope and central zone in layer 0–100 cm within the two thickets ($P < 0.05$), with a mean of 2.4 times more water in the central zone. In the two thickets and the four zones, abundant rainfalls during 1994 produced the highest amount of infiltration (*figure 4*). For the superficial layer 0–10 cm, the same difference occurred in available water for the plants between thickets before and after the wall was built ($P > 0.05$). Consequently, the difference observed could not be due to the erection of the wall but only to a natural spatial heterogeneity. There was no statistical difference in available water of this layer between upslope and central zone within the two thickets.

Densities of *Microchloa indica* in the upslope and the central zones were the same ($P > 0.05$) within the two thickets over the study time in the six transects. There was a difference between the two thickets ($P < 0.001$) in the mean densities of *Cyanotis lanata*. However, it was of the same order before and after the wall was built (103 plants·m^{-2} in the control and 409 plants·m^{-2} in the other thicket). Consequently, it was not due to run-on deprivation. Unlike *Microchloa indica*, there was a difference ($P < 0.001$) in densities of *Cyanotis lanata* between upslope and the centre of the thickets (twelve times more plants·m^{-2} in the

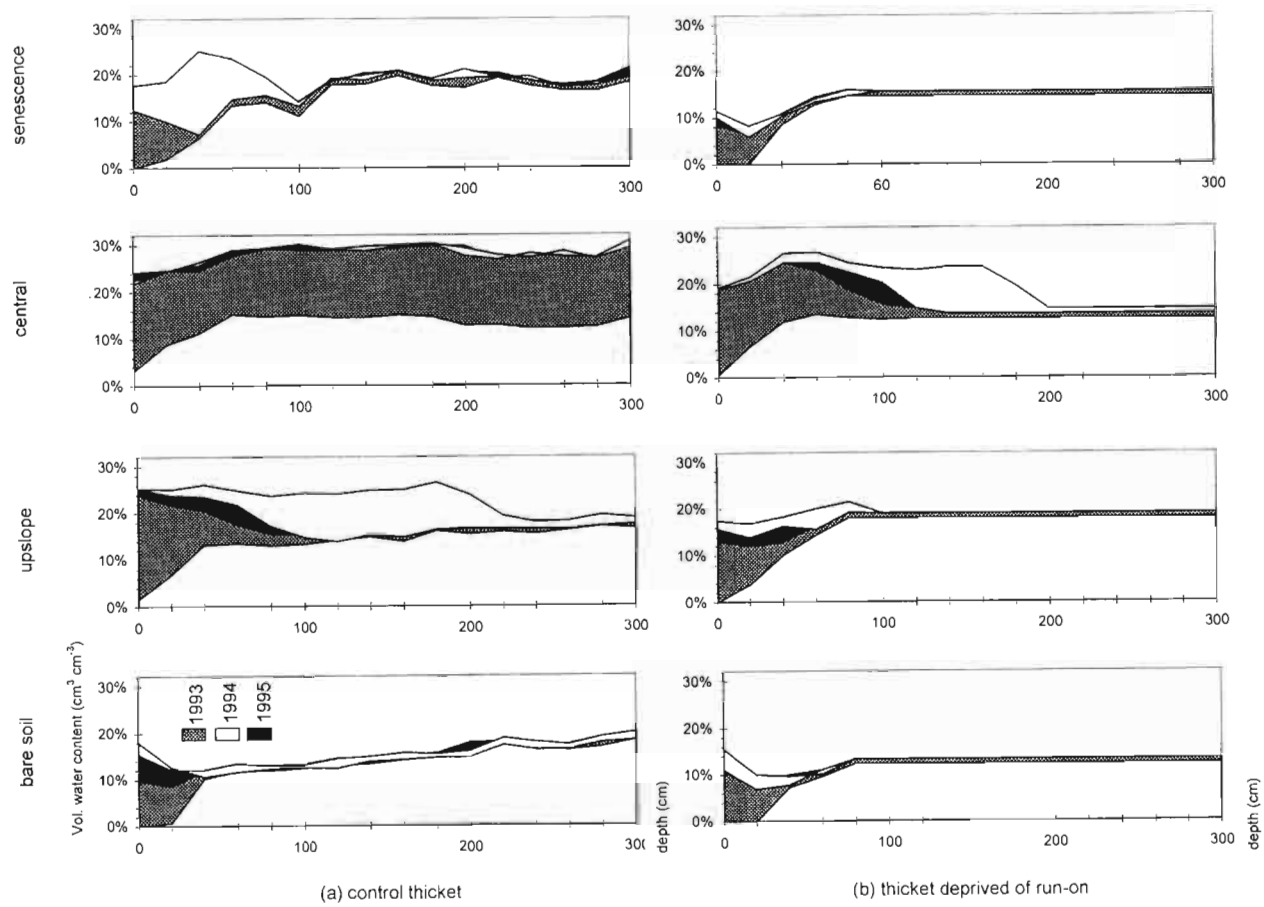

Figure 4. Minimum and maximum moisture profiles over 3 years in four vegetation zones in (a) the control thicket and (b) the thicket deprived of run-on.

centre on the six transects over the whole study time). Also, there were more plants belonging to the group 'remaining species' in the centre than the upslope of the two thickets ($P < 0.05$).

Virtually no difference occurred between the two thickets in *Combretum micranthum* phenology (*figure 5b*).

3.2. Changes resulting from the construction of the wall

An obvious wall effect was observed in the amount of total water stored. Maximum moisture percentage was lower and infiltration depth was shallower every year in all zones of the thicket deprived of run-on than in the control one (*figure 4*). The greatest decrease of infiltration due to the wall effect occurred in the centre of the thicket. Indeed, the moisture front was more than 5.40 m deep in the control thicket (not plotted on *figure 4* because of its scale) against 1.40, 1.20 and 2 m in 1993, 1995 and 1994, respectively, without run-on contribution. The moisture front passed the bottom of the tube, which indicated that a deep drainage occurred. This drainage was completely suppressed in the thicket deprived of run-on during the monitoring years (*figure 4*). The senescence zone was hardly supplied with run-on water except during the wet year (1994) during which it benefited greatly. In the layer 0–100 cm, the amount of stored water available for the plants was similar in the two thickets before the wall was constructed, and was greater in the control thicket after the wall was built ($P < 0.05$). This indicated the effect of run-on deprivation on water availability for the shrubs.

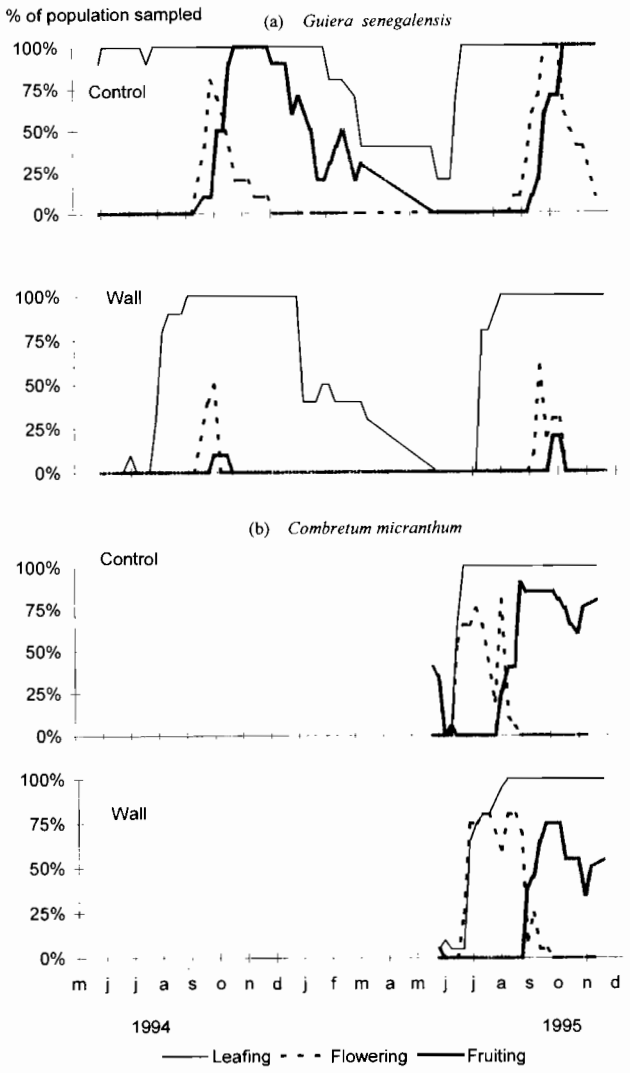

Figure 5. Phenological spectra over 2 years in the control thicket (Control) and the thicket deprived of run-on (Wall) of (a) *Guiera senegalensis* and (b) *Combretum micranthum*.

The difference in mean densities of *Microchloa indica* between thickets were significantly reversed before and after the wall was built ($P < 0.001$). Indeed, the means were 195 plants·m^{-2} in the control thicket and 862 plants·m^{-2} in the other one before the wall was built, and they shifted to 430 and 361 plants·m^{-2} respectively over the two following years. Consequently, the wall appeared as the probable cause of the drop in the thicket deprived of run-on since the difference between thickets remained the same every year after construction ($P > 0.05$). Before the wall was built, mean densities of the group 'remaining species' were significantly lower in the control thicket than in the other, but significantly higher after ($P = 0.002$). The density dropped almost to 50 % behind the wall while it increased in the control thicket. Construction of the wall could be the main cause since the difference between thickets remained statistically stable during the 2 years following construction (1993, 1994).

Figure 5a indicated that population of *Guiera senegalensis* suffered from a strong reduction in the number of shrubs flowering and fruiting in the thicket deprived of run-on compared to the population in the control thicket. The maximum percentage of reproducing shrubs and the duration of the two sexual reproduction phases, that took place at the beginning of the dry season, strongly decreased behind the wall. Although the leafing phase was less disturbed, it suffered a reduction in amplitude and duration of the period when maximum percentage of the population was leafing. For the same species, the two leaf water potential (daily minimum and predawn) decreased quickly after the break of the rains in the thicket behind the wall compared to control (*figure 6a, b*). This indicated plant stress linked to a reduction in availability of water in the rooting zone of the thicket deprived of run-on. Although reduced, a similar effect was recorded in *Combretum micranthum* physiology (*figure 6c*).

4. DISCUSSION

In the study site, at the scale of the bare zone and the thicket just downslope, obviously the run-on flow from the bare zone contributed mainly to the total infiltration in the central zone of the thicket. Its contribution was much less in the upslope vegetated zone. It was negligible downslope of the thicket except when a long and abundant wet season, with regular distribution of rains, occurred as was the case in 1994. The central zone benefited from the highest infiltration capacity that could reach 500 mm during a single rainy event [8]. Cracks in the rooting zone as well as activity of foraging termites mainly contribute to this high infiltration rate [6, 19]. The infiltration capacity in the central zone was so high that even a considerable reduction of water input by run-on did not induce a great deficit of water content available to the shrub, i.e. in layer 0–1 m. In this zone, the rainfall and the negligible run-off taking place in the upslope vegetation zone (about 2 % of total rain [8]) provided enough water to *Combretum micranthum* for it to complete its life cycle, especially as it overlapped with the rainy season ('arido-passive' species, i.e. metabolically inactive during the dry season [7]). If *Combretum micranthum* was affected, the consequences were not

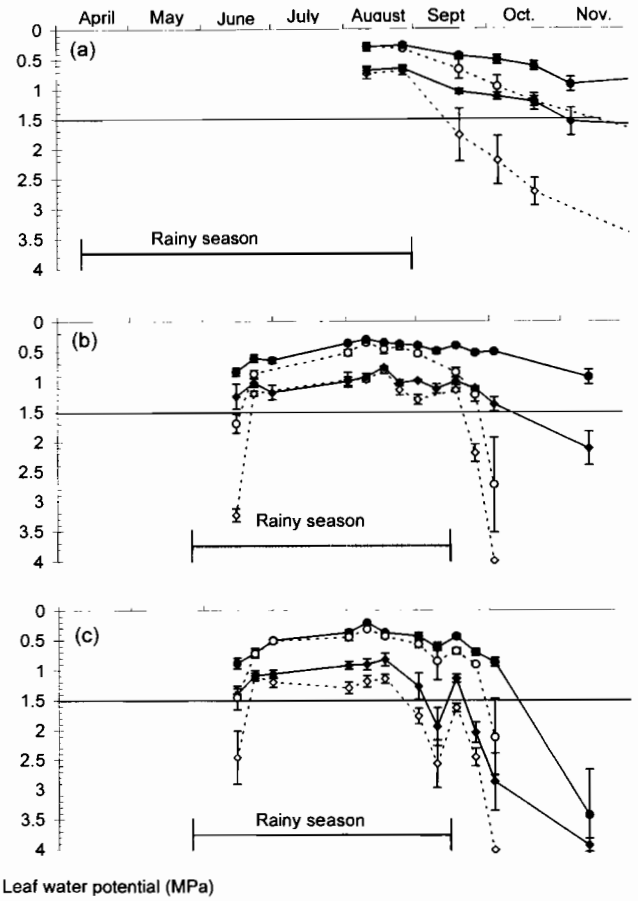

Figure 6. Seasonal changes in the predawn and daily minimum leaf water potentials over 2 years in the control thicket and the thicket deprived of run-on: (a) *Guiera senegalensis* during 1994, (b) *Guiera senegalensis* during 1995, (c) *Combretum micranthum* during 1995. The rainy period is indicated. Solid line and symbols, control thicket; dashed line and open symbols, thicket deprived of run-on; circles, predawn potential; diamonds, daily minimum potential; error bars, confidence intervals (P = 5 %).

visible (within 3 years) in the whole plant functioning, despite some disturbance observed at the organ scale. Unlike *Combretum micranthum*, *Guiera senegalensis* suffered seriously from a lack of water in the upslope zone of the thicket deprived of run-on. That led to a delay and a concentration of the leafing-out stage and to a drastic decrease in the reproductive rate. A combination of two probable causes can be suggested: its reproduction started at the end of the rainy season, when the soil was drying ('arido-active' species [7]) and the species was located in an area (upslope) where there was 2.4 times less available water for the plants than in the central zone of the thicket. When this zone was supplied only with precipitation providing less than 20 % of overall moisture, and corresponding to a drop of 45 % in soil moisture as compared to the control thicket, shrubs were strongly affected. Response of shrubs to run-on deprivation depended both on the life cycle and the location of the species along the water resource gradient.

Contrary to the shrub rooting zone, there was neither a 'wall effect' nor a 'zone effect' in the rooting layer of annual plants. There, water resource was mainly controlled by direct rainfall and evaporation. Consequently, decreases in mean densities of *Microchloa indica* and 'remaining species' in the dammed thicket could not be caused by a decrease in soil water content available to the plants. The wall has probably stopped the possible input of plant seeds carried by the runoff flows from the upslope zone in natural conditions [21]. The presence of annual plants located along the upslope border of the wall where an irregular and thin covering of sand and dust had gradually accumulated supports this interpretation.

Microchloa indica was as abundant in the central zone than upslope (no zone effect). That means its domination upslope [21] was due to the significant lower densities of the other species compared to the central zone (significant zone effect).

5. CONCLUSION

Run-on did not contribute to water storage in layer 0–10 cm, and thus did not supply the annual herbaceous cover which probably depends mainly on microheterogeneity of the bumpy soil surface.

The central zone of the study thickets benefited the most from run-on. Even so, most of the supply from run-on to this zone was lost for the woody vegetation through deep drainage; despite this, the zone was a favourable habitat for vegetation as it supported the greater number of species. For instance, some Sudanian woody species were observed there (*Gardenia sokotensis* Hutch., *Combretum nigricans* Lepr.). It had such a high infiltration capacity that rainfall input, without run-on contribution, was sufficient to maintain dominant shrubs in quite good conditions at least for a long while (several years). This suggested that the run-off/run-on pattern was not as essential to vegetation performance in the central zone than in the upslope one. Although the run-on contribution was much less to the upslope zone than to the central one, it seemed of primary importance for the survival of shrubs which are located upslope (*Guiera senegalensis*). The result on the upslope zone fully supports the

conventional opinion that a banded pattern is necessary for optimal vegetation function [18].

Acknowledgments

We are very grateful to D. Freudenberger (CSIRO, Div. Wildlife and Ecology, Canberra, Australia) for his help in statistics, and J. Aronson (CEFE-CNRS Montpellier, France) for the improvement in the English. This research was partially supported by SAvanna on the Long Term (SALT), centre-project of the Global Change Terrestrial Ecosystems project, and the programme Hydrological and Atmospheric Pilot Experiment in Sahel (HAPEX-Sahel).

REFERENCES

[1] Ambouta K., Contribution à l'édaphologie de la brousse tigrée de l'ouest Nigérien, Docteur-ingénieur thesis, Université de Nancy, 1984, 125 p.

[2] Bristow K.L., Van Zyl W.H., De Jager J.M., Measurement of leaf water potential using the J14 press, J. Exp. Bot. 32 (1981) 851–854.

[3] Cornet A., Delhoume J.P., Montana C., Dynamics of striped vegetation patterns and water balance in the Chihuahuan desert, in: During H.J., Werger M.J.A., Willems J.H. (Eds.), Diversity and Pattern in Plant Communities, Academic Publishers, The Hague, 1988, pp. 221–231.

[4] Couchat P., Carre C., Marcesse J., Ho J., The measurement of thermal neutron constants of the soil: application to the calibration of neutron moisture gauges and to the pedological study of the soil, in: Schrack R.A., Bowman C.D. (Eds.), Nuclear Cross-Sections and Technology, US Department of Congress, 1975, pp. 516–579.

[5] Cuenca R.H., Brouwer J., Chanzy A., Droogers P., Galle S., Gaze S.R., Sicot M., Stricker H., Angulo-Jaramillo R., Boyle S.A., Bromley J., Chebhouni A.G., Cooper J.D., Dixon A.J., Fies J.C., Gandah M., Gaudu J.C., Laguerre L., Lecocq J., Soet M., Steward H.J., Vandervaere J.P., Vauclin M., Soil measurements during HAPEX-Sahel intensive observation period, J. Hydrol. 188-189 (1997) 224–266

[6] Eldridge D.J., Nest of ants and termites influence infiltration in a semi-arid woodland, Pedobiologia 38 (1994) 481–492.

[7] Evenari M., Adaptations of plants and animals to the desert environment, in: Evenari M., Noy-Meir I., Goodall D.W. (Eds.), Hot Deserts and Arid Shrublands. Ecosystems of the World, Elsevier, Amsterdam, 1985, pp. 79–92.

[8] Galle S., Ehrmann M., Peugeot C., Water balance on a banded vegetation pattern. A case study of tiger bush in western Niger, Catena 00 (1999) (in press).

[9] Grouzis M., Sicot M., Une méthode d'étude phénologique de populations d'espèces ligneuses sahéliennes : influence de quelques facteurs écologiques, in: Le Houérou H.N. (Ed.), Les fourrages ligneux en Afrique. État actuel des connaissances. Colloque sur les fourrages ligneux en Afrique, CIPEA, Addis-Ababa, 1980, pp. 231–237.

[10] Hicks S.K., Lascano R.J., Wendt C.W., Onken A.B., Use of a hydraulic press for estimation of leaf water potential in grain sorghum, Agron. J. 78 (1986) 749–751.

[11] Hutchinson J., Dalziel J.M., Flora of West Tropical Africa, Crown Publishers, London, UK, 1954–1972.

[12] Jones C.A., Carabaly A., Estimation of leaf water potential in tropical grasses with the Campbell-Brewster hydraulic press, Trop. Agric. 57 (1980) 305–307.

[13] Le Barbe L., Lebel T., Rainfall climatology of the central Sahel during the years 1950-1990, J. Hydrol. 188-189 (1997) 43–73.

[14] Le Floc'h E., Caractérisation morphologique des stades et phases phénologiques dans les communautés végétales, Ph.D. thesis, U.S.T.L. Montpellier-II Univ., CNRS-CEPE doc No. 45, 1969, 132 p.

[15] Ludwig J.A., Tongway D.J., Spatial organisation of landscapes and its function in semi-arid woodlands, Australia, Landsc. Ecol. 10 (1995) 51–63.

[16] Mauchamp A., Rambal S., Lepart J., Simulating the dynamics of a vegetation mosaic: a spatialized functional model, Ecol. Model. 71 (1994) 107–130

[17] Montaña C., The colonization of bare areas in two phase mosaics of an arid ecosystem, J. Ecol. 80 (1992) 315–327.

[18] Noy-Meir I., Desert ecosystem structure and function, in: Evenari M., Noy-Meir I., Goodall D.W. (Eds.), Hot Deserts and Arid Shrublands. Ecosystems of the World, Elsevier, Amsterdam, 1985, pp. 93–103.

[19] Ouedraogo P., Rôle des termites dans la structure et la dynamique d'une brousse tigrée soudano-sahélienne, Ph.D. thesis, Univ. P.-et-M.-Curie Paris-VI, Paris, 1997, 282 p.

[20] Peugeot C., Esteves M., Galle S., Rajot J.L., Vandervaere J.P., Runoff generation processes: results and analysis of field data collected at the East Central Supersite of the HAPEX-Sahel experiment, J. Hydrol. 188-189 (1997) 179–202.

[21] Seghieri J., Galle S., Rajot J.L., Ehrmann M., Relationships between the soil moisture regime and the growth of the herbaceous plants in a natural vegetation mosaic in Niger, J. Arid Environ. 36 (1997) 87–102.

[22] Slatyer R.O., Methodology of a water balance study conducted on a desert woodland (*Acacia anuera* F. Muell.) community in central Australia, Unesco Arid Zone Res. 16 (1961) 15–26.

[23] Sojka R.E., Sadler E.J., Camp C.R., Arnold F.B., A comparison of pressure chamber, leaf-press and canopy temperature for four species under humid conditions, Environ. Exp. Bot. 30 (1990) 75–83.

[24] Winkel T., Rambal S., Influence of water stress on grapevines growing in the field: from leaf to whole-plant response, Aust. J. Plant Physiol. 20 (1993) 143–157.

Acta Oecologica **20** (3) (1999) 219–224 / © Elsevier, Paris

Forum

Seedling occurrence in alpine treeline conifers: A case study from the central Rocky Mountains, USA

Stephan Hättenschwiler [a*], William K. Smith [b]

[a] *Institute of Botany, University of Basel, Schönbeinstrasse 6, CH-4056 Basel, Switzerland.*
[b] *Department of Botany, University of Wyoming, Laramie Wyoming 82071, USA.*
* *Corresponding author (fax: +41 61 267 35 04; e-mail: haetten@ubaclu.unibas.ch)*

Received January 20, 1999; revised February 10, 1999; accepted February 12, 1999

Abstract — Information concerning the occurrence of very young (1- to 10-year-old) tree seedlings in the alpine treeline ecotone is rare. Seedling occurrence of the dominant conifers *Picea engelmannii* and *Abies lasiocarpa* was measured in the treeline ecotone of the Medicine Bow Mountains, Wyoming (central Rocky Mountains, USA), an area composed of elongated tree islands separated by open meadows (ribbon forest) that grade into the closed forest. No seedlings were found on the windward sides of tree islands, while a mean of 0.6 seedlings·m^{-2} occurred on the leeward (downward) sides. These values compared to the 4.2 seedlings·m^{-2} in the closed forest. In addition, a strong correspondence was found between snowpack depth and seedling abundance, with depths that were either too shallow (< 0.5 m) or too deep (> 1.5 m) associated with fewer or no seedlings. *A. lasiocarpa* seedlings made up much less of the overall seedling population in the ribbon forest (6 %) than in the closed forest (22 %). Seedling establishment in this portion of the alpine treeline ecotone appears to be occurring at a low rate that differs between the two dominant species and may be strongly influenced by wind-driven snow accumulation patterns. © Elsevier, Paris

***Abies lasiocarpa* / *Picea engelmannii* / ribbon forest / snow effects / treeline ecotone**

1. INTRODUCTION

Seedling establishment is a key component in the process of succession and ultimate plant distribution patterns [3, 12]. Seedling life stage is especially crucial at distributional boundaries, or within ecotones such as those found at the alpine treeline, and seedling establishment may be an important factor in evaluating the stability of these treelines. The observed elevational and latitudinal occurrence of the alpine and arctic treelines have been discussed extensively [1, 9, 15, 23, 24]. In addition, a considerable number of studies dealing with the success of tree regeneration at treeline suggest that global climate change may be monitored using treeline dynamics (see review [22]). Despite this continuing interest in the origin and persistence of treelines, there are almost no quantitative analyses of the natural occurrence of very young (1- to 10-year-old) seedlings within alpine treeline ecotones, except some studies documenting establishment and survival of planted seedlings and sown seeds (e.g. [2, 13]), and some observational remarks on seedling occurrence (e.g. [1, 4]).

The purpose of the present study was to quantify the natural occurrence of young (1- to 10-year-old) tree seedlings of the two dominant species *Picea engelmannii* Perry ex Engelm. and *Abies lasiocarpa* (Hook.) Nutt. within the upper treeline ecotone of the Medicine Bow Mountains of the south-central Rocky Mountains, USA, in comparison to the adjacent closed forest. This transitional ecotone between closed, subalpine forest and open, alpine meadow is composed of elongated islands of trees which are usually separated by tens of metres of open meadow, forming a ribbon-like pattern (ribbon forest). This ribbon forest ecotone is common in the central Rocky Mountains from

Colorado to Montana [1, 4] and similar patterns of banded vegetation have been observed in *Nothofagus* forests in Argentina [21]. We also evaluated the relationship between seedling occurrence in this portion of the treeline ecotone and the strong pattern of winter snow deposition that occurs, a potentially important factor for seedling survival in winter and summer.

2. MATERIALS AND METHODS

2.1. Study sites

Study sites were located in the Medicine Bow Mountains of south-eastern Wyoming approximately 65 km west of Laramie, Wyoming (41°21' N, 106°14' W) at an elevation of near 3 360 m. The climate is characterized by very cold winters (minimum air temperature below –40 °C), and cool summers (daytime maximum < 25 °C). Precipitation in the subalpine zone varies from about 650 to 750 mm per year, coming predominantly in the form of winter and spring snows [5, 16] which is redistributed considerably by wind. West and south-west winds during winter and spring can be very strong, often averaging over 10 $m \cdot s^{-1}$ [10, 16]. The closed subalpine forest at our study site was > 500 years old (estimated using the diameter-age relationship described in Oosting and Reed [18]) and composed of *P. engelmannii* and *A. lasiocarpa*. Above an elevation of about 3 300 m, elongated tree islands composed of these two species are found in more wind-exposed sites, with their long axes perpendicular to the prevailing WSW winter winds. Billings [4] defined the term 'ribbon forest' for this special forest type. Smaller tree islands with 'flagged trees' blend into low-lying krummholz mats at higher elevation in the ecotone, or at more wind-exposed sites even at lower elevations. Both *P. engelmannii* and *A. lasiocarpa* can reproduce asexually by layering which extends the width of both tree islands and krummholz mats [6]. The area of our study sites has a typical gradient of krummholz mats (about 1 m in height), followed by small tree islands at lower elevation (tree heights of 1.5 to 3 m), and then longer ribbon-like tree islands (tree heights of 3 to 10 m) that grade into the closed forest (tree heights of 10 to 20 m). For more detailed descriptions of the characteristic ribbon forest-type treeline ecotone see Arno and Hammerly [1] and Billings [4].

2.2. Experimental design

In September 1992, sample transects were established parallel to the direction of the prevailing winter winds on the south-west and north-east sides of ten randomly selected tree islands (composed of about twenty to thirty trees with a maximum height of near 10 m) within an area of about 5 ha. This enabled an evaluation of the association between wind exposure and winter snow deposition on seedling occurrence, i.e. windward and leeward sides of each tree island. Ten transects in the same cardinal orientation to tree islands were also placed randomly in the adjacent closed forest within an area of about 3 ha. A set of three 1-m^2 quadrats were established at a distance of 1, 5 and 10 m from both the leeward and windward edges of the tree islands. Three 1-m^2 quadrats were established along transects in the closed forest at the same distance and cardinal direction as for the leeward transects established in the ribbon forest. Seedling counts of *P. engelmannii* and *A. lasiocarpa* were taken for four age classes (current 1, 2, 3–5 and 6–10 years old). The height of these seedlings were found to range between 2 and 7 cm. Seedling age was estimated based on the presence of cotyledons (1 year), or the number of bud scars and leaf whorls. Seedlings with both cotyledons and primary leaves were considered 2 years old. Based on our experience with these and also with other treeline conifer seedlings of known age, these age estimates are considered to be fairly accurate.

Snow depths were measured during March 10 to 21, 1990 and March 16 to 18, 1991 at 2-m intervals on the windward and leeward sides of five different tree islands that were chosen as representative.

Three-way analysis of variance (ANOVA) was used to test for the effects of forest type (ribbon forest vs. closed forest), species (*P. engelmannii* vs. *A. lasiocarpa*) and quadrat position along the transect (1, 5 and 10 m) on the variable seedling density. Seedling age structure was compared between forest types and species using separate one-way ANOVAs (forest type or species as factor). Percentage data (seedling age structure) were first arcsine transformed prior to ANOVAs to meet the requirement of normal distribution.

3. RESULTS

In the ribbon forest, no seedlings of either species were found on the windward, SW side of any tree island, and thus data from these transects were not included in the statistical analyses. Therefore, comparisons between the ribbon and the closed forest are based on seedling abundance measured on the leeward, NE sides of tree islands. Mean seedling occurrence (both species) was significantly greater in the closed forest (4.2 seedlings·m^{-2}, n = 30 quadrats) than in the ribbon forest (0.6 seedlings·m^{-2}, n = 30 quadrats) (*figure 1*, *table I*), and the total number of seed-

Table I. Three-way ANOVA for the dependent variable seedling density and the independent factors forest type (ribbon and closed), tree species (*P. engelmannii* and *A. lasiocarpa*) and quadrat position (three quadrats along each transect), $n = 10$ transects.

Factors	df	Sum of squares	Mean square	F-value	*P*-value
Forest type (F)	1	99.0	99.0	32.65	< 0.001
Tree species (Sp)	1	57.4	57.4	18.93	< 0.001
Quadrat (Q)	2	4.9	2.4	0.80	0.451
F × Sp	1	23.4	23.4	7.72	0.006
F × Q	2	3.3	1.6	0.54	0.585
Sp × Q	2	1.1	0.5	0.18	0.839
F × Sp × Q	2	2.1	1.0	0.34	0.712
Error	108	327.5	3.0		

lings was more than seven times greater in the closed forest. There were more seedlings of *P. engelmannii* than of *A. lasiocarpa* in both the ribbon and the closed forest (*figure 1*). Also, seedling species composition differed between the two forest types (*table I*) with only 6 % of all seedlings in the ribbon forest being *A. lasiocarpa*, compared to 22 % in the closed forest. In contrast, the corresponding overstory canopies were composed of about 60 and 35 % of *A. lasiocarpa* (tree density) in the ribbon forest and the closed forest, respectively.

Over 90 % of all seedlings found for both species and within both forest types were either 1- or 2-year-old (*figure 2*). Sixty-nine percent of all *P. engelmannii* seedlings were older than 1 year in the ribbon forest compared to only 26 % in the closed forest (*figure 2*, $P < 0.05$, $n = 10$ transects). The age structure of *A. lasiocarpa* seedlings cannot be compared between the two forest types, because only one *A. lasiocarpa* seedling was found in the ribbon forest. However, compared to *P. engelmannii*, there were relatively more *A. lasiocarpa* seedlings older than 1 year in the closed forest (64 % of all *A. lasiocarpa* seedlings found, $P < 0.05$, $n = 10$ transects).

Seedling abundance for both species was similar along the transects in both forest types (no overall and no interactive quadrat effects, *table I*). Accordingly, the frequency of seedling occurrence was rather homogeneous, except in the ribbon forest in quadrats 5 m away from the tree island edge (*figure 1*). At this quadrat position, no single seedling of either species was found (quadrat position effect for the ribbon forest alone: $P < 0.09$) which also corresponded to high snow depths (*figure 3*). Low snow depth (0.1–0.2 m) on windward sides of islands was also associated with the absence of seedlings (*figure 3*).

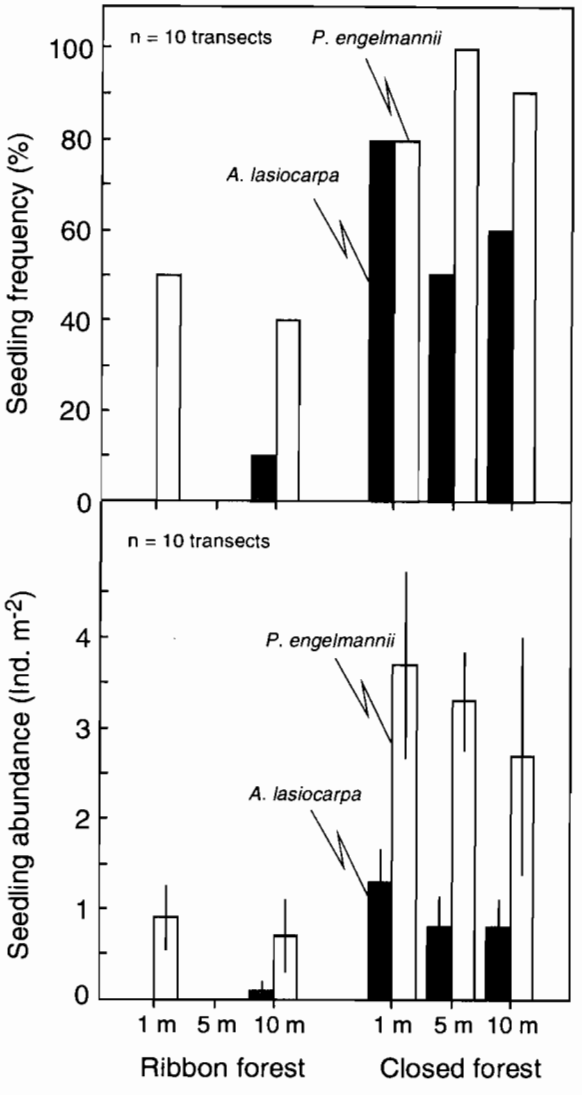

Figure 1. Frequency (above) and abundance (below) of *P. engelmannii* and *A. lasiocarpa* seedlings within ten 1-m^2 quadrats at three different positions (1, 5 and 10 m) on the NE side of the tree islands (left) in the ribbon forest and within the adjacent closed forest (right). Seedling frequency is the number of quadrats with at least one seedling present and is expressed in per cent of the total number of quadrats ($n = 10$). Seedling abundance is the average number of seedlings per quadrat (means of ten transects ± standard errors).

4. DISCUSSION

A mean maximum seedling abundance of 0.9 seedlings·m^{-2} (*figures 1, 3*) in the ribbon forest at

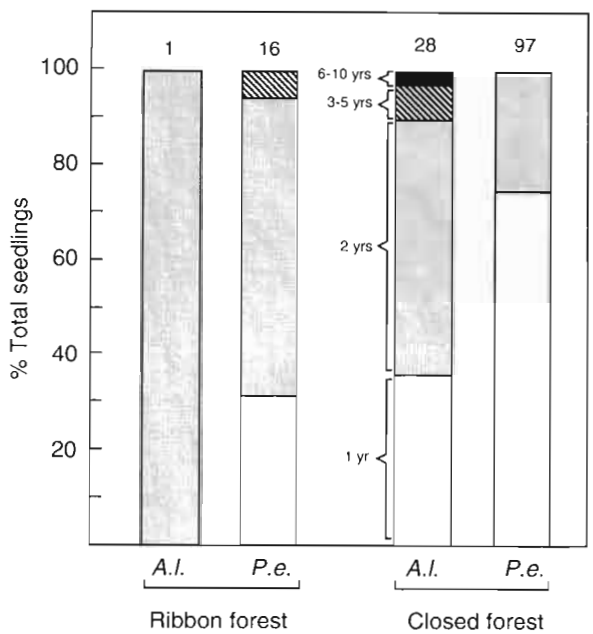

Figure 2. Age distribution of *P. engelmannii* and *A. lasiocarpa* seedlings along ten transects in the ribbon forest and the adjacent closed forest. Total seedling numbers of ten transects × three quadrats are indicated above the bars; age classes are as indicated.

the end of the growing season, suggests a relatively low seedling establishment over the last 10 years, at least. These findings are in contrast to previous reports of no seedling recruitment in the same area [4], or in similar areas [9, 20] of the Rocky Mountains. Although there were substantially more seedlings in the adjacent closed forest, the proportion of *P. engelmannii* seedlings was smaller, and were much younger on average than seedlings found in the ribbon forest.

These differences in abundance and age structure between the two forest types did not correspond to the current species dominance observed in the corresponding overstory canopies, where *P. engelmannii* dominates in the closed forest, but *A. lasiocarpa* is more abundant in the ribbon forest (see also [1, 4]). Seedling abundance, therefore, may be explained by species-specific seedling establishment success rather than by the occurrence of seed trees. *P. engelmannii* has been shown to germinate more rapidly at lower temperatures than *A. lasiocarpa* [14], and this difference was enhanced at high light intensities [19]. A more rapid germination at lower temperature has been recognized as a potential adaptation for drought avoidance, enabling a better correspondence with available soil moisture from snow melt-out in the spring. The higher temperature requirements for *A. lasiocarpa* germina-

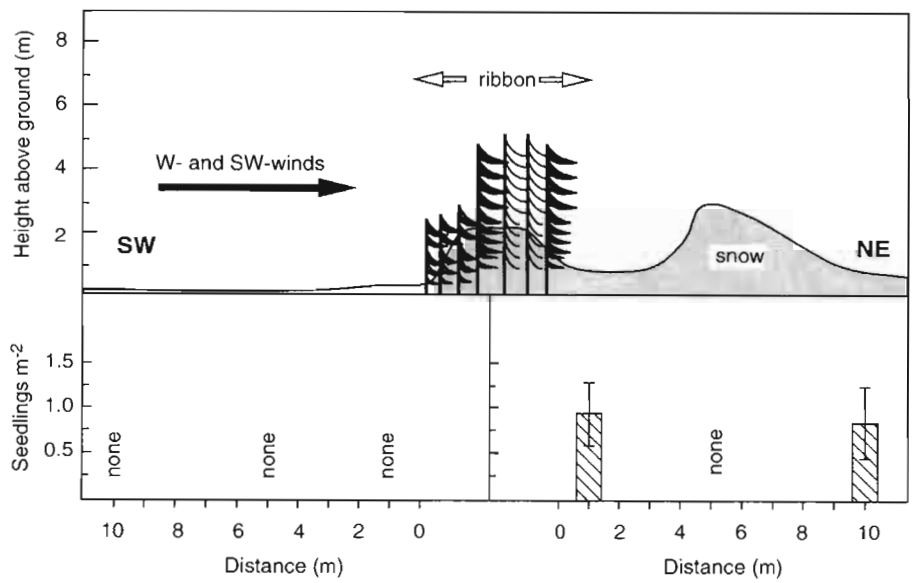

Figure 3. Above: Schematic representation of the snow depths on the windward and leeward sides of a typical tree island in the ribbon forest (based on measurements in March 1990 and 1991). Snow accumulation depths and spatial distribution vary according to the width of the tree island and height of the island trees (the snowbank forms at a distance equal to approximately half the height of the tallest island trees). Below: Mean seedling abundance (± standard error) measured on the upwind and leeward sides of the tree islands in the ribbon forest for a total of ten transects on each side. Seedling ages and numbers were counted at 1, 5 and 10 m from both the upwind and downwind sides of the tree islands.

tion may shorten the already brief period when optimal temperature and soil moisture availability overlap in the ribbon forest. Consequently, seedlings of *P. engelmannii* in the ribbon forest appear to show greater survival compared to *A. lasiocarpa* seedlings.

On the other hand, young seedlings of *A. lasiocarpa* have been shown to establish better on a litter layer compared to *P. engelmannii*, possibly because of a longer tap root [8, 14], and they are also considered to be more shade tolerant than *P. engelmannii* [14]. Consequently, seedlings of *A. lasiocarpa* in the closed forest survive better relative to those of *P. engelmannii*, as indicated here by the greater abundance of older age classes of *A. lasiocarpa*.

In contrast to the adjacent closed forest, we observed a spatial pattern of seedling occurrence that could be associated with the existence of tree islands and their observed influence on snow deposition patterns in the ribbon forest. No seedlings were found on the windward sides of individual tree islands where snow depths were minimal, while seedlings on the leeward sides of tree islands were found only at microsites where accumulative snow depths were between 0.5 and 1.5 m. Thus, an optimal snow depth may be necessary for maximum seedling establishment, with depths that are too shallow or too deep resulting in less successful establishment. Too much snow accumulation could inhibit seedling establishment because of the shortened growth season and inadequate carbon balance [4, 18]. An additional negative factor of too much snow may be snow creep and its sheering effect on seedlings under the snowpack. In contrast, microsites with relatively shallow snow depths, such as those on the windward sides of tree islands, may not provide enough water for the growth and survival of conifer seedlings during summer. It has been reported previously that summer soil water availability in the ribbon forest is determined mainly by snow accumulation patterns during winter [17]. Also, in the same closed forest of the Medicine Bow Mountains, Cui and Smith [7] concluded that a greater seedling mortality in the understory at more sun-exposed microsites appeared to be the result of water stress. The potentially lethal effects of blowing snow, leaf cuticle abrasion, and extreme desiccation reported for upper treeline conifers [10, 11] could also contribute to, or could even be the primary cause of, seedling mortality on the windward sides of tree islands. We conclude that wind-driven snow impacts in this typical ribbon-forest treeline ecotone may be a dominant influence on the observed occurrence of these very young conifer seedlings. Snow distribution patterns in turn are affected by adult tree islands which co-determine seedling occurrence and, thus, may be important to the stability and maintenance of this upper treeline.

Acknowledgments

Field assistance by Monique Allen is gratefully acknowledged. Comments and discussions by Jay Arnone, Christian Körner and three anonymous referees on earlier drafts of the manuscript are appreciated.

REFERENCES

[1] Arno S.F., Hammerly R.P., Timberline: Mountain and Arctic Forest Frontiers, The Mountaineers, Seattle, Washington, 1984.

[2] Barbour M.G., Pavlik B.M., Antos J.A., Seedling growth and survival of red and white fir in a Sierra Nevada ecotone, Am. J. Bot. 77 (1990) 927–938.

[3] Bazzaz F.A., The physiological ecology of plant succession, Annu. Rev. Ecol. Syst. 10 (1979) 351–371.

[4] Billings W.D., Vegetational pattern near alpine timberline as affected by fire-snowdrift interactions, Vegetatio 19 (1969) 192–207.

[5] Bliss L.C., A comparison of plant development in microenvironments of arctic and alpine tundras, Ecol. Monogr. 26 (1956) 303–337.

[6] Cooper W.S., Reproduction by layering among conifers, Bot. Gaz. 52 (1911) 369–379.

[7] Cui M., Smith W.K., Photosynthesis, water relations and mortality in *Abies lasiocarpa* seedlings during natural establishment, Tree Physiol. 8 (1990) 37–46.

[8] Day R.J., The microenvironments occupied by spruce and fir regeneration in the Rocky Mountains, Canadian Forest Branch Publication 1037, 1964.

[9] Griggs R.F., The timberlines of northern America and their interpretation, Ecology 27 (1946) 275–289.

[10] Hadley J.L., Smith W.K., Wind effects on needles of timberline conifers; seasonal influence on mortality, Ecology 67 (1986) 12–19.

[11] Hadley J.L., Smith W.K., Influence of leaf surface wax and leaf area-to-mass ratio on cuticular transpiration in conifers, Can. J. For. Res. 20 (1990) 1306–1311.

[12] Harper J.L., The Population Biology of Plants, Academic Press, New York, 1977.

[13] Hättenschwiler S., Körner C., Responses to recent climate warming of *Pinus sylvestris* and *Pinus cembra* within their montane transition zone in the Swiss Alps, J. Veg. Sci. 6 (1995) 357–368.

[14] Knapp A.K., Smith W.K., Factors influencing understory seedling establishment of engelmann spruce (*Picea engelmannii*) and subalpine fir (*Abies lasiocarpa*) in southeast Wyoming, Can. J. Bot. 60 (1982) 2753–2761.

[15] Körner C., A re-assessment of high elevation treeline positions and their explanation, Oecologia 115 (1998) 445–459.

[16] Linsday J.H., The effect of environmental factors on the leaf water balance of conifers, M.Sc. thesis, University of Wyoming, Laramie, 1967.

[17] Oberbauer S.F., Billings W.D., Drought tolerance and water use by plants along an alpine topographic gradient, Oecologia 50 (1981) 325–331.

[18] Oosting H.J., Reed J.F., Virgin spruce-fir forest in the Medicine Bow Mountains, Wyoming, Ecol. Monogr. 22 (1952) 69–91.

[19] Patten D.T., Light and temperature influence on engelmann spruce seed germination and subalpine forest advance, Ecology 44 (1963) 817–818.

[20] Pearson G.A., Forest types in the Southwest as determined by climate and soil, US Department of Agriculture Technical Bulletin 247, 1931.

[21] Puigdefábregas J., Gallart F., Biaciotto O., Allogia M., del Barrio G., Banded vegetation patterning in a subantarctic forestof Tierra del Fuego, as an outcome of the interaction between wind and tree growth, Acta Oecol. 20 (1999) 135–146.

[22] Rochefort R.M., Little R.L., Woodward A., Peterson D.L., Changes in sub-alpine tree distribution in western North America: a review of climatic and other causal factors, Holocene 4 (1994) 89–100.

[23] Tranquillini W., Physiological Ecology of the Alpine Timberline, Springer-Verlag, Berlin, Heidelberg, New York, 1979.

[24] Wardle P., An explanation for alpine timberlines, N. Z. J. Bot. 9 (1971) 371–402.

ACTA
OECOLOGICA
INTERNATIONAL JOURNAL OF ECOLOGY

INSTRUCTIONS TO AUTHORS

The aims and scope of *Acta Oecologica* are presented at the front of this issue.

The text should be written in English.

There are no page charges.

Manuscripts should be sent to: Chiara Marchetti, NIOO-CTO, P.O. Box 40, NL 6666 ZG Heteren, The Netherlands. The original and two copies are required, each accompagnied by figures and tables. Authors are invited to suggest the names of potential referees.

Manuscript preparation

Manuscripts should be typed, double spaced, on one side only, with a 5 cm margin.

The title page should contain the full title, a short running title, author's name(s), affiliation address(es), address for correspondence, Fax number, e-mail.

Full papers

Articles should be divided into the following sequence sections: title page, abstract, keywords, introduction, material and methods, results, discussion, conclusion, acknowledgements, references, tables, legends of figures and figures.

An abstract not exceeding 250 words is required for articles. The abstract should indicate the main results and conclusions.

Methods should be explained in sufficient detail to permit replication.

Forum

The Forum section is reserved for short papers containing critical discussion of current issues in ecology, and welcomes comments and viewpoints on previously published papers

Units

Use the form: $\mu L \cdot h^{-1} \cdot mg^{-1}$.

Use standard international units (SI).

References

Journal titles should be abbreviated according to the List of serial title word abbreviations (standard ISO) published by the ISSN International Centre, 20, rue Bachaumont, 75002 Paris, France.

References cited should be listed in alphabetical order, and this reference list is numbered in ascending order.

The numbering shall be used when citing references in the text. List numbers in numerical order in square brackets.

The following models for the reference list cover all situations. The punctuation must be followed exactly.

[1] Begon M., Harper J., Towsend C., Ecology. Individuals, populations and communities, Blackwell Scientific Publications, London, 1990, 945 p.

[2] Grant B., Dunham A., Thermally imposed time constraints on the activity of the desert lizard *Sceloporus meriami*, Ecology 69 (1988) 167-176.

[3] Petal J., The role of ants in ecosystems, in: Brian M.V. (Ed.), Production ecology of ants and termites, IBP 13, Cambridge University Press, Cambridge, 1978, pp. 293-325.

Tables and figures

In the text, write: *figure 1*, *table IV*, etc.

Tables should be numbered with roman numerals, each on a separate sheet, and contain only horizontal rules. All tables should have complete but brief headings.

Figure legends should be typed on a separate sheet. All illustrations are to be considered as figures and numbered consecutively throughout the text. Adopt preferably a width to allow 1/2 or 1/4 reduction (final size 8 or 16 cm wide).

If photographs are included, 3 sets of originals are required with high contrast on glossy paper. Colour illustrations carry an extra charge.

Acceptance of papers

After revision and final acceptance, the manuscript should preferably be provided on a high density (HD) disk labelled with: the type of computer used in MS-DOS or format Mac Intosh, the type of software and version number, all file names and author's name(s). The corresponding printed version should be supplied. Once your text is typed, save as an RTF (Rich Text Format) file.

Page proofs

Page proofs will be sent to the first author and should be returned to the Editor within 48 hours of receipt. Alterations in the text, other than corrections, may have to be charged to the author and could seriously delay publication.

Offprints

Twenty-five offprints of each paper and one copy of the journal issue will be provided free of charge. Additional offprints may be purchased. Send an order form with the proofs.

For permission to reproduce material from *Acta Oecologica*, please apply to the Editor-in-Chief.

On acceptance, papers become the copyright of the journal.

ACTA
OECOLOGICA
INTERNATIONAL JOURNAL OF ECOLOGY

1999

Vol. 20 • No 3

May
June

CONTENTS

Banded Vegetation Patterns – Special Issue